International Ocean Discovery Program Expedition 360 Preliminary Report

Southwest Indian Ridge Lower Crust and Moho

The nature of the lower crust and Moho at slower spreading ridges (SloMo Leg 1)

30 November 2015–30 January 2016

Henry J.B. Dick, Christopher J. MacLeod, Peter Blum, and the Expedition 360 Scientists

IODP
INTERNATIONAL OCEAN DISCOVERY PROGRAM

Publisher's notes

Core samples and the wider set of data from the science program covered in this report are under moratorium and accessible only to Science Party members until 30 January 2017.

This publication was prepared by the *JOIDES Resolution* Science Operator (JRSO) at Texas A&M University (TAMU) as an account of work performed under the International Ocean Discovery Program (IODP). Funding for IODP is provided by the following international partners:

National Science Foundation (NSF), United States
Ministry of Education, Culture, Sports, Science and Technology (MEXT), Japan
European Consortium for Ocean Research Drilling (ECORD)
Ministry of Science and Technology (MOST), People's Republic of China
Korea Institute of Geoscience and Mineral Resources (KIGAM)
Australia-New Zealand IODP Consortium (ANZIC)
Ministry of Earth Sciences (MoES), India
Coordination for Improvement of Higher Education Personnel, Brazil (CAPES)

Portions of this work may have been published in whole or in part in other International Ocean Discovery Program documents or publications.

Disclaimer

Copyright

Citation

Dick, H.J.B., MacLeod, C.J., Blum, P., and the Expedition 360 Scientists, 2016. *Expedition 360 Preliminary Report: Southwest Indian Ridge lower crust and Moho.* International Ocean Discovery Program. http://dx.doi.org/10.14379/iodp.pr.360.2016

ISSN
World Wide Web: 2372-9562

April 2016

Expedition 360 participants

Expedition 360 scientists

Henry J.B. Dick
Co-Chief Scientist
Department of Geology and Geophysics
Woods Hole Oceanographic Institution
MS #8, McLean Laboratory
Woods Hole MA 02543-1539
USA
hdick@whoi.edu

Christopher J. MacLeod
Co-Chief Scientist
School of Earth and Ocean Sciences
Cardiff University
Main Building, Park Place
Cardiff CF10 3AT
Wales
macleod@cardiff.ac.uk

Peter Blum
Expedition Project Manager/Staff Scientist
International Ocean Discovery Program
Texas A&M University
1000 Discovery Drive
College Station TX 77845-9547
USA
blum@iodp.tamu.edu

Natsue Abe
Physical Properties Specialist/Downhole Measurements
Institute for Research on Earth Evolution (IFREE)
Japan Agency for Marine-Earth Science and Technology
2-15 Natsushima-cho
Yokosuka Kanagawa 237-0061
Japan
abenatsu@jamstec.go.jp

Donna K. Blackman
Physical Properties Specialist/Downhole Measurements
Scripps Institution of Oceanography
University of California, San Diego
LaJolla CA 92093-0225
USA
dblackman@ucsd.edu

Julie A. Bowles
Paleomagnetist
Department of Geosciences
University of Wisconsin-Milwaukee
Lapham Hall 366
Milwaukee WI 53201
USA
bowlesj@uwm.edu

Michael J. Cheadle
Structural Geologist
Department of Geology and Geophysics
University of Wyoming
1000 University Avenue, Department 3006
Laramie WY 82071
USA
cheadle@uwyo.edu

Kyungo Cho
Inorganic Geochemist
Department of Environmental Exploration Engineering
Pukyong National University
Yongso-ro, Nam-Gu
Busan
Republic of Korea
whruddh@hanmail.net

Jakub Ciążela
Inorganic Geochemist
Institute of Geology
Adam Mickiewicz University
ul. Maków Polnych 16
61-606 Poznan
Poland
ciazela@amu.edu.pl

Jeremy R. Deans
Structural Geologist
Department of Geosciences
Texas Tech University
125 Science Building, MS 1053
Lubbock TX 79409
USA
jeremy.deans@ttu.edu

Virginia P. Edgcomb
Microbiologist
Department of Geology and Geophysics
Woods Hole Oceanographic Institution
220 McLean Laboratory MS#8
Woods Hole MA 02543
USA
vedgcomb@whoi.edu

Carlotta Ferrando
Structural Geologist
Géosciences Montpellier
Université de Montpellier
34095 Montpellier Cedex 05
France
carlotta.ferrando@gm.univ-montp2.fr

Lydéric France
Igneous Petrologist
Centre de Recherches Pétrographiques et Géochimiques (UMR 7358)
CNRS
Université de Lorraine
54501 Vandœuvre les Nancy
France
lyde@crpg.cnrs-nancy.fr

Biswajit Ghosh
Igneous Petrologist
Department of Geology
University of Calcutta
35 Ballygunge Circular Road
Kolkata West Bengal 700019
India
bghosh_geol@hotmail.com

Benoît M. Ildefonse
Structural Geologist
Géosciences Montpellier
Université de Montpellier
34095 Montpellier Cedex 05
France
benoit.ildefonse@umontpellier.fr

Mark A. Kendrick
Inorganic Geochemist
Research School of Earth Sciences
The Australian National University, Acton
Acton ACT 2601
Australia
mark.kendrick@anu.edu.au

Juergen H. Koepke
Metamorphic Petrologist
Institut fuer Mineralogie
University of Hannover
Callinstrasse 3
30167 Hannover
Germany
koepke@mineralogie.uni-hannover.de

James A.M. Leong
Metamorphic Petrologist
School of Earth and Space Exploration
Arizona State University
550 East Tyler Mail PSF #686
Tempe AZ 85287
USA
jmleong@asu.edu

Chuanzhou Liu
Igneous Petrologist
Institut of Geology and Geophysics
Chinese Academy of Sciences
19 Western Beitucheng Road
Beijing 100029
China
chzliu@mail.iggcas.ac.cn

Qiang Ma
Metamorphic Petrologist
School of Ocean and Earth Science
Tongji University
1239 Siping Road
Shanghai
China
tongjimaqiang@hotmail.com

Tomoaki Morishita
Igneous Petrologist
Kanazawa University
College of Science and Engineering
Kakuma-machi
Kanazawa Ishikawa 920-1192
Japan
moripta@staff.kanazawa-u.ac.jp

Antony Morris
Paleomagnetist
School of Geography, Earth and Environmental Sciences
University of Plymouth
Drake Circus
Plymouth PL4 8AA
United Kingdom
a.morris@plymouth.ac.uk

James H. Natland
Igneous Petrologist
Rosenstiel School of Marine and Atmospheric Science
University of Miami
Miami FL 33156
USA
jnatland@rsmas.miami.edu

Toshio Nozaka
Metamorphic Petrologist
Okayama University
Department of Earth Sciences
Okayama 700-8530
Japan
nozaka@cc.okayama-u.ac.jp

Oliver Pluemper
Structural Geologist
Institute of Earth Sciences
Utrecht University
Budapestlaan 4
3584CD Utrecht
Netherlands
o.plumper@uu.nl

Alessio Sanfilippo
Igneous Petrologist
Kanazawa University
College of Science and Engineering
Kakuma Kanazawa 920-1192
Japan
spessio84@gmail.com

Jason B. Sylvan
Microbiologist
Department of Oceanography
Texas A&M University
Eller O&M Building, Room 716
College Station TX 77843
USA
jasonsylvan@tamu.edu

Maurice A. Tivey
Paleomagnetist
Department of Geology and Geophysics
Woods Hole Oceanographic Institution
360 Woods Hole Road
Woods Hole MA 02543
USA
mtivey@whoi.edu

Riccardo Tribuzio
Metamorphic Petrologist
Diparmento scienze della Terra
Università degli studi di Pavia
Via Ferrata 1
27100 Pavia
Italy
tribuzio@crystal.unipv.it

Luis G.F. Viegas
Structural Geologist
Instituto de Geosciencias
Universidade de Sao Paulo
Rua do Lago 562
Sao Paulo SP
Brazil
lgviegas@gmail.com

Education and outreach

Lucas Kavanagh
Education/Outreach Officer
315 Arnold Avenue
Victoria BC V8S 3L6
Canada
l.kavanagh@me.com

Marion Burgio
Education/Outreach Officer
1291 Avenue de l'amiral
Landrin
64110 Jurancon
France
marion.burgio@gmail.com

Alejandra Martinez
Education/Outreach Officer
2424 Elizabeth Circle
Eagle Pass TX 78852
USA
seafoamgreen@gmail.com

Jiansong Zhang
Education/Outreach Officer
Xinhua News Agency Shanghai Branch
Research Department
62 Hengshan Road
Shanghai
China
13311669691@163.com

Siem Offshore AS officials

Terry Skinner
Master of the Drilling Vessel

James Samuel McLelland
Offshore Installation Manager

Technical support

Heather Barnes
Assistant Laboratory Officer

Susan Boehm
X-ray Laboratory

Adam Bogus
Physical Properties Laboratory

Michael Cannon
Marine Computer Specialist

Etienne Claassen
Marine Instrumentation Specialist

William Crawford
Senior Imaging Specialist

Roy Davis
Laboratory Officer

Aaron de Loach
Physical Properties Laboratory

David Fackler
Applications Developer

Edwin Garrett
Paleomagnetics Laboratory

Jan Jurie Kotze
Marine Instrumentation Specialist

Zenon Mateo
Core Laboratory

Aaron Mechler
Thin Section Laboratory

Stephen Midgley
Operations Superintendent

Erik Moortgat
Chemistry Laboratory

Chieh Peng
Assistant Laboratory Officer

Vincent Percuoco
Chemistry Laboratory

Alyssa Stephens
Publications Specialist

Kerry Swain
Logging Engineer

Steven Thomas
Marine Computer Specialist

John Van Hyfte
Drilling Engineer

Rui Wang
Applications Developer

Abstract

International Ocean Discovery Program (IODP) Expedition 360 was the first leg of Phase I of the SloMo (shorthand for "The nature of the lower crust and Moho at slower spreading ridges") Project, a multiphase drilling program that proposes to drill through the outermost of the global seismic velocity discontinuities, the Mohorovičić seismic discontinuity (Moho). The Moho corresponds to a compressional wave velocity increase, typically at ~7 km beneath the oceans, and has generally been regarded as the boundary between crust and mantle. An alternative model, that the Moho is a hydration front in the mantle, has recently gained credence upon the discovery of abundant partially serpentinized peridotite on the seafloor and on the walls of fracture zones, such as at Atlantis Bank, an 11–13 My old elevated oceanic core complex massif adjacent to the Atlantis II Transform on the Southwest Indian Ridge.

Hole U1473A was drilled on the summit of Atlantis Bank during IODP Expedition 360, 1–2 km away from two previous Ocean Drilling Program (ODP) holes: Hole 735B (drilled during ODP Leg 118 in 1987 and ODP Leg 176 in 1997) and Hole 1105A (drilled during ODP Leg 179 in 1998). A mantle peridotite/gabbro contact has been traced by dredging and diving along the transform wall for 40 km. The contact is located at ~4200 m depth at the drill sites but shoals considerably 20 km to the south, where it was observed in outcrop at 2563 m depth. Moho reflections have, however, been found at ~5–6 km beneath Atlantis Bank and <4 km beneath the transform wall, leading to the suggestion that the seismic discontinuity may not represent the crust/mantle boundary but rather an alteration (serpentinization) front. This then raises the interesting possibility that a whole new planetary biosphere may thrive due to methanogenesis associated with serpentinization. The SloMo Project seeks to test these two hypotheses at Atlantis Bank and evaluate carbon sequestration in the lower crust and uppermost mantle.

A primary objective of SloMo Leg 1 was to explore the lateral variability of the stratigraphy established in Hole 735B. Comparison of Hole U1473A with Holes 735B and 1105A allows us to demonstrate a continuity of process and complex interplay of magmatic accretion and steady-state detachment faulting over a time period of ~128 ky. Preliminary assessment indicates that these sections of lower crust are constructed by repeated cycles of intrusion, represented in Hole U1473A by approximately three upwardly differentiated hundreds of meter–scale bodies of olivine gabbro broadly similar to those encountered in the deeper parts of Hole 735B.

Specific aims of Expedition 360 focused on gaining an understanding of how magmatism and tectonism interact in accommodating seafloor spreading, how magnetic reversal boundaries are expressed in the lower crust, assessing the role of the lower crust and shallow mantle in the global carbon cycle, and constraining the extent and nature of life at deep levels within the ocean lithosphere.

Summary

International Ocean Discovery Program (IODP) Expedition 360 was the first leg of Phase I of the SloMo (shorthand for "The nature of the lower crust and Moho at slower spreading ridges") Project, a multiphase drilling program that proposes to drill through the outermost of the global seismic velocity discontinuities, the Mohorovičić seismic discontinuity (Moho). The Moho corresponds to a compressional wave velocity increase from ~6.7 km/s to between 7.6 and 8.6 km/s, typically at ~7 km beneath the oceans. Since the work of Adams and Coker (1906), Adams and Williamson (1923), and Wrinch and Jeffreys (1923), the Moho has generally been regarded as the boundary between crust and mantle; however, an alternative model, that the Moho is a hydration front in the mantle (Hess, 1960, 1962), has recently gained credence upon the discovery of abundant partially serpentinized peridotite on the seafloor and on the walls of fracture zones. One such location is Atlantis Bank, an 11–13 My old elevated oceanic core complex massif adjacent to the Atlantis II Transform on the Southwest Indian Ridge (SWIR).

IODP Hole U1473A was drilled on the summit of Atlantis Bank during Expedition 360, 1–2 km away from two previous Ocean Drilling Program (ODP) holes: Hole 735B (drilled during ODP Leg 118 in 1987 and ODP Leg 176 in 1997) and Hole 1105A (ODP Leg 179 in 1998). A mantle peridotite/gabbro contact has been traced for 15 km at ~4200 m depth along the transform wall ~11.5 km to the west. Moho reflections have, however, been found at ~5–6 km beneath Atlantis Bank, leading to the suggestion that the seismic discontinuity may not represent the crust/mantle boundary but rather an alteration (serpentinization) front (Muller et al., 2000). This raises the interesting possibility that a whole new planetary biosphere may thrive due to methanogenesis associated with serpentinization. The SloMo Project seeks to test these two hypotheses at Atlantis Bank and evaluate carbon sequestration in the lower crust and uppermost mantle.

Located on the north-central part of Atlantis Bank, 2.2 km north-northeast of Hole 735B, Hole U1473A was drilled 789.7 meters below seafloor (mbsf) into massive gabbro cut by isolated dikes. The shallower part of the hole has been affected by faulting: in the upper 469 m, seven distinct fault systems were encountered, ranging from 5 cm thick cataclasite bands to a 50 m thick carbonate-veined chlorite-rich fault zone. Over this interval, we obtained 44% recovery under relatively poor drilling conditions. From 469 mbsf to the bottom of the hole, however, drilling conditions were excellent, similar to Hole 735B, with 96% recovery in the lowermost 212 m interval cored (577.5 to 789.7 mbsf). Hole U1473A is the deepest hole ever drilled from the seafloor into ocean crust during a single 2 month expedition. The hole is in good condition overall and, after minor remediation (including the fishing of a piece of steel dropped in the bottom of the hole during logging at the end of Expedition 360), can be reoccupied during SloMo Leg 2.

A primary objective of SloMo Leg 1 was to explore the lateral variability of the stratigraphy established in Hole 735B. Comparison of Hole U1473A with Holes 735B (Dick et al., 2000) and 1105A (Casey et al., 2007) allows us to demonstrate a continuity of process and complex interplay of magmatic accretion and steady-state detachment faulting over a time period of ~128 ky. Preliminary assessment indicates that these sections of lower crust are constructed by repeated cycles of intrusion, represented in Hole U1473A by approximately three upwardly differentiated hundreds of meter–scale bodies of olivine gabbro broadly similar to those encountered in the deeper parts (>500 mbsf) of Hole 735B.

The gabbro bodies in Hole U1473A are transposed by intense locally pervasive ductile deformation, with extensive intervals of sheared porphyroclastic to ultramylonitic gabbro (often Fe-Ti oxide rich) forming a 600 m thick crystal-plastic shear zone. Notably, shear sense is both normal and reversed in the upper section of the hole but predominantly reversed in the lower part. Similar relationships are also seen in Hole 735B; all are probably a response of the Atlantis Bank oceanic core complex to flexure during exhumation. Deformation is noticeably less intense toward the bottom of Hole U1473A, with primary subophitic igneous textures often well preserved in the lowermost 200 m. Overall, the presence of such exten-

sive crystal-plastic deformation in Hole U1473A and elsewhere at Atlantis Bank demonstrates that magmatic accretion took place in a highly dynamic environment, beginning while the gabbros were partially molten and continuing as they cooled and were exhumed tectonically from beneath the rift valley floor.

The average composition for Hole U1473A is very similar to Hole 735B, with Mg# of 71 and 0.7 wt% TiO_2. However, H_2O contents averaging 1.0 wt%, even in petrographically fresh samples, are much higher than expected for pristine gabbro cumulates. Most of the gabbros drilled in Hole U1473A are olivine gabbro, with lesser but still significant proportions of gabbro and oxide-bearing gabbro. The relationship between these rock types is complex and ranges from simple interlocking igneous contacts between undeformed gabbros with subparallel coarse to pegmatitic oxide gabbro layers, to isolated patches of oxide- and pyroxene-rich gabbro intercalated with the olivine gabbro, to oxide concentrations that indicate local migration of late Fe-Ti oxide-rich melts along active shear zones. The Fe-Ti–rich oxide gabbro and gabbronorite occurrences, whether in layers and patches or within shear zones, appear to have crystallized from evolved interstitial melt compacted out of the olivine gabbro cumulates and record the migration of these melts through the section. Evidence for percolation of more primitive melts through the section is also ubiquitous, with fine-grained microgabbros intruding or replacing the coarse olivine gabbro. Approximately 1.5% of the section consists of late magmatic felsic veins, ranging in composition from diorite to trondhjemite. These may represent the final stages of fractionation of the melts intruded to form the gabbros or may instead be produced by reheating and partial anatexis of the section by successive intrusive events. Several diabase dikes intruded gabbros that had been altered under granulite to greenschist facies conditions. These include granoblastic hornblende diabase dikes that may have partially melted the crystal-plastically deformed gabbro host to form trondhjemite. Overall, the bulk of the gabbros are too fractionated to be in equilibrium with the mid-ocean-ridge basalt (MORB) hanging wall, reflecting a complex evolution beyond initial intrusion of basaltic melt.

The Hole U1473A section has undergone static hydrothermal alteration, extensive recrystallization associated with crystal-plastic deformation, and alteration associated with veining and with late cataclastic deformation. Static alteration occurs throughout the hole, ranging from <3% to 90%, with locally intense veining and characterized by colorless amphibole, talc, serpentine, and clay minerals after olivine; however, away from fault zones, much of the section is very fresh. Formation of near-ubiquitous brown hornblende and secondary clinopyroxene reflect near-solidus conditions, whereas other assemblages reflect amphibolite to subgreenschist facies. Clay minerals are the last alteration products, reflecting temperatures <150°C. Amphibolite facies alteration and overprinting clay mineral formation are significant largely at shallow depths, whereas intervals displaying greenschist facies alteration are found sporadically throughout the hole. Carbonate with or without clay and oxidative reddish clay replacement of olivine is also more conspicuous in intervals disturbed by faulting, whereas deeper in the hole microveins filled with chlorite, with or without amphibole, are more typical.

Felsic veins in Hole U1473A often have high abundances of secondary sulfides and clay minerals as well as replacement of primary plagioclase by albitic and occasionally secondary quartz, showing that these were pathways for large volumes of hydrothermal fluids. This observation was also made for Hole 735B. A key similarity between Holes U1473A, 735B, and 1105A is the occurrence of amphibole veins, which is largely limited to the shallower sections of the holes.

Specific objectives of SloMo Leg 1 included drilling through a magnetic reversal that was projected to lie several hundred meters below seafloor at Site U1473: from reversely polarized at the surface to normally polarized at depth. Virtually all intervals drilled in Hole U1473A have positive inclinations, indicating, in the Southern Hemisphere, a reversed polarity magnetization that places the hole within geomagnetic polarity Chron C5r.3r, as in Hole 735B. Magnetizations are sufficient to account for the observed sea-surface anomalies at Atlantis Bank. A clear reversal boundary was not reached during Expedition 360; however, thermal demagnetization revealed characteristic remanence with negative inclination (normal polarity) in narrow altered intervals in the lower part of the hole, leading us to suggest that we are entering a reversal transition near the bottom of Hole U1473A. Three intervals with statistically significant differences in inclination downhole may document differential block rotations due to faulting.

Background and objectives

Expedition 360 constituted the first leg of the multiphase SloMo Project that aims ultimately to drill through the Moho seismic discontinuity at Atlantis Bank at the ultraslow-spreading SWIR (Figure **F1**). By penetrating this fundamental seismological boundary, the SloMo Project will test the hypothesis that the Moho, at least at slow- and ultraslow-spreading ridges, represents an alteration boundary such as the lower limit of mantle lithosphere serpentinization rather than the igneous crust–mantle transition (Figure **F2**). If the latter, the igneous crust/mantle boundary could lie at any depth above the seismic boundary.

The site chosen for this deep drill hole is Atlantis Bank, an elevated flat-topped massif at ~700 m water depth on the east flank of the north-south–trending Atlantis II Transform (Figure **F3**) (Dick et al., 1991b). The Moho here lies at ~5.5 km below the platform summit (Figure **F4**) (Muller et al., 2000). The principal aim of Expedition 360 was to drill as deep as possible through lower crustal gabbro and to leave a hole open and ready to be deepened during subsequent expeditions. A target depth of 1300 mbsf was originally estimated, derived from prior experience of drilling conditions at Atlantis Bank and assuming a nominal 4 days contingency time for weather and operational issues; however, this depth was not achieved largely because the number of days available to us for coring during Expedition 360 was substantially less than planned (see **Operations**).

On the basis of local geological knowledge from site survey investigations, it was thought unlikely that the igneous crust/mantle boundary would be encountered or a significant amount of peridotite recovered during Expedition 360 itself. The aim of future SloMo expeditions is to reoccupy and deepen the hole with the overall goal of penetrating the crust–mantle transition, which is believed to be as much as ~2.5 km above the Moho (see below). Additional drilling, potentially using the riser D/V *Chikyu*, is likely to be necessary to penetrate the Moho itself at ~5 km below seafloor (Figure **F4**).

The SloMo Project is not simply focused on the ultimate goal of drilling the crust/mantle boundary; equally important is what we learn on each step of the journey on the way. By recovering a substantial section of the igneous lower crust at Atlantis Bank, Expedition 360 was designed to address specific key challenges set out in the IODP Science Plan 2013–2023 (**http://www.iodp.org/science-plan-for-2013-2023**). This document, representing the consensus

of the global ocean drilling community, posits that in order to understand the inherent connections between the Earth's interior and its surface environment we must address fundamental questions about basic plate tectonic processes. Central among these questions are how seafloor spreading and mantle melting lead to the creation of oceanic lithosphere at mid-ocean ridges, and what controls the architecture of the ocean crust thus formed (IODP Science Plan Challenge 9). Constraining the composition, diversity, and architecture of the lower ocean crust and shallow mantle is critical to understanding the global geochemical cycle, particularly the exchange of heat, mass, and volatiles between the Earth's interior, oceans, and atmosphere.

At slow- and ultraslow-spreading ridges, the lower crust uniquely preserves that critical link where magmatic and tectonic processes directly reflect plate dynamics, melt input, and the mantle flow pattern. We now know that at such ridges a substantial portion of plate spreading is accommodated in the lower crust by tectonic extension due to faulting and, in places, ductile deformation (e.g., Mutter and Karson, 1992). Large-offset "detachment" normal faults exert a strong control on melt distribution and transport in the lower crust and delivery to the seafloor. This is in marked contrast to fast-spreading ridges, where it is accepted that the crust principally undergoes magmatic accretion by the injection of melt into the lower crust, diking, and eruption of magmas on the seafloor; thus, rollover and corner flow by ductile flow accompanying mantle upwelling and plate spreading is believed to be mostly limited to the mantle. However, at slower spreading ridges, which are cooler and support only ephemeral magma chambers, the lower crust can potentially support a shear stress. As a consequence, with lower rates of magma supply and colder, stronger lithosphere formed directly beneath the ridge axis, slower spreading ridges have very different morphologies and crustal architectures. Thus, as stated in IODP Initial Science Plan Challenge 9, a full picture of crustal architecture and accretion can only be drawn if both fast- and slow-spreading environments are addressed.

Specific aims of Expedition 360, the first leg of Phase I of the SloMo Project, therefore focused on gaining an understanding of how magmatism and tectonism interact in accommodating seafloor spreading, how magnetic reversal boundaries are expressed in the lower crust, assessing the role of the lower crust and shallow mantle in the global carbon cycle, and constraining the extent and nature of life at deep levels within the ocean lithosphere. These are explained further in **Scientific objectives** below.

Geological setting

The SWIR with a full spreading rate of 14 mm/y lies at the slow end of the mid-ocean-ridge spreading-rate spectrum. The ridge trends approximately southwest–northeast for most of its length, spreading almost due north–south. Between ~52°E and 60°E, it is offset by a series of closely spaced long-offset transform faults. One of these, the Atlantis II Transform at 57°E (Fisher and Sclater, 1983), offsets the SWIR sinistrally by 200 km (Dick et al., 1991b) (Figure **F1**). Between this transform and the Novara Transform ~140 km to the east, the spreading axis is divided into two segments, AN-1 and AN-2, separated by a 17 km offset nontransform discontinuity at 57°20′E and 57°54′E (Mendel et al., 1997; Hosford et al., 2003; Baines et al., 2007). The spreading rate here is asymmetric: at the short westerly Segment AN-1 adjacent to the northern ridge/transform intersection of the Atlantis II Transform, magnetic anomalies reveal rates of 8.5 mm/y to the south and 5.5 mm/y to the north, and the transform has been lengthening by 3 mm/y for at least the past 20 My (Dick et al., 1991b; Hosford et al., 2003; Baines et al., 2007). At ~20 Ma, a 10° counterclockwise change in regional spreading direction put the Atlantis II Transform into transtension for a period of ~12 My (Dick et al., 1991b, Hosford et al., 2003; Baines et al., 2007, 2008).

Immediately to the east of the Atlantis II Transform, parallel to it and on a flow line directly south of spreading Segment AN-1, is an elevated transverse ridge (Figure **F1**). It consists of a series of uplifted blocks connected by saddles that rise to as little as 700 meters below sea level (mbsl) (Dick et al., 1991b). Atlantis Bank (32°43′S, 57°17′E) forms the shallowest and northernmost portion of this ridge, 95 km south of the SWIR axis (Figures **F1**, **F3**). The bank consists of a raised dome ~40 km long by ~30 km wide, rising from 5700 m at the base of the transform wall to 700 m on a ~25 km^2 flat-topped wave-cut platform at its crest and then drops to 4300 m on its eastern flank across two prominent transform-parallel east-dipping normal faults (Dick et al., 1991b; Baines et al., 2003; Hosford et al., 2003).

Site surveys of the Atlantis Bank area have included multibeam, magnetics, and gravity surveys, as well as rock sampling using seabed rock coring, a remotely operated vehicle (ROV), submersible dives, and dredging (Dick et al., 1991b; MacLeod et al., 1998; Arai et al., 2000; Kinoshita et al., 1999; Matsumoto et al., 2002). A high-resolution bathymetric map of the ~25 km^2 summit region compiled from narrow-beam echo soundings (Dick et al., 1999) shows the platform consists of a broadly flat surface ranging from ~750 to 689 m water depth (Figure **F5**). ROV survey results show the central pavement to be bare rock, locally knobbly igneous outcrop (largely gabbro) surrounded on its periphery and locally on its surface by limestone, in some places ripple marked, and carbonate-cemented pebble conglomerate. Morphologically the platform is interpreted as a set of partially eroded sea stacks surrounded by beach gravel and limestone pavement (see below).

Hole 735B is located at the southwest corner of the flat surface of the Atlantis Bank platform (32°43.395′S, 57°15.959′E, 731 m water depth) (Figures **F3**, **F5**). During Legs 118 and 176, the hole was drilled to a total of 1508 mbsf with 87% core recovery, all in gabbro (sensu lato) ~11 Ma in age (Robinson, Von Herzen, et al., 1989; Dick et al., 2000). Further operations during Leg 179 drilled the 158 m deep Hole 1105A in the center of the platform (32°43.13′S, 57°16.65′E; Pettigrew, Casey, Miller, et al., 1999), also in gabbro and with similar overall core recovery rates.

Employing the British Geological Survey's 5 m diamond rock drill and 1 m "BRIDGE"-oriented corer during site survey Cruise JR31 on the RRS *James Clark Ross*, MacLeod et al. (1998) drilled 42 successful cores on the surface of this platform region, recovering igneous rocks in 33 of them (Figure **F5**). The cores reveal continuous gabbro outcrop on the platform surface, with diabase at two locations and serpentinized peridotite along with pillow-basalt breccia drilled at its southern tip. The two lattermost occur where the flat platform narrows into a north–south spine (32°44.5′S). Many of the gabbroic rocks in the shallow drill cores and seen in *ROPOS* ROV images from the surface of the platform are mylonitic, displaying intense crystal-plastic deformation with shallow fabrics. In Hole 735B, crystal-plastic deformation of oxide gabbro and olivine gabbro was likewise found to be strong in the uppermost 500 m but diminished markedly downsection (Robinson, Von Herzen, et al., 1989; Cannat et al., 1991; Dick et al., 1991a; Miranda and John, 2010). Considered together, it is apparent that the upper surface of Atlantis Bank represents a detachment fault damage zone representing a high-temperature "plutonic growth fault" active during

the accretion of the gabbroic lower crust and responsible for its exhumation. This "hot" detachment must have rooted at the top of a continuously replenished crystal mush zone close to the midpoint of the AN-1 spreading ridge (Dick et al., 1991a, 2000; Natland and Dick, 2001, 2002). Numerous inliers of dikes intercalated with gabbro occur across the eastern side of the bank (Figure **F3**), demonstrating that the detachment footwall passed through the zone of active diking beneath the rift valley (Dick et al., 2008). Magnetic anomalies hosted within the gabbro massif indicate an age from 10.7 to 14.5 Ma (Dick et al., 1991b; Allerton and Tivey, 2001; Hosford et al., 2003); hence emplacement of gabbro into the footwall of a single detachment fault must have been continuous for ≥3.74 My, accruing a total slip of at least 38.9 km (e.g., Baines et al., 2007). Inclinations of paleomagnetic remanence directions from Holes 735B and 1105A and JR31 seabed drill cores are consistently ~20° steeper than expected for the latitude of Atlantis Bank and are interpreted as indicating a southward tilt of this magnitude subsequent to cooling of the section through the Curie temperature of magnetite (580°C) (Kikawa and Pariso, 1991; Dick, Natland, Miller, et al., 1999; Pettigrew, Casey, Miller, et al., 1999; Allerton and Tivey, 2001).

Submersible observations at Atlantis Bank (Kinoshita et al., 1999; Matsumoto et al., 2002) show that the detachment fault surface is preserved over large regions in the deeper waters on both sides of the platform. The damage zone and underlying gabbro are well exposed by high-angle normal faulting on the eastern side of the complex and in headwalls of large landslips on the western flank. Here, lower temperature fault rocks are present in addition to the amphibolite facies mylonite. These chloritized and weathered fault gouge and talc-serpentine schists, preserved locally on the fault surface (Dick et al., 2001; Miranda and John, 2010), are very similar to fault rocks found on the Mid-Atlantic Ridge core complexes (e.g., MacLeod et al., 2002; Escartín et al., 2003, Schroeder and John, 2004; Dick et al., 2008).

The absence of the low-temperature fault rocks on the flat surface of the Atlantis Bank platform compared to its flanks suggests they have been removed, a deduction entirely consistent with the long-held supposition (Dick et al., 1991b; Palmiotto et al., 2013) that Atlantis Bank was once an ocean island, and its flat top results from erosion at sea level followed by subsidence to its present level. Shallow drilling and dredging on the summit and uppermost flanks of the Atlantis Bank platform have amply verified this supposition. Indurated carbonates were drilled at 24 sites from the periphery of the platform and were also recovered in dredges from its flanks (MacLeod et al., 1998, 2000; Palmiotto et al., 2013). Although some (recent) carbonate sand was recovered, most of the sediments are indurated bioclastic limestone (skeletal packstone to wackestone; MacLeod et al., 2000) of Miocene to Pleistocene age (Palmiotto et al., 2013). The sediments contain abundant macrofauna, primarily bryozoans, mollusks, algal nodules, and echinoids, but also some solitary corals. Benthic and, in some instances, large planktonic foraminifers are common. Whereas Palmiotto et al. (2013) suggest a water depth of ~100–200 m based upon assemblages in dredged carbonates from the flanks of the platform, green algal (dasyclad) assemblages in drill cores from the platform summit (G. Della Porta and V.P. Wright, pers. comm., 1999; MacLeod et al., 2000) indicate water depths at wave base or shallower, demonstrating that the platform was at sea level and probably above. How much material has been removed by subaerial erosion is not known, potentially 100–200 m with reference to the inferred thickness of the detachment fault damage zone. ROV observations of steep sides up to 10 m, locally even 50 m, at the gabbro pavement flanks on the platform summit may represent coastal cliffs and small sea stacks resulting from the dispersal of wave energy on the flanks of the island during erosion.

The Atlantis II Transform transverse ridge, on which Atlantis Bank lies, is clearly analogous to oceanic core complex massifs found on the Mid-Atlantic Ridge (e.g., Cann et al., 1997; Tucholke et al., 1998; MacLeod et al., 2002, 2009; Smith et al., 2006; Dick et al., 2008), although here, as elsewhere along the SWIR (Cannat et al., 2006; Sauter et al., 2013), the prominent spreading direction–parallel corrugations that are characteristic of the flat surfaces of the Atlantic oceanic core complexes are not so obvious and are potentially present only on the down-dropped terrace on the eastern side of Atlantis Bank (Figures **F1**, **F3**); furthermore, the Atlantis II Transform transverse ridge was clearly uplifted far above the surrounding seafloor. Whereas flexural uplift of detachment fault footwalls to form oceanic core complexes is typically 1 ± 0.5 km relative to surrounding seafloor of similar age (Tucholke et al., 1998; Lavier et al., 1999), the Atlantis II transverse ridge has been uplifted by 3 km (Baines et al., 2003). Dick et al. (1991a) and Baines et al. (2003) propose that the original detachment-related uplift at the ridge/transform intersection was accentuated by an additional phase of flexural uplift, imparted upon the transform in response to the change of spreading direction on the SWIR at 19.5 Ma, and accommodated by the reactivation as normal faults of originally transform-related north–south structures.

One consequence of the Atlantis II transverse ridge relative uplift is that the crust/mantle boundary, as mapped by dredging and submersible traverses, is exposed along its western wall for a distance of nearly 40 km (Figure **F3**). This boundary was encountered at several locations during *Shinkai 6500* dives in landslip headwalls and debris slopes. The boundary lies at ~4660 m water depth west of the drill sites but shoals considerably 20 km to the south, where it was located in outcrop by a *Shinkai 6500* dive at 2563 m water depth (Kinoshita et al., 1999; Matsumoto et al., 2002). Upslope to the east of these dives, Dives 467 and 459 crested the landslip headwalls and encountered the more gently sloping detachment fault footwall at 3000 and 1755 m, respectively, potentially indicating gabbro layer thicknesses as little as 1500 and 2895 m. Elsewhere along the western flank of Atlantis Bank, serpentinized peridotite was recovered in dredges from as shallow as 2000 m water depth (Dredge JR31-DR8), though in other nearby places only at >3000 m depth. At the southern end of the platform summit itself, serpentinized harzburgite was drilled at a water depth of 839 m (Site JR31-BGS12). Highly altered peridotite sampled at several locations above the peridotite/gabbro contact on the transform wall consists largely of talc-serpentine schist that likely overlies the gabbro massif. This and the presence of serpentinized peridotite pebbles in sedimentary (beach) conglomerates lying on gabbro near the edge of the platform suggest that a discontinuous talc-serpentine sheet was intruded along the detachment fault from where the fault cut massive peridotite in the transform fault zone (Dick et al., 2001). This sheet is now preserved locally on the detachment surface. The serpentinite drilled at Site JR31-BGS12 on the southern end of the platform, however, is relatively massive harzburgite with well-preserved pseudomorphs of pyroxene. Possible origins of this particular serpentinite outcrop include a peridotite screen in gabbro similar to those drilled at Atlantis Massif in Integrated Ocean Drilling Program Hole U1309D (Blackman, Ildefonse, John, Ohara, Miller, MacLeod, and the Expedition 304/305 Scientists, 2006), an enclave of less deformed and altered serpentinized peridotite in the original detachment fault shear zone, or juxtaposition via a north-dipping ridge-parallel normal fault that demarcates the southernmost end of the flat platform at 32°44.4′S.

A wide-angle seismic refraction survey of the Atlantis II Transform region found the Moho at 5 ± 1 km beneath Atlantis Bank (Muller et al., 1997, 2000; Minshull et al., 1998) (Figure **F4**). The direct geological constraints outlined above offer strong support to the inference that the Moho cannot represent the (petrological) crust/mantle boundary in this region. Whereas Muller, Minshull, and colleagues also concluded that it could be a serpentinization front, they based this conclusion on the geochemical argument that the igneous crustal thickness there was originally ~4 km (based upon rare earth element inversions), and with the basaltic carapace removed by detachment faulting, the remainder was likely to be ~2 to 2.5 km thick. However, they admit this interpretation is nonunique, primarily because of the overlap in *P*-wave seismic velocity between gabbro and ~20%–40% partially serpentinized peridotite (e.g., Miller and Christensen, 1997).

At what level is the (petrological) crust/mantle boundary likely to lie beneath Atlantis Bank? Projecting the detachment surface to the locations of the traversed crust/mantle boundary described above indicates that the crustal thickness at these points prior to mass wasting on the transform wall was significantly <3 km, whereas the depth to the Moho below the transform wall remains approximately constant (Figure **F4**). Given that the elevated core complex massif is produced by flexure during uplift into the rift-mountains because of a spreading direction change (Baines et al., 2003), it seems reasonable to conclude that the mapped boundary is most likely to project approximately subhorizontally or even be elevated beneath the center of Atlantis Bank, consistent with the igneous crustal thickness of 2–2.5 km suggested by Minshull et al. (1998).

Scientific objectives

Previous ODP operations at Atlantis Bank drilled 1508 m deep Hole 735B and 158 m deep Hole 1105A. Both holes recovered long sections of gabbro, consisting largely of olivine gabbro, subordinate amounts of oxide gabbro, and minor troctolite and leucocratic veins (Dick et al., 1991a, 2000; Pettigrew, Casey, Miller, et al., 1999). On the basis of our previous site survey, we selected Site AtBk6, located on the northern edge of the Atlantis Bank platform 1.4 km north of Hole 1105A and 2.2 km north-northeast of Hole 735B, as the most suitable location for a deep-penetration drill site (Figures **F3**, **F5**).

Three contingency sites identified at Atlantis Bank were Site AtBk4 (serpentinized peridotite Site JR31-BR12) at the southern end of the platform, Site AtBk5 in gabbro at the northern edge of the platform, and Site AtBk2 in gabbro and dikes at 1700 m water depth on the down-dropped terrace east of the main elevated platform (Figures **F3**, **F5**). These sites were envisaged not as alternatives to the deep-penetration site but as single-bit spud-ins in case weather conditions were not sufficiently calm to allow the hard rock reentry system to be deployed at the beginning of the cruise.

Drilling at our principal Site AtBk6 (now Site U1473) during Expedition 360, in lithologies similar to those at previous drill Sites 735 and 1105, was designed to allow us to tackle a number of specific science questions (see below).

1. *What is the igneous stratigraphy of the lower ocean crust?*

   Analysis of drilling results in Hole U1473A should allow us to determine the extent to which the igneous, metamorphic, and structural stratigraphy found in Holes 735B and 1105A is laterally continuous across the wave-cut platform on Atlantis Bank. In combination with Holes 735B and 1105A and the existing surface mapping, new drilling should provide a 3-D and possibly 4-D view of the lateral continuity and evolution of the lower crust and its emplacement process.

2. *How much mantle is incorporated into the lower crust?*

   An unanticipated finding in cores from Hole U1309D at the Atlantis Massif on the Mid-Atlantic Ridge was the incorporation of significant volumes of hybridized mantle peridotite within the gabbro section (Blackman et al., 2011; Expedition 304/305 Scientists, 2006; Drouin et al., 2009). Comparable screens of mantle rock were not found in either Holes 735B or 1105A. Does this reflect a profound difference between the two different mid-ocean ridges, perhaps due to different magma budgets or accretion mechanisms, or is it simply happenstance that they were not encountered during previous drilling at Atlantis Bank?

3. *What are the modes of melt transport into and through the lower crust?*

   Several different modes of melt delivery and transport were proposed on the basis of observations from Hole 735B cores. These modes include small intrusive cumulate bodies, larger intrusive units on the scale of hundreds of meters, anastomosing channels produced by focused flow and melt-rock reaction, and compaction of late iron titanium–rich melts into shear zones where they hybridized olivine gabbro to iron titanium oxide–rich gabbro and gabbronorite. The continuity and scale of these features cannot be determined from a single deep hole. Results of Expedition 360 drilling should further document the extent and proportion of these features in a younger section of the massif.

4. *How does the lower crust shape the composition of MORB?*

   The complex stratigraphies found in Holes 735B and U1309D differ in significant ways. What common factors, however, influence the composition of MORB? As in Hole 735B, recent work on gabbroic sections from the East Pacific Rise shows that the lower crust acted as a reactive porous filter homogenizing diverse melts that were intruded into it and modifying their trace element contents prior to their eruption to the seafloor (Lissenberg et al., 2013). To what extent does this processes operate uniformly at slower spreading rates?

5. *What is the strain distribution in the lower crust during asymmetric seafloor spreading?*

   Asymmetric spreading produced by detachment faulting is now recognized as one of three major accretionary modes at slow-spreading ridges (symmetric, asymmetric, and amagmatic rifting). Although each of these is important, little is known of how magmatism and tectonism interact, and hence how lower crustal accretion differs in these environments. To date we have been able to determine strain distributions with depth in two deep holes (Holes 735B and U1309D) in two different oceanic core complexes (Atlantis Bank on the SWIR and Atlantis Massif on the Mid-Atlantic Ridge) and found them to differ significantly: far more intense crystal-plastic deformation is found in the upper 500 m of Hole 735B than in Hole U1309D (Figure **F6**). We cannot assess the nature, extent, and role played by high-temperature deformation during lower crustal accretion with isolated 1-D sections. Offsetting and drilling north of Hole 735B will allow us to determine the continuity of strain distribution from Holes 735B and 1105A across the Atlantis Bank core complex and thereby assess the role and broader significance of synmagmatic deformation in this tectonic environment.

6. *What is the nature of magnetic anomalies?*

An important goal of Expedition 360 was to drill through a magnetic reversal boundary in oceanic crust for the first time and to determine what controls magnetic anomalies in plutonic rocks.

Magnetic anomaly "stripes" are detectable across the Atlantis II transverse ridge, including Atlantis Bank and its wave-cut platform (Dick et al., 1991b; Allerton and Tivey, 2001; Hosford et al., 2003; Baines et al., 2007, 2008). Whereas most of the platform is reversely magnetized, as are the gabbro intervals of Holes 735B and 1105A (Kikawa and Pariso, 1991), a narrow normally polarized zone ~2 km wide is present near its northern end. This zone is equated to anomaly Chron C5r.2n (11.592–11.647 Ma; Allerton and Tivey, 2001; Baines et al., 2008) (Figure **F7**). The zone is detectable on sea-surface (Dick et al., 1991b; Hosford et al., 2003) and deep-towed magnetic profiles (Allerton and Tivey, 2001), as well as in the JR31 seabed drill cores; however, the precise location of the boundary in each case is slightly offset. Because the sea-surface magnetization signal is derived from a much greater volume of rock than the near-bottom signal in the cores, Allerton and Tivey (2001) deduced from the sense of offset that the magnetic anomaly boundaries are inclined. They modeled the southern limit of the anomaly as a planar boundary dipping ~25° toward the south, suggesting that the surface represented either an isotherm corresponding to the Curie point or the edge of an intrusion. Alternatively, the form of the southern edge of the anomaly may have been modified by faulting: extensive brittle deformation and cataclasis is observed in shallow drill cores from the location of the southern reversal boundary, possibly corresponding to a north-dipping east-west–striking normal fault at the kink/narrowing of the platform summit at 32°41.8′S. If so, the reversal boundary is likely to dip more steeply than the 25° proposed by Allerton and Tivey (2001). For this reason, Hole U1473A was sited at the northern end of the main platform, just south of this normal fault, to encounter the reversal boundary at as a shallow a depth as possible.

7. *What is the role of the lower crust and shallow mantle in the global carbon cycle?*

Serpentinization and weathering of ultramafic rocks as well as alteration of basalts are known, under the right conditions, to cause the formation of carbonates. Such carbonates are present in the form of extensive veining in serpentinized peridotite at the southern edge of the Atlantis Bank platform (shallow drill Site JR31-BGS12/contingency drill Site AtBk4) and in partially serpentinized and weathered peridotite from the southern transform wall at 32°50′S (*Kaiko* ROV Dives 173 and 174).

The extent of these reactions in the lower crust is to date largely unknown. We do not expect that carbon sequestration will be a significant process in the lower ocean crust based on Holes 735B and U1309D; however, the possibility exists that Expedition 360 may penetrate the base of the lower ocean crust, and thus offer the first opportunity to determine if carbon sequestration is significant in the mantle below it.

8. *Is there life in the lower crust and hydrated mantle?*

A primary objective of the SloMo Project is to determine the microbiology of the lower crust, the potential serpentinized mantle above the Moho, and the underlying mantle to address IODP Science Plan Challenge 6 "What are the limits of life in the subseafloor?"

Starting in the 1990s, microbiologists accompanying ODP and Integrated Ocean Drilling Program expeditions have documented the presence of microbial life in deeply buried sediment and the basaltic basement (Fisk et al., 1998; Parkes et al., 1994; Mason et al., 2010). Evidence for active microbial life has been detected as deep as 2458 mbsf (Inagaki et al., 2015), and the introduction of molecular biology into marine ecology has led to great advances in our understanding of microbial life below the seafloor (Biddle et al., 2008; Cowen et al., 2003; Inagaki et al., 2006; Mason et al., 2010; Edgcomb et al., 2011; Orsi et al., 2013a, 2013b). Much of the microbiology performed during ODP and Integrated Ocean Drilling Program expeditions has concentrated on sediment (e.g., ODP Leg 201 to the Peru margin), with the notable exception of expeditions to the Juan de Fuca Ridge (Cowen et al., 2003; Lever et al., 2013; Jungbluth et al., 2013), Atlantis Massif (Mason et al., 2010), North Pond (Orcutt et al., 2013), and Louisville Seamounts (Sylvan et al., 2015).

Because it was never expected that mantle rocks be encountered during the first phase of SloMo, the aim of microbiology sampling during Expedition 360 was to explore for evidence of microbial life at depth within the crystalline lower oceanic crust, about which little is known. It is nevertheless possible that indirect inferences may be drawn as to the likely processes at work at greater depths from a microbial perspective from postcruise analysis of the gabbros drilled during the expedition. Olivine-rich gabbros can host serpentinization, a process that produces hydrogen, which can serve as an electron donor for microbial metabolism. Serpentinization can also be an abiotic methanogenic process through Fischer Tropsch type reactions (CO_2 reduction with H_2 in aqueous solution; Proskurowski et al., 2008), thus potentially providing an additional source of carbon (in addition to carbon dioxide that may be present) for life in the deep crust. Complex organic matter and lipids in serpentinites suggest microorganisms inhabit mantle rock exhumed at the seafloor (Delacour et al., 2008; Ménez et al., 2012). In cores from Hole U1309D (Atlantis Massif), small subunit ribosomal RNA gene sequence analyses indicated that heterotrophic microorganisms putatively capable of hydrocarbon oxidation are present in lower crustal rocks (Mason et al., 2010). Delacour et al. (2008) point out that organics in these systems likely have both biotic and abiotic sources. Abiotic synthesis of organics during serpentinization is a way of providing energy to deep-seated communities, but inorganic redox fluid-mineral reactions may also be mined directly for metabolic energy (e.g., Shock, 2009). Apart from energy constraints, the distribution of permeability and fluid flow impose strong constraints on the presence and activity of subseafloor life that can only be accurately determined by drilling. During Expedition 360, microbiologists focused on exploring evidence of life using culture-based approaches, molecular analyses, and enzyme assays. Efforts were focused on rock sections showing evidence of alteration or fracturing within all lithologies encountered.

Site survey

The broad location of the deep-penetration SloMo legacy hole that we were to drill during Expedition 360 was the north central part of Atlantis Bank, south of the inferred north-dipping fault that coincides with the bathymetric offset of the platform at 32°42′S. We believed this location would be away from the influence of the fault zone yet close to the (south dipping) magnetic reversal boundary we inferred we would encounter in the subsurface; furthermore, it would be sufficiently distant from Holes 735B and 1105A to allow us to assess kilometer-scale variability of magmatic and tectonic processes associated with lower crustal accretion.

The site selected for deep drilling (proposed Site AtBk6) had been cored during the 1998 site survey Cruise JR31 as Site JR31-BR8, determined to be located at 32°42.3402′S, 57°16.6910′E, on the

basis of an acoustic transponder network deployed during Cruise JR31 on the *James Clark Ross* (MacLeod et al., 1998). From a seafloor photograph taken from the BRIDGE drill camera the site was part of an extensive bare-rock pavement outcrop (Figure **F8**). Drill Core JR31-BR8 consisted of 1.1 m of oxide-bearing olivine gabbronorite with a thin mylonitic shear zone.

As soon as we reached Atlantis Bank following the transit from Sri Lanka, we headed directly for Site AtBk6. Once on site, an advanced piston corer (APC)/extended core barrel (XCB) bit, bit sub, drill collars, and 5 inch drill pipe assembly was made up and lowered to 668 meters below rig floor (mbrf). The subsea camera system was installed and lowered to just above the bit to conduct a survey to select a site appropriate for drilling. The survey strategy was to proceed in a square "spiral" pattern increasing at 10 m intervals away from the Site AtBk6 start point until a sufficiently flat bare-rock spot at least 5 m in diameter was located. The drill pipe and camera were raised and lowered by up to several meters as required by the seafloor morphology.

No suitable site was found at Site AtBk6 or during the initial 50 m × 50 m survey (Figure **F9**); rather than the bare-rock pavement photographed at Site JR31-BR8, we observed white sediment plus scattered dark (gabbro) blocks on a near-flat surface deepening slightly to the northwest (Figures **F9**, **F10A–F10B**). The reason for the disparity with what was previously observed at apparently the exact same location is not known but probably indicates some absolute offset of some tens of meters in the navigation of the JR31 transponder survey.

The initial 50 m × 50 m survey spiral revealed a dense boulder field and possible outcrop at the southwestern corner of the box; accordingly, the survey was extended south and southwest by a further 50 m. Within this area, an irregular steep-sided outcrop of dark gabbro was identified, north-northwest elongated, ~30 m wide by >60 m long, and rising abruptly by as much as ~10 m above the surrounding carbonate sediment-covered seafloor. The top of this outcrop was flat and formed either of bare gabbro exposures or else was covered by a thin cap of indurated carbonate. After further investigation of this flat bare-rock pavement following a total of 5.5 h of survey, a suitable location for Hole U1473A was found (Figure **F10E**) at 32°42.3622′S, 057°16.6880′E (710.2 mbsl), 40 m south of the original start point.

Principal results

Site U1473

Hole U1473A is located at 32°42.3622′S 57°16.6880′E, in 710.2 m water depth on the north central part of Atlantis Bank, 2.2 km north-northeast of Hole 735B and 1.4 km north of Hole 1105A. During Expedition 360, Hole U1473A was drilled to a total depth of 789.7 mbsf, recovering 469.4 m of core with an average of 59% recovery over the entire interval (>96% over the lower 200 m of the hole). This constitutes the deepest igneous rock penetration from the seafloor during a single R/V *JOIDES Resolution* expedition to date.

Igneous petrology

Hole U1473A cores are composed of a variety of gabbroic lithologies, from primitive olivine gabbros to evolved oxide-rich gabbros, cut by felsic veins (~1.5% of the total) and rare diabase dikes. Eight lithologic units were defined within the gabbroic sequence, primarily on the basis of changes in mineral modes, grain size, and texture but also based on the presence and relative importance of other igneous features such as igneous layering and felsic material (Figure **F11**). Magnetic susceptibility and bulk-rock geochemical variations were also considered when defining these units.

Primary magmatic textures of gabbros to ~400 mbsf are mostly erased by intense crystal-plastic deformation; when preserved, primary textures are mostly subophitic and locally granular. The main lithology is olivine gabbro (76.5%), followed in abundance by disseminated-oxide gabbro (9.5%; oxide content between 1% and 2%), gabbro (sensu stricto; 5.1%), oxide gabbro (3.7%; oxide content >5%), oxide-bearing gabbro (3.7%; oxide content between 2% and 5%), and felsic veins (1.5%). Oxide abundance decreases slightly downhole, with the exception of the lowermost intervals (deeper than ~650 mbsf) within which a larger proportion of oxide-bearing lithologies was recovered. Oxide-bearing gabbro and oxide gabbro are usually characterized by strong localized crystal-plastic deformation; however, in contrast, those in the deepest part of Hole U1473A (Unit VIII) are essentially undeformed. Formation of oxide gabbro is most likely related to the percolation of late-stage melts through an existing olivine gabbro framework, an inference that is supported by the near-ubiquitous presence of interstitial brown amphibole and rims around clinopyroxene and/or olivine. When located around olivine, brown amphibole is also associated with orthopyroxene rims. These late-stage melt-related features are less abundant in fresh and undeformed samples from the deeper levels of the hole. The felsic veins consist of leucodiorite, quartz diorite, diorite, trondhjemite, and rare tonalite, locally containing oxide minerals. They tend to be concentrated in specific zones or horizons, with trondhjemite predominating deeper than 500 mbsf.

Several diabase dikes were found at various depths in Hole U1473A. They intrude gabbros that had experienced previous crystal-plastic deformation under conditions ranging from amphibolite up to granulite facies. Most of the dikes have diabasic textures; however, the larger granulite facies dikes have local assemblages of granoblastic brown amphibole, plagioclase, clinopyroxene, and orthopyroxene near their contacts with the gabbro, reflecting recrystallization likely at 800°C or higher. Likely associated centimeter-scale dikelets may consist entirely of the granulite assemblage. From textural relationships, some dikes appear to have locally partially melted the adjacent gabbro to form the felsic veins.

Igneous layering, defined by modal and grain size variation, is well developed in Units II and VII (91–175 and 578–642 mbsf, respectively). Grain size variability in the layering is generally also accompanied by modal variation. In most cases, contacts between different layers are subparallel to each other, though less commonly irregular contacts are also found. The dominant olivine gabbro is largely coarse grained but locally displays considerable variability, ranging from fine to very coarse grained. Grain size variations in olivine gabbro may be locally associated with igneous layering but are mainly found within irregular olivine gabbro domains with sutured contacts.

In several respects Hole U1473A displays similarities to the other two holes drilled at Atlantis Bank (Holes 735B and 1105A; Dick et al., 2000; Casey et al., 2007) (Figure **F12**). Similar igneous processes operated in the genesis of the plutonic section as a whole. Most striking is the first-order observation that the plutonic sections in Holes 735B and U1473A are mainly composed of olivine gabbro (>75%) with numerous intercalations of gabbros containing oxides (~15% of the sections). The level and volume of oxide and disseminated-oxide gabbros vary considerably between the Atlantis Bank drill sites. It is probable that more of the section was removed by erosion at Site U1473 compared to Site 735, making direct cor-

relation of the sections relative to the detachment fault surface difficult. Intensely deformed and/or oxide-rich intervals are abundant in the upper portion of Hole 735B and decrease rapidly deeper than 600 mbsf, are abundant in 158 m deep Hole 1105A, and although present in Hole U1473A, occur intermittently downhole with a larger abundance of likely related disseminated-oxide gabbro.

Felsic rocks are also found ubiquitously across Atlantis Bank (e.g., Baines et al., 2008) and at all three drill sites. These rocks are represented by veins or patches that are reported to be associated with oxide gabbros in Hole 735B (Dick et al., 2000) and with olivine gabbro in Hole 1105A (Casey et al., 2007) but are found cutting both rock types in Hole U1473A. Locally, some dike margins are invaded by felsic melts that were most likely generated by hydrous contact metamorphism of the previously hydrothermally altered host gabbro. Other felsic veins may be the product of extreme fractionation of the gabbroic melts or even local anatexis of gabbros due to subsequent gabbro intrusive cycles (e.g., Koepke et al., 2004). Troctolite and troctolitic gabbro found in Hole 735B and, in the first case, interpreted as representing injection of primitive melts into the crystallizing olivine gabbros, were not encountered in Hole U1473A.

Another common feature of the three holes drilled at Atlantis Bank is the occurrence of 100–400 m thick igneous lithologic units defined by variations in texture, grain size, mode, and geochemical composition. These units are mirrored by variations in whole-rock geochemical compositions, which reveal apparent upward-differentiating geochemical trends, as defined by decreases in Mg#, Cr, and Ni contents and increases in Y (Figure **F13**) (see **Geochemistry** below). Each of the lithologic units is in turn characterized by internal heterogeneity in composition and texture on a meter scale, also documented in the other gabbroic sections sampled at Atlantis Bank. This heterogeneity was likely governed by complex interplay between magmatic processes (new melt injections, fractional crystallization, melt-rock reaction, and late-stage melt migration) and deformation.

Taken as a whole, the igneous stratigraphies of Holes 735B, 1105A, and U1473A document directly comparable processes occurring in all three locations over a lateral scale of >2 km and vertical scale of ≥1.5 km. This leads us to suggest that this portion of the Atlantis Bank plutonic section is relatively homogeneous laterally. Key features are (i) the occurrence of olivine gabbro as the principal lithology; (ii) the ubiquitous presence of disseminated-oxide, oxide-bearing, and oxide gabbros and their greater abundance at the shallower structural levels; and (iii) the presence of ~100–400 m thick olivine gabbro units showing upward-differentiating geochemical trends that may represent discrete magma bodies. Whereas the different drill holes display striking similarities between each other overall, we do not attempt to correlate igneous units directly from hole to hole; instead, we prefer to emphasize the similarity in overall igneous accretion processes.

How applicable are the conclusions we draw from drilling at Atlantis Bank to other oceanic core complex gabbro massifs or, indeed, plutonic accretion processes at (slow-spreading) mid-ocean ridges in general? In partial answer to this question, we may compare the igneous architecture documented at Atlantis Bank with that of the gabbro body drilled at Atlantis Massif, the oceanic core complex at 30°N on the Mid-Atlantic Ridge (Hole U1309D; Blackman et al., 2011; Expedition 304/305 Scientists, 2006). The most striking difference is related to the lithologic variability of the two sections. In particular, Atlantis Bank is dominated either by olivine gabbro or oxide-bearing gabbro (only), whereas Atlantis Massif contains a much broader range of lithologies, with a dominant lithology of gabbro (sensu stricto; Figure **F12**) rather than olivine gabbro and lesser amounts of olivine gabbro and oxide gabbros. An even more significant difference is the abundance of troctolite and the presence of relict mantle peridotite horizons in Hole U1309D. Particularly significant are olivine-rich troctolites formed by reaction of mantle peridotite with basalt melt (e.g., Drouin et al., 2009), as well as minor dunite between the gabbro bodies, which were not found at Atlantis Bank. These major differences in igneous stratigraphy at Atlantis Bank and Atlantis Massif demonstrate that significant variability exists in the mode of accretion and internal differentiation of magmatic bodies in the lower crust between oceanic core complexes, likely reflecting variations in magma supply and accompanying tectonic setting, spreading rate, and thermal regime along ocean ridges.

Geochemistry

The Hole U1473A lithologies are dominated by moderately evolved olivine gabbro with Mg# between 82 and 66. Mg# co-varies with other petrogenetic indicators such as Ca#, Ti, Y, Cr, and Ni. The variations in Cr and Ni concentrations cannot be explained by modal mineralogy but are attributed to the composition of pyroxene and olivine in the rock.

Downhole variation plots show major discontinuities in Mg#, Cr, Ni, and Ca# at ~60–90, 300, and ~700 mbsf (Figure **F13**). The discontinuities are interpreted as defining upwardly evolving units of magma intruded in individual intrusive events. The discontinuities are remarkably similar to those seen in Hole 735B (Figure **F6**) (Dick et al., 2000) and are interpreted as defining upwardly evolving units of magma intruded in individual events. However, oxide gabbros occur in centimeter-scale intervals throughout the section and are significantly more evolved than the background olivine gabbro, providing evidence for the migration of late-stage melts over minimum distances of tens to hundreds of meters.

The average composition calculated for Hole U1473A is very similar to that of Hole 735B, with Mg# of 71 ± 3 and TiO_2 of 0.7 ± 0.2 wt%. The average composition of the Atlantis Bank gabbros is slightly more evolved than that of Atlantis Massif (Hole U1309D; Godard et al., 2009), although their standard deviations overlap. They are both, however, substantially more fractionated than the bulk lower crust average calculated for Hess Deep (fast-spread lower crust) by Gillis et al. (2014), although we note that the Hess Deep calculation is based on extrapolation from relatively short drilled sections and thus is only an approximation of the composition of the East Pacific Rise lower crust.

Hole U1473A gabbros have H_2O contents of 0.2–8 wt% (mean = 1.0 ± 0.9 wt%, median = 0.8 wt%), much higher than expected in pristine cumulates. Even petrographically fresh samples (thin section alteration intensity 0–2) have mean H_2O contents of 0.8 ± 0.6 wt% (median = 0.7 wt%). The abundance of H_2O decreases with depth and is therefore likely to be controlled mostly by deep and near-pervasive infiltration of seawater through the crustal section. Examination of altered and fresh sample pairs indicates that the alteration did not significantly alter major element compositions or the trace element concentrations investigated. This is consistent with the infiltration of low-salinity seawater-derived fluids with limited potential for mobilizing other elements.

CO_2 is below detection limit in many of the samples investigated, but concentrations of up to 2 wt% were obtained for altered rocks in the carbonate-veining zone (~210–580 mbsf). A surprise was that four of the carbonate-rich samples investigated are dominated by up to 0.5 wt% of inorganic carbon rather than CO_2. These

high concentrations are similar to the range reported for clay-rich alteration of glass on the seafloor and may be related to clay alteration in the gabbros. The amount of organic carbon present is a factor of 10 higher than determined for the majority of serpentinites investigated previously. This is an intriguing result and may require that low-temperature alteration minerals of gabbro be added to the list of potential microbial habitats in the subseafloor.

Metamorphic petrology

Hole U1473A gabbros show three distinct modes of alteration: (1) static hydrothermal alteration, (2) alteration associated with crystal-plastic deformation, and (3) alteration associated with cataclastic deformation.

Static background alteration is pervasive, with alteration mineral abundance estimated from macroscopic description ranging from <3% to 90% (Figure **F14**). Although alteration mineral abundance may locally exceed 60% in intervals of intense veining or faulting (4% of Hole U1473A cores), in 78% of cores background alteration mineral abundance is <30%. This is very similar to the figure for Hole 1105A (83% of cores contain <30% background alteration). Static alteration minerals consist mainly of (i) colorless amphibole, talc, serpentine, and clay minerals after olivine; (ii) secondary clinopyroxene and brown to green or colorless amphibole after clinopyroxene; (iii) colorless amphibole and talc after orthopyroxene; and (iv) secondary plagioclase and chlorite after primary plagioclase. These minerals occur in different abundances in each core or hand specimen and indicate variable temperature conditions for alteration. Textural relationships document overprinting of lower temperature over higher temperature assemblages during the gabbroic sequence cooling. The formation of the secondary clinopyroxene and brown amphibole association most likely took place at near-solidus temperatures (>800°C). Brownish green and green amphibole and tremolite/actinolite + chlorite ± talc assemblages formed at amphibolite to greenschist facies metamorphic conditions (700°–400°C). The assemblage of secondary plagioclase + chlorite + pale-green amphibole (actinolite) with minor amounts of zoisite and titanite indicates greenschist facies conditions (450°–350°C). Serpentinization of olivine most likely took place at temperatures in the range 350°–200°C (i.e., lower than greenschist facies alteration but higher than that of clay mineral formation). Clay minerals are the latest products of alteration at lowest temperatures (<150°C). Downhole trends in background alteration correlate with the distribution of metamorphic veins outlined below.

Amphibole veins and amphiboles replacing primary mafic minerals are dominant at shallower levels (<240 mbsf), as they are in Hole 735B, whereas carbonate or carbonate-clay veins are conspicuous at 180–580 mbsf (Figure **F14**). Oxidative reddish clay-mineral replacement of primary minerals is also significant from the seafloor to 580 mbsf. In these intervals, it is common that millimeter-wide veins have alteration halos that are up to centimeters wide. At deeper levels (>580 mbsf), microveins filled with chlorite ± amphibole are more abundant than the millimeter-wide veins.

Felsic veins are typically more altered than host gabbros. The most apparent feature is the replacement of primary plagioclase, and sometimes quartz, by secondary plagioclase, which has a characteristic whitish milky appearance and often has fluid inclusions. Together with association of a relatively high abundance of secondary sulfide and patches of clay minerals in these veins, this implies that the felsic veins were pathways for large volumes of hydrothermal fluids, as also found in Hole 735B (Dick et al., 1991a), particularly at lower temperatures (subgreenschist facies). Local occurrence of biotite in host gabbros is evidence for metasomatic alteration related to felsic vein intrusion.

Neoblasts formed by crystal-plastic deformation typically consist of olivine, plagioclase, and clinopyroxene with minor brown amphibole and Fe-Ti oxide minerals. This mineral assemblage indicates near-solidus temperature conditions (>800°C). Amphibolite mylonites composed of brown-green hornblende and plagioclase, typically associated with minor Fe-Ti oxides, locally develop in thin discordant mylonitic bands. Amphibolite facies mineral assemblages also occur in the halos associated with amphibole veins. Amphibolite mylonites and amphibole-vein halos show cooling of the gabbroic sequence to temperature conditions pertaining to the transition from ductile to brittle regime (~700°C).

Intervals recording intense cataclastic deformation have abundant carbonate and brownish clay mineral(s). Clays and carbonates show textural relationships indicative of their simultaneous formation, and some of the carbonates show a signature of plastic deformation. These observations show that cataclastic deformation took place in association with alteration at low temperatures (<150°C).

Structural geology

The internal structure of the Hole U1473A cores reflects a complex interplay of magmatic and tectonic processes that span a broad range of temperatures, from contemporaneous magmatic intrusion and high-temperature crystal-plastic deformation down to late low-temperature brittle faulting. As a whole, Hole U1473A samples a 600 m thick zone of intense crystal-plastic deformation cut by a later brittle high-angle fault zone with a damage zone that extends to ~570 mbsf. The variety, distribution, and intensity of the preserved structures are consistent with synkinematic exhumation and cooling in the Atlantis Bank oceanic core complex.

Undeformed parts of Hole U1473A cores preserve weakly developed magmatic fabrics defined by the shape-preferred orientation of plagioclase crystals and decimeter-scale igneous layering. The transition from magmatic flow to solid-state crystal-plastic deformation is marked by an increase in plagioclase recrystallization and common development of tapered twins and undulose extinction.

Crystal-plastic deformation occurs throughout Hole U1473A (Figure **F15**). In moderate to intense crystal-plastic deformation zones, the relationship of magmatic to crystal-plastic fabrics is obscured. Crystal-plastic deformation is extensively developed throughout the top 600 m of Hole U1473A. In detail, the deformation is heterogeneous with meter- to 10 meter–scale zones of dominantly porphyroclastic shear zones separated by relatively weakly deformed gabbros. Locally, deformation intensity increases and true mylonitic zones can be found at ~200–210 and ~220–230 mbsf. Rare thin ultramylonites are heterogeneously developed and commonly crosscut the porphyroclastic foliation. The dip of the crystal-plastic fabrics averages 10°–40°, although, locally, the dip can progressively increase and steepen to vertical. Folding of the fabrics is more common in the upper part of the core. Shear sense indicators are dominantly reversed, an observation confirmed by analysis of shear sense indicators in thin sections. Even in discrete intervals that display little or no macroscopically visible crystal-plastic deformation, thin sections generally reveal weak crystal-plastic overprints. The majority of these intervals reveal narrow zones of incipient plagioclase recrystallization, especially at the boundaries of pyroxene crystals, and pyroxene microfracturing.

Weak to moderate crystal-plastic fabrics commonly have a strong shape-preferred orientation defined by large elongated plagioclase and pyroxene crystals. Given the limited amount of recrystal-

lization observed it appears unlikely that ductile deformation could have caused the alignment of the larger crystals. Therefore, it is more likely that plagioclase and pyroxene were originally aligned by magmatic flow and subsequently overprinted by localized crystal-plastic deformation. Additionally, the grain size layering may have acted as a favored planar anisotropy for a subsequent crystal-plastic fabric to nucleate. In some examples, the layering has a strong crystal-plastic overprint, particularly when the layering has a moderate dip. In other examples, the layering is "necked" and truncated by ductile shear zones.

The conditions over which ductile deformation occurred in Hole U1473A range from near-solidus granulite grade to amphibolite grade (see **Metamorphic petrology**). The distribution of amphibole within mylonites is not restricted to the top of the hole and extends to at least ~670 mbsf. Several examples of multiple generations of crystal-plastic fabrics with variations in shear sense, dip magnitude, dip direction, and metamorphic grade can be observed in Hole U1473A cores. In some examples, the older mylonite has moderate dip and reversed shear sense, whereas the younger crosscutting mylonite has a subhorizontal dip and normal shear sense. In others, moderately dipping reversed-sense porphyroclastic fabrics are crosscut by subvertical normal-sense mylonites. In each case amphibole is more prevalent in the younger crosscutting fabric. The deformation mechanisms remain the same during granulite and amphibolite grade deformation and are dominated by subgrain rotation recrystallization. This variability in crosscutting relationships indicates a changing strain field through time, with the early crystal-plastic fabrics primarily preserving granulite conditions, whereas the younger fabrics reflect amphibolite facies conditions. That the differences in metamorphic facies may be associated with differences in shear zone orientation and shear sense does not accord with the prediction of simple extension at the ridge axis and suggests that the lower oceanic crust deformation path is complex and protracted.

Evidence exists for contemporaneous brittle and crystal-plastic deformation. Fractures in clinopyroxene in Hole U1473A gabbros are filled with plagioclase crystals, whereas magmatic ilmenite locally fills cracks in both plagioclase and pyroxene porphyroclasts, indicating that melt was present while fracturing occurred. This can reasonably be anticipated where the crystal/melt ratio is high, as a load-bearing framework can form that can accommodate strain by brittle deformation (Handy et al., 2007). In other examples, plagioclase porphyroclasts have fractures filled with fine-grained recrystallized plagioclase indicating that plagioclase was capable of deforming contemporaneously by brittle (i.e., fracturing) and ductile (i.e., recrystallization) deformation mechanisms. These features have been described in granitoids (e.g., Blumenfeld and Bouchez, 1988) and are interpreted as the transition from magmatic to crystal-plastic conditions, during which submagmatic to crystal-plastic foliations may develop.

Amphibole veins, both brown (hornblende) and pale green (actinolite) amphibole, exhibit a wide variety of crosscutting relationships with crystal-plastic fabrics. Amphibole veins commonly cut the crystal-plastic foliation at high angle and may transpose (bend) an older crystal-plastic fabric, indicating that vein formation occurred at moderate to high temperatures. In other cases, older crystal-plastic fabrics may be simply offset across an amphibole vein, suggesting relatively lower temperature deformation. The relationship between crystal-plastic fabrics and veins is complex (Figures **F15**, **F16**). Crystal-plastic fabrics are overprinted and offset by brittle fractures and local faults with dominantly normal shear sense; however, reversed shear sense is also observed in brittle structures. In most cases, the fractures and faults within plagioclase and pyroxene are filled with amphibole. These microstructural relationships suggest that the brittle-ductile overprint occurred at lower temperatures, mainly ranging from amphibolite to greenschist facies conditions. Some of the shear zones contain Fe-Ti oxides, which are significantly weaker compared to silicate phases (e.g., Till and Moskowitz, 2013). We suggest that discrete parts of the shear zone were still deforming by ductile deformation mechanisms, whereas other zones were deforming by fracturing. The resulting microstructures are characterized by coeval ductile and brittle deformation mechanisms that were activated by variations in the thermal gradient, composition, and grain size.

Fe-Ti oxide-rich domains are heterogeneously distributed throughout Hole U1473A, as demonstrated by the distribution of magnetic susceptibility, which is an approximation for the proportion of Fe-Ti oxide minerals (see **Petrophysics**). The relationship between deformation and the presence of Fe-Ti oxides can be cryptic, with examples of Fe-Ti oxides occurring in both deformed and undeformed samples. There are 26 ultramylonites within Hole U1473A to 789 mbsf, 18 of which correlate with a peak in magnetic susceptibility. Most susceptibility peaks that do not correlate with the presence of an ultramylonite instead correlate with the presence of a mylonite; however, the two largest contiguous zones of deformation, the 10 m thick mylonites from 201 to 210 mbsf and from 219 to 228 mbsf, do not correlate with peaks in magnetic susceptibility and are Fe-Ti oxide poor.

No clear evidence has been found from the cores for crystal-plastic deformation having predated or been contemporaneous with intrusion of the individual geochemically defined coarse olivine gabbro units. However, the felsic veins appear to have been synkinematic: some of the late-magmatic felsic veins were deformed along with the gabbros, whereas others, themselves undeformed, clearly crosscut plastically deformed gabbro. The dikes that cut the Hole U1473A section were intruded under a range of conditions likely ranging from upper amphibolite to subgreenschist facies conditions; although none exhibited crystal-plastic deformation, the enclosing gabbros generally do. Taken together with the clear relationship between late evolved oxide gabbros and discrete shear zones, it may be concluded that deformation commenced almost immediately after crystallization of the main gabbro body or bodies, whereas late-stage interstitial melts were still present. Continuing deformation led to the exhumation and cooling during extension along a detachment shear zone that formed the oceanic core complex.

Seven discrete fault systems were identified in Hole U1473A based on the presence of fault rocks and fractured intervals (Figure **F17**). They range from discrete 5 cm thick cataclasites at the top of the hole to a major fault zone at 411–469 mbsf. An eighth discrete fault may exist at ~570 mbsf; otherwise, no faulted intervals were encountered at greater depths. In each case, the faulted and fractured zones correspond to intervals of borehole enlargement, reduced core recovery, increased penetration rates, and in some instances to drilling difficulties (see **Operations**). The 50 m thick fault zone at 411–469 mbsf consists of chlorite-rich and carbonate-rich breccias and correlates with an increase in carbonate veining. Taken in conjunction with evidence for a negative temperature anomaly in downhole logs from this depth (see **Petrophysics**), it appears that the fault zone controls an active hydrologic system. Carbonate veining is positively correlated with fault rock intensity in most of the faulted intervals above and below the 411–469 mbsf

fault zone (Figure **F16**). The downhole frequency of carbonate veins increases toward the major fault zone and then decreases below it, correlating with the damage zone of the fault as defined by the fracture density of the rocks (Figure **F17**). The background alteration and olivine alteration increases with the degree of carbonate veining, suggesting that low-temperature olivine alteration is enhanced in the vicinity of carbonate veins. This is supported by macroscopic core observations displaying the pronounced red-stained (oxidative) alteration of olivine in the vicinity of the carbonates (see **Metamorphic petrology**). These smaller fault zones may too be the focus of active fluid flow.

The following are the main structural conclusions from IODP Hole U1473A:

- Multiple generations of felsic veins, most with a crystal-plastic overprint, provide evidence for a protracted history of melt generation and deformation.
- Hypersolidus magmatic fabrics and grain size layering provide anisotropies that preferentially cause the nucleation of crystal-plastic fabrics.
- A 600 m thick zone of intense crystal-plastic shearing is present within Hole U1473A (Figure **F15**). It represents high-temperature deformation related to the detachment fault zone; however, it does not correlate directly with the deformed interval at the top of Hole 735B.
- Multiple generations of crystal-plastic fabrics with different orientations, shear sense, and metamorphic grade attest to a protracted history of ductile deformation.
- Shear sense is predominantly normal in the upper 50 m of Hole U1473A but tends to be reversed at greater depths. This same observation is made in Hole 735B but with the transition at ~450 mbsf.
- A strong correlation exists between the presence of Fe-Ti oxides and that of mylonite, ultramylonite, and magmatic contacts; however, the modal abundance of Fe-Ti oxide does not seem to correlate with deformation, and weaker crystal-plastic fabrics tend not to correlate with the presence or absence of Fe-Ti oxide.
- The transition from crystal-plastic to brittle deformation is associated with granulite to amphibolite and, in some cases, greenschist facies alteration by way of ductile, semibrittle, and brittle deformation mechanisms. The degree of greenschist grade deformation is, however, much less in Hole U1473A than in previously reported sample suites from the surface of Atlantis Bank (e.g., Miranda and John, 2010).
- Amphibole veins are concentrated in the upper 400 m of Hole U1473A (Figure **F16**) and either deflect or offset older crystal-plastic fabrics at a high angle. Brittle overprint of high-temperature crystal-plastic fabrics is relatively limited and restricted to the upper ~300 m of the hole.

A 50 m thick high-angle fault zone, defined by several fault breccias, abundance in carbonate veins, enlargement in borehole size, and reduction of in situ borehole resistivity, occurs from 411 to 469 mbsf. A temperature anomaly associated with this zone suggests the fault is hydrologically active. Six other smaller fault zones are identified at shallower levels within Hole U1473A (Figure **F17**). All corresponded to lowered core recoveries, increased penetration rates, and, in some cases, problematic drilling conditions.

Paleomagnetism

Remanence measurements were made on archive section halves from Hole U1473A. This generated demagnetization data at more than 12,000 measuring points downhole. Virtually all intervals have positive inclinations indicating that the sampled gabbroic rocks hold a reversed polarity magnetization, consistent with the interpretation of marine magnetic anomalies (Allerton and Tivey, 2001) that places Hole U1473A within geomagnetic polarity Chron C5r.3r (Gradstein et al., 2012). Moreover, the sampled gabbros carry sufficiently strong magnetizations to account for the observed magnetic anomalies over Atlantis Bank.

The archive section-half data were subject to principal component analysis (PCA) using a processing and filtering scheme designed to rapidly identify the highest quality highest coercivity components for subsequent tectonic interpretation. The resulting principal component data allow division of the hole into upper and lower zones with statistically different inclinations (Figure **F18**). Thermal demagnetization data from discrete samples subject to the same filtering for reliability support this division. The boundary between major inclination zones corresponds to the fault zone observed at 411–469 mbsf, from a mean value of ~72° shallower than 403 mbsf to a mean value of ~61° deeper than 403 mbsf. A narrow zone of steeper inclinations (mean = 73.3°) is also seen between 737 and 750 mbsf. Compared to the expected dipole inclination of 51.3°, these results imply a significant but variable rotation of the Atlantis Bank footwall since acquisition of magnetization, with the major change across the fault zone likely reflecting differential rotation across this structure.

Although the greater part of Hole U1473A carries reversed polarity magnetization, thermal demagnetization of discrete samples and alternating field demagnetization of archive section-half pieces reveals characteristic remanences with negative inclinations in some narrow zones of altered gabbro (around ~564, 678, and 749 mbsf). The presence of these zones within broader intervals of reversed polarity indicates (near-) complete remagnetization of these rocks during a subsequent normal polarity period. The timing of the alteration cannot be uniquely determined from these data, but the presence of these components in the lower part of the hole suggests that the reversal boundary between reversed geomagnetic polarity Chron C5r.3r and normal polarity Chron C5r.2n may occur in close proximity to the current bottom of Hole U1473A.

Petrophysics

Core sections were measured in data loggers for magnetic susceptibility, gamma ray attenuation (GRA) density, and natural gamma radiation (NGR). Magnetic susceptibility was measured on both whole-round sections and archive halves, using a pass-through sensor coil and a contact probe, respectively. The measured magnetic susceptibility varies over the whole instrument range (10,000 instrument units; i.e., ~0.1 SI); high magnetic susceptibility values (>1000 instrument units) are ubiquitously related to abundant magnetite in gabbroic lithologies. The dominant olivine gabbro lithology has relatively low susceptibility that does not exceed a few hundred instrument units. At the centimeter to decimeter scale, high values of magnetic susceptibility indicate oxide-rich intervals, seams, and patches.

NGR from the gabbro cores is consistently very low (≤1 count/s). Several isolated peaks up to ~10 counts/s were observed in the vicinity of felsic veins. In the lower part of the hole (deeper

than ~575 mbsf), these narrow peaks often correlate with the highest magnetic susceptibility signals, indicating the presence of magnetite in the felsic veins.

GRA density estimates range from 2.1 to 3.2 g/cm^3 and average ~2.65 g/cm^3. Estimates are slightly less variable in the bottom of the hole (below the major fault zone at ~411–462 mbsf) than in shallower sections, with an average value of about 2.67 g/cm^3.

Density and porosity were determined for 186 samples. Grain density ranges from 2.88 to 3.13 g/cm^3 and averages 2.98 g/cm^3. It does not vary significantly downhole, except for a slightly higher variability above the major fault zone at ~411–469 mbsf. Porosity is generally very low; it ranges from 0.1% to 4.2% and averages 0.6%.

Compressional seismic velocity was measured at room pressure and temperature along three mutually perpendicular directions on 2 cm × 2 cm × 2 cm cubic samples. A total of 184 gabbroic samples from Hole U1473A were measured, 94% of which were olivine gabbro. V_P ranges from 5930 to 7150 m/s, with an average of 6734 m/s and an average standard deviation of 25 m/s. Above the major fault zone at ~411–469 mbsf, V_P shows a modest increasing trend over the interval ~280 to ~400 mbsf, from ~6700 to ~7100 m/s. This progressive increase does not continue deeper in the hole; below the major fault zone, V_P is lower on average (6646 m/s) than in the upper part of the hole (6795 m/s), with a similar range of local-scale variability. Local trends of decreasing V_P over a few tens of meters match trends of increasing porosity and correspond to more fractured intervals and fault zones. The measured apparent anisotropy of V_P is generally low, ranging from 0.1% to 10.9% and averaging 2.2%; the slowest average V_P of the three measured directions is parallel to the core axis (~6708 m/s).

Thermal conductivity was measured on 86 samples from archive halves. It ranges from 1.77 to 2.52 W/(m·K) and averages 2.28 W/(m·K). The standard deviation of the measurements is <2% (0.66% on average). Olivine gabbro conductivities are in the same range as those measured during previous oceanic crust drilling expeditions. Deeper than ~450 mbsf, the average thermal conductivity is slightly higher (2.36 W/[m·K]) than in the upper part (2.21 W/[m·K]). This may partly reflect the general change in background alteration at the bottom of the hole; deeper than 570 mbsf, the olivine is less altered and secondary clays are absent (Figure **F14**).

Downhole logs were successfully acquired at the end of drilling operations using three tool strings: a modified "triple combo" (NGR spectroscopy, bulk density, bulk resistivity, and magnetic susceptibility), a Formation MicroScanner (FMS)-sonic string (seismic velocity and electrical resistivity imaging), and an ultrasonic string (acoustic imaging). Each tool string also measured total NGR and borehole temperature. The borehole diameter measured by the triple combo tool string shows significant variations in the upper part of the hole to ~570 mbsf and a much more regular and clean shape deeper, where core recovery averaged 96%. Intervals where the hole diameter is very variable and/or out of gauge correspond to low recovery and/or faulted material identified in the core. The presence of fault zones at ~411–469 mbsf is indicated by low electrical resistivity and low bulk density. A negative temperature excursion recorded by the temperature tool on each run also places the base of a major fault that introduces colder fluid into the borehole at ~469 mbsf.

In the bottom part of the hole (deeper than ~570 mbsf), V_P averages about 6840 m/s, significantly higher than shallower than 570 mbsf, where it is generally about 6300–6400 m/s away from fault zones.

Microbiology

Microbiology sampling during Expedition 360 focused on exploring evidence for life in the lower crust and hydrated mantle using culture-based and culture-independent approaches, microscopy, and enzyme assays. Sampling efforts focused on cores with evidence of alteration or fracturing within all lithologies encountered. In total, 68 whole-round samples (4–22 cm long) were collected for microbiological analysis. Adenosine triphosphate (ATP) was quantified from all samples and ranged from below detection to 5 pg/cm^3 (mostly <1 pg/cm^3), indicating the presence of a subsurface biosphere in Atlantis Bank. Samples collected for postcruise research include fixed samples for cell counts to quantify microbial biomass and frozen samples for DNA, RNA, and lipid extraction to describe the diversity (DNA and lipids) and activity (RNA) of the microbial community. A total of 38 samples were inoculated into as many as 10 different kinds of microbial media targeting specific prokaryotic iron-reducing microbes, sulfate-reducing bacteria, sulfur-oxidizing microbes, archaeal methanogens, and eukaryotic fungi. These will be analyzed during postcruise research. In addition, for 12 samples we established nutrient addition experiments testing nutritional constraints on microbial biomass in this environment. Enzyme activity assays were conducted using substrates for alkaline phosphatase, leucine aminopeptidase, and arginine aminopeptidase at 15 sample depths in Hole U1473A. These experiments are ongoing, but initial analysis indicates the presence of very low alkaline phosphatase activity, whereas enzyme activity for both peptidase substrates was below detection.

Finally, a new microbial contamination tracer, perfluoromethyl decaline (PFMD), was used for contamination testing for the first time. PFMD was run during coring operations for 10 samples and was routinely detected in the drilling fluids, usually on the outside of uncleaned cores, and rarely above detection on the outside of cleaned cores. It was below detection on the inside of cores, indicating that penetration of drill fluids to the interior of whole-round drill cores where we collected our samples is unlikely. We ran three runs of the commonly used tracer perfluoromethylcyclohexane (PMCH) at the end of the cruise for comparison. It was more difficult to clean the core exteriors successfully with this more volatile tracer, and PMCH was detected on occasion on core interiors.

Hole 1105A redescription

During the 11 day transit from Colombo, Sri Lanka, to Site U1473 at Atlantis Bank, the Expedition 360 science party reexamined the cores drilled during Leg 179 in Hole 1105A (Pettigrew, Casey, Miller, et al., 1999; Casey et al., 2007). This activity involved rigorously describing the cores and many of the accompanying thin sections with the primary purpose of familiarizing the science party with the material likely to be encountered at the new Site U1473, situated 1.4 km to the north. The science party developed templates for the description of the igneous, metamorphic, and structural features of the cores and thin sections to establish core description protocols for the new Site U1473 cores. An additional benefit of redescribing Hole 1105A cores is that the data generated are in a format directly comparable with those for Hole U1473A.

In general, our findings were very similar to those produced by the Leg 179 scientists; however, with a larger science party to work on the cores, some of the information collected is new. We include this information in a separate site chapter of the expedition report in the Expedition 360 *Proceedings*, as a basis for direct comparison with the results of drilling at Site U1473. In addition, we were able to

make certain physical properties measurements on Hole 1105A cores, including section-half magnetic susceptibility measurements, that had not been possible during Leg 179. It is important to note here that the observations made on the Hole 1105A cores by the Expedition 360 scientific party augment rather than replace those made by the Leg 179 scientists.

Igneous petrology

Our observations on the igneous petrology of this section are summarized below and then briefly compared with those made during Leg 179. The 30 cores recovered from Hole 1105A are composed of gabbroic rocks and related felsic veins (Pettigrew, Casey, Miller, et al., 1999; Casey et al., 2007). The gabbroic rocks are mostly coarse grained with subophitic to granular textures and are variably deformed. Subophitic textures dominate in undeformed samples. The main lithologies are oxide gabbro and olivine gabbro, followed in abundance by gabbro (sensu stricto). A significant proportion of the olivine gabbro and gabbro intervals contain small amounts of oxides and are referred to as disseminated-oxide gabbro (1%–2% oxides) and oxide-bearing gabbro (2%–5% oxides). On the whole, gabbroic rocks with oxides >1% dominate deeper than 35 mbsf, and they tend to be more plastically deformed than other lithologies. Oxides are particularly abundant and probably crystallized from percolating evolved melts. In these deformed gabbros, oxides are not obviously affected by plastic deformation, and thus apparently crystallized after dynamic recrystallization of the silicates. Some rare undeformed oxide gabbros are also observed. Thin intrusions of fine-grained olivine gabbro occur between 60 and 75 mbsf. Numerous felsic veins occur throughout the core and are concentrated at 15–65 and 138–158 mbsf. Detailed observations of the corresponding thin sections allow us to document the evolution of late-stage melts within a crystallizing mush and to track the origin of magmatic oxide minerals where they are particularly enriched.

When compared with Hole 735B gabbros (Robinson, Von Herzen, et al., 1989; Dick, Natland, Miller, et al., 1999), Hole 1105A is more enriched in oxide-bearing varieties (disseminated-oxide gabbro, oxide-bearing gabbro, or oxide gabbro) and therefore represents a section of crust that is more evolved overall than that recovered in Hole 735B. The oxide-rich section of Hole 1105A is both thicker and more enriched in oxides than the principal oxide-rich portions of Hole 735B (Units III and IV; 170.2–274.1 mbsf). Deformation grade and alteration patterns are also different, and a downhole differentiation trend similar to that observed for Hole 735B oxide gabbro is questionable for Hole 1105A whole-rock compositions but may be more evident when considering mineral compositions (Dick, Natland, Miller, et al., 1999; Dick et al., 2002; Pettigrew, Casey, Miller, et al., 1999; Casey et al., 2007). If the Hole 1105A section is equivalent to any portion of Hole 735B, the most likely candidate would be Units III and IV (170.2–274.1 mbsf; Casey et al., 2007). Nevertheless, given the mismatch in comparisons presented above and as discussed in Casey et al. (2007), Hole 1105A may not represent a single layer connected directly with Hole 735B; rather, it may instead record the manifestation of a similar process, dominated by the percolation of evolved melts that have the potential to precipitate oxides and concentrate them in high-porosity regions located in the shallowest levels of the sections. In Hole 735B, these regions clearly correspond to units affected by crystal-plastic deformation; however, such a relationship is less evident in Hole 1105A. The shallowest section of Hole 1105A (15–40 mbsf) is composed of material that is less evolved (olivine gabbro) and less deformed than in the deeper sections and is similar to several units recovered lower in Hole 735B. In Hole 735B, most felsic veins are associated with oxide gabbro (e.g., Natland et al., 1991), a relationship that is not observed in Hole 1105A.

When compared with results of Leg 179 (Pettigrew, Casey, Miller, et al., 1999), we have defined fewer intervals: 108 during Expedition 360 versus 141 during Leg 179. Their modal content estimates are on average also quite different from ours, resulting in different proportions of rock types (olivine gabbro was 39% during Expedition 360 versus 43% during Leg 179, gabbro was 21% versus 36%, respectively, and oxide gabbro was 41% versus 21%, respectively). Our values as presented above have been adjusted to match Leg 179 descriptions, since during Leg 179 disseminated-oxide gabbro (defined as having oxide content from 1% to 2%) and oxide-bearing gabbros (oxide content from 2% to 5%) were included within the gabbros.

The units defined for Hole 1105A during Leg 179 and Expedition 360 are relatively similar to each other. Four units were defined both during Leg 179 (two subunits in Unit II) and during Expedition 360. The transition between Units I and II are relatively close (<10 m difference), the transition between Units IIA and IIB of Leg 179 and between corresponding Units II and III of Expedition 360 also differ by <10 m, and the transition between Units IIB and III of Leg 179 is 4 m deeper than the transition between Units III and IV of Expedition 360. Leg 179 scientists also defined a Unit IV in the deepest part of Hole 1105A, but this distinction was not made during Expedition 360.

Metamorphic petrology

Most gabbros in Hole 1105A (83%) have <30 vol% of secondary minerals formed by static alteration; intervals of extensive static alteration (≥60 vol%) are rare (<3% of the total). The intensity of static alteration shows no trend with depth in the hole. Olivine and plagioclase are generally the most and the least altered phases, respectively. Plagioclase is substantially altered only where the host rock shows intense veining or cataclasis. Felsic veins tend to be substantially more altered than their host gabbros.

High-temperature alteration is largely associated with crystal-plastic deformation. The neoblastic minerals (plagioclase, olivine, and clinopyroxene, the latter locally associated with minor brown amphibole) document crystal-plastic deformation under granulite to upper amphibolite facies conditions. The high-temperature alteration is also locally manifested by static replacement of magmatic clinopyroxene by secondary clinopyroxene and minor brown hornblende.

Subsequent phases of metamorphism are recorded in veins and by static alteration minerals. Veins filled with brownish green hornblende forming up to 1 mm long crystals are presumed to have formed under amphibolite facies conditions. Other veins are characterized by pale-green actinolitic amphibole needles associated with chlorite. These veins likely developed under greenschist facies conditions.

The moderate-temperature static alteration minerals vary in conjunction with the primary mineral. In particular, variable replacement modes were observed for olivine. Olivine is commonly altered to talc and minor oxide aggregates, frequently with an outer rim of chlorite where it is in contact with plagioclase. A less frequent mode of olivine alteration is represented by local aggregates of chlorite and pale-green amphibole in coronae along plagioclase contacts. Clinopyroxene is altered along rims, cleavage surfaces, and microveins into green to pale-green amphibole. Plagioclase hydrothermal alteration is mostly confined to development of chlorite

along the contacts with primary mafic minerals and within microveins, in many instances in association with minor secondary plagioclase.

Abundant veins filled with clay minerals record hydrothermal alteration under oxidative subgreenschist facies conditions. Veins of this type are conspicuous in a few intervals in association with significant cataclastic deformation. In these intervals, olivine and pyroxene are mainly replaced by reddish brown clay minerals or by mixtures of clay and iron oxyhydroxides. Similar clay and carbonate veins and brownish clay pseudomorphs after olivine and pyroxene occur in host gabbros near the cataclastic zones. Low-temperature carbonate veins are also present toward the bottom of Hole 1105A.

Structural geology

The distribution and intensity of structures in Hole 1105A—magmatic contacts, veins, and fabrics; crystal-plastic fabrics; alteration veins; cataclastic material and fractures—represent a continuous record of deformation from ductile to brittle. The proportion and overall intensity of gabbroic rocks displaying crystal-plastic fabrics increases downhole, from decimeter-thick discrete mylonites in the top 80 mbsf to meter-thick gneissic porphyroclastic shear zones deeper than 80 mbsf. Intervals of mylonite and ultramylonite, which may overprint earlier magmatic fabrics, are characterized by elongated bands of plagioclase intercalated with bands of pyroxene and are commonly Fe-Ti oxide rich. Crystal-plastic fabrics are shallowly to moderately inclined and commonly display reversed shear sense, although normal shear sense does occur. Fe-Ti oxides are abundant in many samples, ranging from deformed to undeformed, and concentrate near magmatic contacts. Eighty percent of magnetic susceptibility peaks correlate with intervals that contain some evidence for crystal-plastic deformation.

Magmatic fabrics (shape-preferred primary orientations of elongate crystals) are commonly overprinted and obscured by subsequent, near-penetrative crystal-plastic fabrics. Where magmatic fabrics do occur, they are weakly developed. Typically, they are inclined and better developed in finer grained rocks and near magmatic contacts. Magmatic contacts range from intrusive to gradational and sheared, with the majority of contacts being gradational, defined by grain size or modal variations. Magmatic veins are common throughout the top and bottom of Hole 1105A (15–65 and 138–158 mbsf) and are absent from the middle part of the section (65–138 mbsf). Most of the magmatic veins crosscut a previous crystal-plastic fabric and are not themselves plastically deformed; however, in a few instances leucocratic gabbroic veins are observed that have a mylonitic overprint. In some cases, deformation is confined to the vein, whereas the host gabbro is apparently undeformed. These intrusive relationships indicate at least two generations of melt input and deformation. The distribution of magmatic vein dips is bimodal, similar to that seen in Hole 735B.

Five fractured zones are identified in Hole 1105A, two of which are fault zones. These fault zones (at 112 and 127 mbsf) are each ~5 m thick fractured intervals surrounding a core of fault breccia. Discrete fractures are generally planar, some with slickensides. The slickenlines have a steep to moderate rake, indicating oblique to dip-slip. The dip magnitude distribution is not random.

Alteration veins vary in orientation as well as mineralogy: amphibole veins tend to be moderately to steeply inclined, whereas carbonate and clay veins are generally subhorizontal. Amphibole veins are most common at 40–50, 60–70, and 120–130 mbsf, intervals in which other vein fills are rare. Incomplete fill of calcite and clay veins and the correlation of these veins with zones of fracturing are indicative of low-temperature potentially recent fluid flow through the fracture systems. This is consistent with measured downhole logging temperature anomalies at 104–105 and 135–136 mbsf (Pettigrew, Casey, Miller, et al., 1999).

The relative ages, distributions, and orientations of structures, ranging from magmatic contacts to brittle faults, document a down-temperature continuum of deformation, spanning the entire history from magmatic accretion to exhumation. Perhaps the most striking observation is the absence in Hole 1105A of a coherent high-strain porphyroclastic to mylonitic shear zone at the seafloor directly comparable to that documented in Hole 735B 1.2 km to the east-northeast (Robinson, Von Herzen, et al., 1989; Dick et al., 1991a). Given the generally accepted interpretation of Atlantis Bank as an oceanic core complex, the apparent absence of detachment fault shearing at the surface of the platform might best be explained by erosion following the earlier uplift of Atlantis Bank to sea level. Erosion might also explain the absence of a significant brittle overprint at the top of the hole. Most likely, the high-temperature deformation exhibited in Hole 1105A represents a slightly deeper part of the damage zone related to the detachment shear zone below the ridge axis.

Paleomagnetism

Remanence measurements were made on archive halves from Hole 1105A. These had previously been demagnetized at a maximum field of only 20 mT during Leg 179; hence, during Expedition 360 we were able to conduct further stepwise demagnetization up to 50 mT. We thereby generated demagnetization data at >2500 measurement points downhole. These data were subject to PCA using a processing and filtering scheme designed to rapidly identify the highest quality demagnetization data for subsequent tectonic interpretation. Piece-averaged principal components have a mean inclination of 72.5° (determined from 346 archive-half pieces). This value is in good agreement with those obtained previously at Site 753B (71.1°) and from seabed rock drill samples (Allerton and Tivey, 2001). Compared to the expected dipole inclination of 51.3°, the results imply a consistent minimum rotation of the Atlantis Bank footwall of ~20° since acquisition of magnetization.

Petrophysics

New physical properties measurements on section halves and section-half pieces from Hole 1105A were acquired and integrated with the new shipboard core descriptions. Using equipment not available to Leg 179 scientists, we measured point magnetic susceptibility on archive halves and thermal conductivity on discrete samples.

The mean magnetic susceptibility of rocks recovered in Hole 1105A is 1800 instrument units (i.e., ~1800 × 10^{-5} SI). Several intervals have susceptibility much greater than the average value for Hole 1105A and correspond to intervals with a higher abundance of magnetite in oxide or oxide-bearing (olivine) gabbro.

Thermal conductivity was measured on 28 gabbro pieces taken at irregularly spaced intervals along Hole 1105A. Measured values range from 1.804 to 2.981 W/(m·K), with an average of 2.16 W/(m·K). This limited data set from the shallow portion of the section at Atlantis Bank does not show any relation between rock type or alteration and thermal conductivity.

Operations

Expedition 360 was of 61 operational days' duration (30 November 2015–30 January 2016). The expedition achieved the deepest igneous rock penetration from the seafloor on a single *JOIDES Resolution* expedition to date (789.7 mbsf) and recovered 469.4 m of core (59% recovery over the entire interval). The sequence of operational events can be grouped into eight successive episodes (Figure **F19**; Tables **T1**, **T2**).

Summary

Port call and transit to Site U1473 (30 November–16 December)

Expedition 360 spent the first 5.6 days in port in Colombo, Sri Lanka, to offload and load samples, equipment, and supplies. The 2817 nmi transit to Site U1473 took 10.9 days.

Seafloor survey and installing the reentry system (17–19 December)

We established a reentry system using a drill-in casing assembly with a mud motor and underreamer and completed it with a free-fall funnel, at a water depth of 710.2 m. Following a 1.0 day seafloor survey to select the exact drill site, the method and design used for the Site U1473 reentry system took only 1.5 days to install. The drilled depth is 9.5 mbsf, the casing shoe is at 7.4 mbsf, and the top of the cone is at 703.2 mbsl (7.0 m above the seafloor). The casing was not cemented into the hole and the reentry installation proved stable throughout the expedition.

First coring episode (19–30 December)

During this successful 10.3 day coring episode (including 0.6 days waiting on weather [WOW[) we retrieved Cores 360-U1473A-2R through 44R (9.5–410.2 mbsf) with a recovery of 207.0 m (52%), using four rotary core barrel (RCB) drilling bits. Projecting the advance per day of this episode (including WOW) to the total remaining coring time, we would have reached a total depth of >1200 mbsf, close to the 1300 mbsf precruise estimate.

Fishing for roller cones and medical evacuation (30 December–7 January)

Three roller cones were lost in problematic coring conditions at the end of the previous episode while cutting Core 360-U1473A-44R. We made a total of four fishing attempts, first with two fishing magnet runs, then with two reverse circulation junk basket (RCJB) runs, for a total of 2.8 days, without recovering any cones. However, to everyone's surprise, the last RCJB run recovered an unprecedented 0.5 m long, 18 cm diameter core (Core 45M, 410.2–410.8 mbsf). This made it extremely unlikely that we had a roller cone left at the bottom of the hole and we hence decided to resume coring.

Between the first and second fishing run we were obliged to sail to a helicopter rendezvous site near Mauritius for a medical emergency. The 1320 nmi round-trip consumed 5.5 days of operational time.

Second coring episode and two roller cones lost and found (7–12 January)

Cores 360-U1473A-46R through 55R (410.8–481.7 mbsf) were retrieved with a total recovery of 20.0 m (28%). Penetration rates were high, recovery was low, and cores were highly fractured, indicating a weak (faulted) formation. Because of excessive torque and the need for a wiper trip and reaming the hole, we decided to retrieve the drill string, to discover that the RCB bit was missing one of its four roller cones. The second of two RCJB fishing runs that followed recovered one missing roller cone but left three lost cones still unaccounted for. We decided to resume coring; however, Cores 53R through 55R (469.6–481.7 mbsf) had zero recovery. Deployment of depluggers had no effect. We retrieved the drill string and found that the bit had damage attributable to a roller cone. We deployed the fishing magnet and recovered a heavily abraded roller cone that had evidently been stuck in the center of the drill bit and prevented advance and recovery.

Drilling ahead (12–13 January)

We decided to drill ahead without coring for an interval not to exceed 100 m using a tricone bit, which is more robust than the RCB coring bit and therefore more suitable to mitigate potential issues near the bottom of the hole, such as reaming a slightly tight hole. We also wanted to get an idea of how much faster drilling would deepen the hole compared to coring. We drilled ahead from 481.7 to 519.2 mbsf (37.5 m), found that the advance rate was not greater compared to that of coring, and after 1.3 days decided therefore to resume coring.

Third coring episode (13–23 January)

During this coring episode of 9.9 days (including 0.6 day when the pipe was stuck in the hole at 651.9 mbsf), we retrieved Cores 360-U1473A-57R through 89R (519.2–789.2) and recovered 241.4 m (89%) using four RCB coring bits. Coring conditions were ideal for the most part in these less deformed gabbroic rocks. We arguably recovered the single longest piece of igneous rock ever (2.85 m) in Core 84R. On 18 January the drill string got stuck in the hole and it took 15 h to get back into coring operations. Nevertheless, as with the first coring episode, extrapolating the average daily advance during this episode (including stuck time) over the total number of coring days available, we would have reached >1200 mbsf.

Successful logging and mechanical bit release problem (23–30 January 2016)

We conducted successful wireline logging runs with (1) the "triple combo" tool string, (2) the FMS-sonic tool string, and (3) the Ultrasonic Borehole Imager (UBI). When the drill string was recovered, the mechanical bit release (MBR) top connector was missing the sleeve retainer ring, which was presumed to have fallen into the bottom of the hole. We first used a fishing magnet trying to recover the ring without success. Next we deployed a coring bit in the hope that the missing part may have dropped onto the seafloor when the previous RCB bit was released prior to logging; however, we immediately experienced excessive torque that was attributed to contact with metal at the bottom of the hole. The presence of the sleeve retainer ring at the bottom of Hole U1473A was confirmed with a subsequent RCJB deployment, which recovered three rounded boulders with tool marks that fit the sleeve retainer perfectly. At this point in time we had to leave Site U1473 and get underway for Mauritius.

Port call and transit to Site U1473 (30 November–16 December)

Expedition 360 (SWIR lower crust and Moho) began with the first line ashore at the Unity Container Terminal Berth in Colombo, Sri Lanka, at 1100 h on 30 November (UTC + 5.5 h). The Co-Chief Scientists, IODP technical staff, and the Expedition Project Manager boarded the ship. The remainder of the science party and the ship's crew boarded the vessel on the second day of the port call (1 December).

Port call activities took place from 30 November through 5 December and included routine offloading of cores and miscellaneous freight from Expedition 359 and loading of miscellaneous drilling equipment, expedition stores, and food for Expedition 360. Activities also included offloading 5½ inch and 5 inch drill pipe for inspection and refurbishment, loading 295 joints of new 5 inch drill pipe, and pumping 900 metric tons of marine gas oil from barges to the ship's fuel tanks. On 4 December, the port authority required the ship to move from the Unity Container Terminal berth to the JCT Transfer Jetty to complete port call operations, including pumping of 60 metric tons of barite and 54 metric tons of sepiolite from trucks into the ship's bulk tanks. Loading of all supplies was concluded at 1800 h on 5 December and the last line was released at 2018 h, getting the ship under way to the Atlantis Bank at full speed of 11.2 kt.

During the transit, ship time was changed by –0.5 h on 6 December and by –1.0 h on 7 December, resulting in UTC + 4 h, which was the time zone for the remainder of Expedition 360. Plans for the reentry installation were finalized and all reentry hardware was located and inspected. Ship tours were given to the science party. The hydraulic release tool (HRT) was assembled in preparation for running the drill-in casing system. Appropriate space-out drawings were completed, defining the drill-in casing program. The dual elevator handler was overhauled and all other drilling and coring equipment had the prespud maintenance checks completed.

On 13 December the ship's speed was reduced and the course changed to maneuver around the center of tropical depression Ex-Bohale. On 16 December we arrived at the coordinates for proposed primary Site AtBk6 (32°42.3402′S, 57°16.6910′E), and at 1700 h we switched to dynamic positioning mode. The 2817 nmi sea voyage was completed in 10.9 days at an average speed of 10.7 kt.

Seafloor survey and installing the reentry system (17–19 December)

On 17 December, an APC/XCB bit, bit sub, drill collars, and new 5 inch drill pipe were made up and lowered to 668 mbrf (bottom-hole assembly [BHA] Run 1). The subsea camera system was installed and lowered to just above the bit in preparation for a survey to select a site appropriate for drilling at or near proposed Site AtBk6. The survey strategy was to proceed in a square spiral pattern, increasing at 10 m intervals away from the start point (Site AtBk6) until a sufficiently flat bare-rock spot at least 5 m in diameter was located. During the survey, the drill pipe and camera were raised and lowered by up to several meters as required by the seafloor morphology. No suitable site was found during the initial 50 m × 50 m survey. The survey was extended to the south by a further 50 m in the direction of the most promising seafloor. After a total of 5.5 h of survey a suitable location for Hole U1473A was found at 32°42.3622′S, 057°16.6880′E (710.2 mbsl), 40 m south of the original start point. Total survey operations lasted from 0530 to 1530 h. After recovery of the camera system and drill pipe, an acoustic beacon was dropped to provide additional positioning information into the dynamic positioning system.

Later on 17 December we began to assemble the drill-in casing reentry system, consisting of a 12¼ inch tricone bit, bit sub, underreamer, and mud motor. A pump-in sub was installed on top of the mud motor and connected with a high-pressure hose to the mud manifold to verify the proper functioning of the mud motor and underreamer. The mud motor began turning at 15–20 strokes/min, and the retractable arms on the underreamer opened at 40 strokes/min and 300 psi. The HRT running tool was attached to the drilling assembly and this entire drilling stinger was racked back in the derrick.

One joint of 13⅜ inch casing was picked up and trimmed to 11.35 m length. The previously assembled drilling stinger was inserted into the casing and the 13⅜ inch casing hanger and the HRT were made up to the casing, with all casing connections stitch-welded. The assembly (BHA Run 2) was lowered to the moonpool and the hard rock landing skirt was welded underneath the casing collar. The entire assembly was lowered to the seafloor and the subsea camera system was run to just above the casing hanger to observe the drill-in process. The top drive was picked up, and drilling in Hole U1473A started at 0535 h on 18 December. During the first hour, drilling was punctuated with erratic torque, which was only detectable by the camera system. Drilling smoothed noticeably after the underreamer was drilled into the seafloor. A bull's eye level mounted on the landing skirt broke off and disappeared from view about 1 h into the drill-in process.

The signals from the two subsea cameras were lost at 1445 h and the camera was pulled to the surface. A backup telemetry pod was installed and the cameras redeployed by 1700 h. Drilling continued without the camera system except while handling the camera frame at the surface. After a period of no advancement, at 1845 h we stopped drilling out of concern that the underreamer and bit assembly may have had a problem. With the 16½ inch cased hole now extending to 11.5 mbsf, we circulated a mud sweep and started recovering the subsea camera system.

The HRT free-fall funnel was assembled and dropped at 2015 h. We observed its successful landing on the 13⅜ inch casing hanger via the redeployed subsea camera system from 1915 to 2045 h. The stinger with bit, mud motor, and underreamer was released from the casing by pumping a release piston down the pipe and into the HRT. The casing dropped ~1.7 m to the bottom of the 16½ inch hole. The camera system and the stinger with HRT, mud motor, underreamer, and bit were pulled clear of the reentry system by 2230 h on 18 December and tripped back to the surface.

With the knowledge that the 13⅜ inch casing had landed on the bottom of the 16½ inch hole, we decided that attempting to cement the casing would not be prudent. If we were unable to push cement into the annulus between the casing and the hole we might instead end up cementing inside the casing and up to the funnel.

First coring episode (19–30 December)

From 0500 to 1215 h on 19 December, the RCB BHA was made up with a C-7 drill bit and lowered to 668 mbrf (BHA Run 3). Next, we deployed the subsea camera system and performed a short survey of the reentry system, which showed that the reentry installation was higher than our initial numbers indicated. Our current estimate has the seafloor at 721 mbrf (710.2 mbsl). The initial drilled depth is 730.5 mbrf (9.5 mbsf), with the casing shoe at 728.4 mbrf (7.4 mbsf). The 12¼ inch rathole was ~2 m deep and the top of the cone is at ~714 mbrf (703.2 mbsl). The reentry installation appeared stable.

We picked up the top drive and reentered Hole U1473A at 1535 h on 19 December (first reentry). At 1745 h after recovering the camera system and washing back to bottom (~2 m of fill), the core barrel was dropped and cutting of the first core (360-U1473A-2R) began. Coring continued through Core 9R (80.4 mbsf), when drill bit use had reached 39.5 h at 1500 h on 21 December. The hole was cleaned and the drill pipe was pulled to the surface, equipped with a new C-7 RCB bit, and redeployed (BHA Run 4). Hole U1473A was reentered for the second time at 2335 h on 21 December. No fill was

recorded at the bottom of the hole. RCB coring resumed at 1315 h on 22 December from 80.4 mbsf. At 0400 h on 24 December, when coring had reached 167.7 mbsf (Core 18R) and bit rotating hours was 42.5 h, the drill string was again retrieved to install a new bit. We reentered Hole U1473A with the third RCB bit at 1137 h on 24 December (BHA Run 5). No fill was detected on bottom and coring resumed at 1415 h from 167.7 mbsf. While cutting Core 19R, the ship's heave continued to increase. The situation worsened while attempting to cut Core 20R. When it became impossible to keep the bit on bottom after a 2.7 m advance, we suspended coring. Core 19R was recovered and the drill string tripped out of the hole and secured with the end of the pipe in the water column at 624 mbsl while we waited on the swell to subside. Ship heave of over 6 m total amplitude was recorded while WOW.

After a 1 h period with heave consistently <4 m, the ship was positioned to reenter Hole U1473A at 1122 h on 25 December. After reentering the hole and lowering the bit to the bottom, no fill was observed and RCB coring continued at 1400 h from 180.1 mbsf, recovering Cores 21R through 34R (313.2 mbsf), when rotation time on the third RCB coring bit reached 41.9 h. The hole was cleaned and the drill string retrieved, with the bit clearing the rotary table at 1755 h on 27 December.

The fourth C-7 RCB bit was made up to the BHA and the drill string was redeployed and reentered Hole U1473A at 0008 h on 28 December. When the drill string was lowered to the bottom of the hole, 1.5 m of soft fill was encountered, which was washed out and followed by another mud sweep to remove the cuttings from the hole. RCB coring resumed at 313.2 mbsf and continued through Core 44R at 410.2 mbsf. At the end of cutting Core 44R, a mud sweep was pumped, which was followed by an increase in drill string torque to ~700 A. The drill string was worked for ~3 h with a combination of excessive pull (50,000 lb), rotation (800 A), and circulation. The drill string became free at 0100 h on 30 December. Core 44R was retrieved and another core barrel was dropped. While attempting to get back on bottom to continue coring, the driller experienced erratic torque, up to 450 A. After a few minutes of attempting to core, the decision was made to pull the drill string even though we had only 34.6 rotating hours on the bit. Upon clearing the rotary table at 0740 h, the bit was found to be missing three out of four roller cones.

This first coring episode with four BHA runs and four RCB bits recovered Cores 2R through 44R (9.5–410.2 mbsf) with 161.3 m recovered (49%). Recovery was below expectations when compared with Hole 735B. Hole conditions and lithologic evidence indicated one or more major fault zones, including one at ~400 mbsf.

Fishing for roller cones and medical evacuation (30 December–7 January 2016)

A new BHA was assembled with a 9 inch Bowen fishing magnet to attempt to retrieve the cones left in the bottom of the hole. Hole U1473A was reentered at 1244 h on 30 December (BHA Run 7), and the fishing magnet was lowered to the bottom of the hole with circulation and slight rotation, in accordance with the Bowen procedures. The drill string was tripped back to the surface and the fishing magnet arrived at the rig floor at 2020 h. The magnet had picked up some magnetic debris (core catcher parts); however, none of the three roller cones was retrieved.

During the trip out of the hole we were informed by the ship's physician of a medical emergency necessitating transfer of the patient to a medical facility for examination and treatment. At 2324 h on 30 December, the ship started the transit toward Mauritius. A helicopter was scheduled and the vessel sailed to a rendezvous point south of Mauritius. A recently formed tropical depression was between the vessel and the meeting point, necessitating a course deviation to the west to avoid the worst of the bad weather. The vessel arrived at the agreed on rendezvous point at 1634 h on 2 January and switched to dynamic positioning mode. The helicopter from the Mauritius Police Department touched down at 1717 h and departed at 1725 h with the patient on board. The ship started the transit back to Site U1473 at 1742 h. It arrived at 1035 h on 5 January, switching from cruise mode to dynamic positioning mode. The total transit distance covered for the medical evacuation was 1320 nmi and it consumed 5.6 days of operational time allocated for Expedition 360.

In preparation for our second attempt to retrieve the three roller cones left at the bottom of Hole U1473A, the BHA was made up with new drill collars and a Bowen fishing magnet with a milling guide and two boot-type junk baskets. Hole U1473A was reentered at 2146 h on 5 January (BHA Run 8; seventh reentry). The bit landed on fill at 316.7 mbsf and was washed to the bottom of the hole with slight rotation. A 30 barrel mud sweep was pumped and the string was worked up and down three times and slowly turned five times. The drill string was retrieved and the fishing magnet arrived at the rig floor at 0800 h on 6 January. The magnet picked up some metal debris from the lost core catcher but none of the missing cones from the main RCB coring bit.

Next, we made up a Gotco RCJB with a milling guide and two boot-type junk baskets and reentered Hole U1473A at 1330 h (BHA Run 9; eighth reentry). The bit was rotated and washed to the bottom of the hole with slight rotation. After tagging the bottom of the hole, a 20 barrel mud sweep was pumped to clean out the hole. The RCJB was worked up and down three times before the flow-deviating steel ball was dropped down the drill pipe to activate the reverse circulation. The driller attempted to advance the bit for 20 min using low weight (2000 lb) before the drill string was tripped back to the surface, clearing the rig floor at 0110 h on 7 January. The RCJB assembly recovered gravel, including a few boulders, of gabbroic and fault rock material but no signs of the missing roller cone parts.

The same RCJB assembly was made up once more and reentered in Hole U1473A at 0555 h (BHA Run 10; ninth reentry). With the bit near the bottom of the hole, two 30 barrel high-viscosity mud sweeps were pumped before the bit was worked up and down from 0845 to 1030 h. Reverse circulation was activated and the driller spent nearly 1 h advancing to ~410.8 mbsf, using greater weight than during the previous run (2000–4000 lb; 200–400 A; 160 strokes/min). The drill string was recovered, clearing the rig floor at 1510 h. To everyone's surprise, the RCJB had recovered an unprecedented 0.5 m long, 18 cm diameter core from a cored interval of 0.6 m (83% recovery). The core was given the core type designation Core 45M. However, none of the roller cones previously lost in the hole were recovered.

Given the tight fit of the RCJB assembly in the hole, it was extremely unlikely that any roller cone bits could have remained at the bottom of the hole. We speculated that the cones may have been lifted out of the hole with one or more of the previous three runs with two fishing magnets and the RCJB (Run 07-FM, Run 08-FMM, Run 09-RCJB) and dropped on the seafloor before they could reach the rig floor, or they could be lodged in the borehole sidewall where breakouts created cavities. On 7 January, we decided to resume RCB coring.

Second coring episode and two roller cones lost and found (7–12 January)

A BHA was assembled with a new RCB C-7 bit and reentered Hole U1473A for the tenth time (BHA Run 11) at 2320 h on 7 January. A wash core barrel was deployed to facilitate the cleaning out of debris before resumption of coring. The last meter of the hole had to be reamed because the RCJB had created a slightly undersized hole. We pumped 50 barrels, then 30 barrels of high-viscosity mud and retrieved the wash core barrel at 0515 h. Another core barrel was dropped and Cores 46R through 52R (410.8–469.6 mbsf) were retrieved with a total recovery of 20.5 m (34%). Penetration rates were high for several cores, with a maximum of 8.9 m/h for Core 48R. In addition, recovery was low and cores were highly fractured, indicating a weak formation. Coring operations included five 30 barrel mud sweeps. Because of excessive torque (500 A) in the lowermost part of the hole, a wiper trip was conducted to condition the hole and 1 h was spent reaming the hole. After advancing through 1.5 m of fill on the bottom of the hole, the bit was advanced 0.6 m for Core 52R, with erratic high torque. Given the large amount of reaming that had been required and despite the low bit hours (12.1 h), we decided to retrieve the drill string, which cleared the rig floor at 1545 h on 9 January 2016. We discovered that the RCB bit was missing one of its four roller cones.

An RCJB with tandem boot junk baskets was assembled and deployed in an attempt to recover the missing cone. The bit reentered Hole U1473A at 2007 h on 9 January and was washed to the bottom of the hole at 469.6 mbsf with circulation and slight rotation.

The RCJB (BHA Run 12) was deployed and worked up and down near the bottom of the hole. After activating reverse circulation by dropping the steel ball down the hole and working some more on the bottom, the drill string was recovered. It cleared the rig floor at 0500 h on 10 January, recovering some gravel but no roller cone.

The RCJB was reassembled with a new mill tooth cutting shoe and catcher assembly and deployed once more (BHA Run 13), reentering Hole U1473A at 0846 h. After a 30 barrel mud sweep, the RCJB was worked and activated again according to protocol. The drill string was retrieved, clearing the rig floor at 1605 h on 10 January. This time the recovery consisted of a large cobble and the lost roller cone.

We decided to resume coring and made up an RCB BHA with a new RCB C-7 bit, lowered it to the seafloor, and reentered Hole U1473A at 2037 h (BHA Run 14; sixth RCB run). The bit was washed to the bottom of the hole, which included a 50 barrel mud sweep after noting 0.5 m of fill at the bottom. Our attempt to cut Core 53R (469.6–470.6 mbsf) from 0015 to 0400 h on 11 January advanced only 1 m and achieved no recovery. Erratic torque was observed during this advance and repeated mud sweeps were pumped. Then we cut Core 54R (470.6–480.3 mbsf), advancing the full 9.7 m but not recovering any core. Based on the assumption that rock had jammed the bit throat, we deployed a deplugger (1045–1130 h) in an attempt to dislodge the obstacle. This was followed with another failed attempt to core (55R; 480.3–481.7 mbsf; 1.4 m advance, no recovery). We ran another bit deplugger and dropped another core barrel; however, no penetration could be achieved. At 1745 h on 11 January, we decided to recover the drill string and the bit cleared the rig floor at 2150 h. Upon inspection, the bit had lost most of the tungsten carbide inserts, particularly toward the inside of the roller cones, and was missing one of the four core guides.

The bit had obviously encountered metal at the bottom of the hole, at a minimum its own missing core guide, and possibly one of the missing cones lost in the hole a few days ago. At 2215 h on 11 January, we began to make up and deploy a fishing magnet with mill tooth guide (FMM) and two boot-type junk baskets in an attempt to recover the metal junk at the bottom of Hole U1473A (Run 15-FMM). We reentered Hole U1473A at 0321 h on 12 January and tagged the bottom of the hole at 0615 h without encountering any fill. Two 30 barrel mud sweeps were pumped while working the magnet and its milling shoe according to protocol. The drill string was retrieved, clearing the rig floor at 1105 h, and we found that the fishing magnet had successfully recovered a heavily eroded roller cone. As we suspected from inspection of the bit from Run 14, the cone had plugged the RCB bit and prevented advancement and recovery of core the previous day. Some gravel was recovered as well in the boot-type junk baskets.

Drilling ahead (12–13 January)

We decided to drill ahead without coring for an interval not to exceed 100 m using a tricone bit. The tricone drilling bit is more robust than the RCB coring bit and therefore more suitable to mitigate potential issues near the bottom of the hole, such as reaming a slightly tight hole. We also wanted to get an idea of how much faster drilling would deepen the hole compared to coring, and we wanted to do that before reaching the modeled depth interval (~600 mbsf or deeper) where we expect to penetrate the magnetic polarity transition from reversed to normal.

We started to make up a 9⅞ inch tricone bit at 1200 h on 12 January, reentered Hole U1473A at 1545 h, washed and reamed down a tight hole to the bottom at 481.7 mbsf, began to drill new hole at 2300 h, and deepened the drilled interval to 519.2 mbsf. Drilling conditions were reasonably good; however, the rate of advance barely matched the rates we had achieved with RCB coring earlier in the hole. We decided in the afternoon of 13 January to switch back to coring. The drill string was retrieved and cleared the rig floor at 2010 h. Inspection of the tricone drill bit showed slight wear of the outside diameter caused by the narrow gauge hole, but the cones and bearings were all in good condition. The wear was severe enough to crack all 4 tungsten carbide bit nozzles.

Third coring episode (13–23 January)

A new 9⅞ inch RCB C-7 bit was made up and deployed to near the seafloor (BHA Run 17; seventh RCB bit), at which point deployment was suspended to allow the rig crew to slip and cut 115 ft of drilling line as part of their routine rig maintenance. Hole U1473A was reentered at 0210 h on 14 January, reamed down from 510.6 to 519.2 mbsf, and cleaned with a 30 barrel high-viscosity mud sweep. When the intended wash barrel was recovered at 0730 h, it surprisingly contained a 0.2 m long freshly trimmed core plus 0.2 m of additional material, which was registered as Core 57R (519.2–519.6 mbsf). We subsequently recovered Cores 58R through 66R (519.6–606.6 mbsf) and recovered 64.9 m (75%). Coring conditions were optimal during this run. Average torque on bottom remained ~350 A and recovery was getting better downhole. Thirty barrel high-viscosity mud sweeps were pumped every 5 m.

With 39.6 h on the bit, we decided at 0700 h on 16 January to retrieve the drill string for another bit change, clearing the rig floor at 1055 h. Upon inspection, the RCB coring bit was intact, with very little wear on the skirt or its tungsten carbide inserts. The inserts on the nose of the bit showed appreciable signs of wear but were intact.

A new 9⅞ inch C-7 bit was made up and, following some rig servicing tasks, reentered Hole U1473A at 1424 h (BHA Run 18; eighth RCB bit). Coring resumed at 1830 h and continued through Core 71R (648.4 mbsf), with 30 barrel mud sweeps pumped as required. At 2215 h on 17 January, we had to suspend coring and pull out of the hole because of high ship heave. Given the time spent on the bit already, we decided to use the down time for an early bit change and retrieved the drill string with the bit clearing the rig floor at 0240 h on 18 January. Run 18 (Cores 67R through 71R) recovered 41.3 m (a staggering 99%).

A new RCB C-7 drill bit was installed and lowered toward the seafloor (BHA Run 19; ninth RCB bit). By that time, the swell had subsided and we reentered Hole U1473A at 0653 h (the eighteenth reentry). RCB coring resumed at 1030 h on 18 January and Core 72R was advanced from 648.4 to 651.9 mbsf with varying torque and mud sweeps every few meters. At 1215 h, the drill pipe became stuck with the bit at 651.9 mbsf, with loss of rotation despite applying torque up to 800 A and overpull up to 175,000 lb. The driller gradually increased the pressure and overpull on the drill string, opening and closing the heave compensator in the process, and was able to work the bit up to 648 mbsf. The pipe suddenly became free at 1400 h and rotation and circulation were reestablished. As we pulled up to 555 mbsf, the torque gradually normalized and we retrieved Core 72R (648.4–651.9 mbsf) at 1615 h. We think that a significant piece of rock fell from higher up in the hole onto the tapered drill collar and the drill string became free when the rock was gradually broken up. The sudden release of energy when freeing the pipe was cause for concern. It was therefore decided to retrieve and inspect the BHA and the drill bit to minimize the overall risk to the hole. Before pulling the drill string, the major traveling equipment on the rig was inspected for any visible damage. While pulling the drill string with the top drive, the torque was carefully monitored; everything appeared normal. The bit arrived back on the rig floor at 2015 h and was inspected. With <2 h of coring time, the bit looked as good as new and was reassembled to the BHA.

Hole U1473A was reentered at 2350 h on 18 January (BHA Run 20; nineteenth reentry) and the bit was lowered to the bottom of the hole without encountering any fill. Coring resumed and Run 20 retrieved Cores 73R through 81R (651.9–721.3 mbsf), recovering 65.6 m (95%). We pumped 30 barrel high-viscosity mud sweeps every 5 m to keep the hole clean. At 0200 h on 21 January, drill bit rotating time had reached 40 h and it was time for a pipe trip to replace the bit. The drill string was retrieved and the bit arrived back on the rig floor at 0635 h on 21 January.

We made up another RCB C-7 coring bit, this time with an MBR to allow us to drop the bit on the seafloor after coring, reenter the hole, and conduct wireline logging without the need for a full pipe trip. The bit was lowered to the seafloor and Hole U1473A was reentered for the twentieth time at 1038 h on 21 January. The bit reached the bottom of the hole without drag or excessive torque and, after a 30 barrel mud sweep, coring resumed at 1515 h. We retrieved Cores 82R through 89R (721.3–789.2 mbsf) and recovered 66.0 m (a whopping 97%), pumping 30 barrel high-viscosity mud sweeps every 5 m and a 50 barrel mud sweep at the end.

Successful logging and MBR problem

At 1445 h on 23 January, we began our wireline logging program for Hole U1473A, which had a total depth of 789.2 mbsf. With the bit near the bottom of the hole, we displaced the hole with 290 barrels of drill water (freshwater) to enhance the salinity (and thus the electrical resistivity) contrast between a relatively small amount of formation pore fluid and a relatively large amount of borehole fluid. We raised the drill bit to 205 mbsf and displaced the upper part of the hole with another 49 barrels of drill water. Next, we pulled the bit out of the hole, clearing the seafloor at 1830 h, and offset the ship 30 m east with the bit ~10 m above the seafloor. Using two wireline runs with the rotary shifting tool (RST), we dropped the drill bit onto the seafloor at 1930 h. Next, we repositioned the ship and reentered Hole U1473A at 2145 h on 23 January (twenty-first reentry), lowering the end of the pipe to 45.5 mbsf. The subsea camera system was recovered and the rig floor prepared for logging.

At 2330 h on 23 January, we began to rig up the logging tools for the first of three logging runs with the triple combo tool string, which measures bulk density, bulk resistivity, spectral NGR, magnetic susceptibility, total gamma radiation, and temperature. The triple combo was deployed at 0045 h on 24 January. The run included a 150 m upward calibration pass from the bottom of the hole and the main upward logging pass from 787.8 mbsf. During the main log, the tool string temporarily lost power at 354.0 mbsf and was dropped back down to 383.1 mbsf before the log was completed. The tool string was back at the surface at 0530 h.

The second run with the FMS-sonic tool string, which measures microresistivity to generate a partial borehole wall image, propagation of compressional and shear waves, total gamma radiation, and temperature, was deployed at 0815 h. After the tool string was run to bottom at 785.5 mbsf, the controller of the heave compensator had to be rebooted to correct a problem. The run included three logging passes. The first was from 785.5 mbsf to just below the end of pipe at 88.9 mbsf. The second pass was from 785.5 to 568.2 mbsf; it was aborted because one of the FMS arms didn't open and the tool was dropped back to the bottom. The third pass was from 785.5 mbsf to the seafloor. The tool string was back at the surface at 1530 h and rigged down by 1645 h on 24 January.

The third run with the UBI tool string, which generates a borehole wall image using ultrasound. The tool string was also configured to measured spectral gamma radiation as well as total gamma radiation and temperature. It was deployed at 1800 h on 24 January. A downhole pass was measured from just above the seafloor to 785.2 mbsf. The uplog started at 778.6 mbsf. A small problem was encountered with an apparent ledge at ~579 mbsf in both directions. The tool string was back on the rig floor at 0330 h on 25 January.

After all logging equipment was rigged down, the drill string was retrieved and cleared the rig floor at 0555 h. Upon inspection of the MBR top connector, we found that the sleeve retainer ring was missing. The locking bolt securing the sleeve retainer was found to be sheared. The most likely situation was that the sleeve retainer backed out during logging operations and fell into the open hole. We therefore needed to retrieve it before we could resume coring. We made up and deployed a fishing magnet with mill guide, reentered Hole U1473A at 1012 h, and reached the bottom of the hole at 789.2 mbsf. A significant amount of fill and hard material was encountered on the way to bottom. A 30 barrel mud sweep was pumped, and the fishing magnet was worked up and down near the bottom of the hole according to protocol (1430–1530 h). The drill string was retrieved and cleared the rig floor at 1850 h. The sleeve retainer ring was not recovered.

Because a small possibility existed that the retainer dropped to the seafloor when the bit was dropped, rather than into the hole, we decided to attempt a coring run. An RCB bit was made up and deployed, reentering Hole U1473A at 2229 h on 25 January. The drill string was washed and reamed to the bottom of the hole at 789.2

mbsf, which included a 30 barrel high-viscosity mud sweep and the deployment and recovery of a wash barrel. Next, a core barrel was dropped at 0315 h on 26 January and an attempt was made at coring. Applying a maximum of 2000–3000 lb of weight and 350 A of torque, the driller noted erratic torque on bottom. After several careful attempts at coring, it became clear that metal junk was preventing advancement. The drill string was retrieved, clearing the rig floor at 1020 h. Upon inspection, the drill bit showed only a few scratches but was otherwise in excellent condition.

The RCJB was made up with a mill tooth cutting shoe and two boot-type junk baskets and deployed in an attempt to retrieve the missing MBR sleeve retainer ring (BHA Run 24). The bit reentered Hole U1473A at 1420 h on 26 January. At 1745 h when the top drive was picked up to lower the pipe to the bottom of the hole, power to the top drive was lost for 5.73 h. The circulation head was installed so we could keep circulating and rising/lowering the drill string while the top drive electrical problem was being repaired. At 2300 h, the top drive was picked up again and the drill string was washed toward the bottom of the hole to complete the fishing attempt. A 30 barrel mud sweep was pumped, and the string was worked up and down three times before the activation ball was dropped down the pipe to trigger reverse circulation. After circulating and rotating on bottom for 80 min, the top drive was set back and the drill string was retrieved, clearing the rig floor at 0545 h on 27 January. The sleeve retainer was not recovered; however, its presence at the bottom of Hole U1473 was confirmed with the recovery of three rounded cobbles that have clear tool marks characteristic of contact with the sleeve retainer.

With no expedition time left, the remaining drill collars were laid out to the drill collar racks and the rig floor was cleaned up and secured for transit. At 0440 h, the single acoustic positioning beacon was recovered. The thrusters and hydrophones were then raised.

A total of 86 RCB cores were taken over a 741.6 m interval with a total recovery of 468.15 m of core. The reverse circulating junk basket recovered a surprise core on one run and other samples on a subsequent run. The total advance for the tool was recorded at 1.1 m with a 1.0 m of material recovered. There were a number of other junk baskets recovered with sample material. With the exception of the last junk basket runs, these were curated and entered into the database against the hole. On the next to last junk basket run, the material was recorded as a ghost core and entered into the database against from 9.5 to 788.2 mbsf. The final RCJB was recorded as an advance of 0.5 m with 0.5 m of material recovered. The overall core recovery for Hole U1473A was 468.65 m over an interval of 742.2 m, yielding a recovery percentage for Hole U1473A of 63.2%. The ghost core was not considered in recovery statistics. The total time spent on Hole U1473A was 868.5 h or 36.19 days.

Transit to Port Louis, Mauritius

At 0830 h on 27 January, the transit to Port Louis, Mauritius, began. Expedition 360 ended at 0800 h on 30 January with the first line ashore.

Education and outreach

Expedition 360 had a team of four Education and Outreach officers on board the ship, including two teachers from France and the USA, one informal educator and podcaster from Canada, and one journalist from China. These officers communicated the goals of the expedition in simple terms to students and the general public across the globe through live webcasts from the ship, online social media, and facilitating interviews between reporters from national and international media outlets and the science party. The officers also developed curriculum and other educational material for students at all age levels.

Webcasts

Using a direct satellite link, iPads, and videoconferencing software, the Education and Outreach team was able to interact with students all over the world to share the scientific goals and progress of the expedition. This format allowed for direct communication between students on shore and scientists aboard the *JOIDES Resolution*. A typical session included a brief demonstration of crust–mantle/Moho models comparing mid-ocean ridges of various spreading rates using samples and diagrams, followed by a laboratory tour that traced the path of a core on board the ship. Events concluded with a question and answer portion that typically included a member of the science party.

Events were organized to school classrooms with students aged 6–19 (with a mean age of 14), teacher workshops, and universities at both the undergraduate and graduate level. A total of 120 events reached 5947 people in 16 countries with 174 shipboard scientist engagements. Demand for these events was overwhelming, and the schedule filled up by mid-January. Teachers were given the option to combine classes within a school or overlap multiple participants of the same language and age level from different locations. A number of these sessions were recorded by teachers for future use and online publication (Table **T3**).

Social media

The Education and Outreach Team maintained four websites for the duration of the expedition: a Facebook page, a Twitter feed, an Instagram account, and a blog at **http://joidesresolution.org**. Each team member took turns contributing to these sites for a combined total of 274 posts, which were viewed 350,065 times and replied to, liked, or shared 15,959 times (Table **T4**). The team also hosted an "Ask Me Anything" session on Reddit, answering 64 questions from the public over the course of 2 h with the help of 6 members of the science party.

Media

Expedition 360 received a significant amount of global media attention. The Education and Outreach Team supported interested journalists by arranging interviews with scientists on board and providing background information, photographs, and video footage. This resulted in a total of 34 written articles in 7 languages, 4 English language radio interviews, and 3 English television broadcasts. Selected highlights from this coverage may be viewed in Table **T5**, and a complete list of coverage during the expedition is in Table **T6**.

In addition, the presence of a Chinese reporter on board generated significant coverage in China. The Xinhua News Agency released about 30 news reports and more than 120 photographs regarding Expedition 360. These reports have been transmitted by many other media outlets and websites in China, which has aroused widespread social interest. In China's largest search engine Baidu, with the keywords "Zhang Jiansong" (the onboard reporter) and "resolution," more than 24,300 search results were returned. Furthermore, after having read these reports, some Chinese journalists performed further interviews with IODP scientists. A video report

was also filed to the Sansha TV station in the Hainan Province, near the South China Sea.

Educational material

The Educators developed Expedition 360 specific curriculum for students and educational material for the general public. This material ranged from classroom activities to digital media, all of which will be published and freely accessible at **http://joidesresolution.org**. In addition, a video version of the ship tour has been produced and is available to share with educators who were unable to participate in live broadcasts during the expedition. In coordination with one of the Co-Chief Scientists, aspects of this video were designed to specifically tie in with a number of key ideas within UK GCSE, AS and A-level national curricula for Geology and Geography.

Prior to the expedition, the Educators made presentations to elementary and secondary schools, sharing their upcoming experience with ~800 teachers and students. One school district in Texas produced a promotional video outlining Expedition 360; this video also encouraged teachers and students throughout the district to participate in the activities planned for the expedition.

In order to prepare classes for webcasts with the ship, images of samples were collected to create in-classroom activities. These images can be used to observe the interaction between seawater and lower crustal rocks in a tectonically active region. These activities aim to help students understand the continuous evolution of plate tectonic theory and the links between the lithosphere and biosphere. Fifteen activities correlated with Texas standards and teaching resources covering four topics that fit with French standards were created during the expedition.

Six 20 min podcast episodes featuring explanations of scientific concepts and interviews with the science party were published with 1500 listeners across 18 countries. One more episode is currently in production and will be posted shortly after the expedition.

Postexpedition projects

All of the Education officers will continue to develop material and engage in outreach activities promoting Expedition 360 and ocean exploration in general after the expedition. They intend to present their work at the 2016 American Geophysical Union Fall Meeting and at other conferences as well as the postcruise meeting. Continued efforts will promote IODP in China by encouraging teachers to sign up for webcasts and sail aboard the *JOIDES Resolution*.

Peripheral rock material (gravelly cuttings otherwise discarded) was collected by the Education and Outreach Team and will be shipped to the US Science Support office and made available to educators for demonstration and instructional use. Further curriculum material will be developed and shared with teachers at state, national, and international levels.

Collaboration will continue with the science party by organizing postexpedition webcasts to communicate the progression of the research progress with students. The science party will be updated regarding outreach opportunities they can become involved in. Video footage was collected and will be edited to communicate the ideas shared among the science party and progression of the atmosphere during the expedition. Audio interviews recorded during the expedition will be further edited to create radio stories for wider distribution and syndication.

Preliminary assessment

Expedition 360 was the first drilling leg of the multiphase SloMo Project that aims ultimately to drill through the Moho at Atlantis Bank on the ultraslow-spreading SWIR. The primary broad-scale objective of Expedition 360 was to establish a pilot hole for ultradeep drilling, as deep as possible in the time available. At Site U1473, we were successful in achieving the deepest igneous rock penetration from the seafloor ever during a single 2-month expedition with the *JOIDES Resolution* (789.7 mbsf). Hole U1473A is open and viable to be substantially deepened; moreover, we were achieving an unprecedented 96% core recovery in the lowermost 200 m of the hole by the end of the expedition.

Operations assessment

We did not reach our precruise target depth of 1300 mbsf. Out of a 61 day expedition, projected to have 42.2 days on site, we ended up with only 22.8 coring days. Had we had a full expedition without operational problems we would likely have had little trouble achieving or exceeding our original target depth. Substantial time (5.5 days) was lost for a medical evacuation to Mauritius and half a day to a late departure from port. Using Colombo as a starting port also entailed an extraordinarily long transit, such that it was a full 17 days after the start of the expedition before we reached the study area. On two occasions we suffered bit failure resulting in roller cones being left in the hole, necessitating a total of 6.6 days of fishing to retrieve the cones. Toward the end of the leg, it was recommended that we use an MBR before logging, which had never produced any problems before, to save a pipe trip and conserve several extra hours for coring after the logging; however, a mechanical failure left a metal sleeve retainer at the bottom of the hole with insufficient time to fish the piece out of the hole. Two abbreviated attempts did not succeed, although they provided evidence that we were very close. The piece is at the bottom of the hole, and the hole is free of fill; hence, it should be routine to fish it out during a future visit. With this fishing and, ideally, minor remediation to cement a fault zone in the upper portion of the hole, we can reoccupy Hole U1473A and deepen it substantially. Drilling conditions at the base of the hole are excellent; noteworthy is the 96% core recovery we obtained in the lowermost 200 m.

Despite of all the issues described, in only 22 days we drilled the deepest single hole ever initiated for a single hard rock leg in the history of ocean drilling. We left an open hole that can be reoccupied and deepened with only minor remediation. An open hard rock hole, where drilling conditions have significantly improved with depth, is quite unusual. An open 800 m hole promising to penetrate a magnetic reversal boundary within the next tens to a few hundreds of meters is worth reoccupying in and by itself, broader SloMo objectives notwithstanding.

Achievement of scientific objectives

As anticipated, we drilled a section of lower crustal gabbro similar to that exposed on the surface of the Atlantis Bank oceanic core complex and recovered in nearby Holes 735B and 1105A. We did not expect to encounter mantle lithologies during the first leg of the first phase of SloMo, nor did we. From the Hole U1473A cores and full suite of downhole logs we will be able to fully address most of our major expedition-specific scientific objectives.

A major objective was to establish whether or not the stratigraphy encountered and processes documented in Hole 735B are

representative of the enormous 400 km^2 gabbro massif mapped over Atlantis Bank, and if they can be reasonably considered as representative. This seems to be the case on the basis of three holes drilled there, from which we are now able to assess the spatial and temporal scales of variability of igneous lower crustal accretion for the first time. Equally important is the comparison between Atlantis Bank (SWIR) and its counterpart the Atlantis Massif oceanic core complex on the Mid-Atlantic Ridge, where the stratigraphy differs profoundly in several aspects. A major long-term objective of SloMo is to establish a seismic laboratory, at which the properties of the lower crust and upper mantle can be directly measured at seismically appropriate scales. We have shown that Atlantis Bank is a (probably uniquely) suitable location for such an endeavor. This in itself is a huge accomplishment.

The one objective we did not meet in full, because of the limited time available to us for coring during Expedition 360, was to cross the magnetic polarity reversal boundary known to be present at depth beneath Atlantis Bank. We did, however, find increasing evidence for opposite polarities in discrete late-stage features in the lowermost cores, indicating that we were entering a zone of polarity transition. Although this evidence in itself provides an important constraint on the mechanisms by which magnetic reversals are recorded in the lower ocean crust, the key interval lies tantalizingly close beneath.

Site selection

Site selection for deep drilling at Atlantis Bank was always going to be to some extent a lottery, in that drilling conditions at depth at a new location were always going to be unknown in detail. The original *James Clark Ross* JR31 site survey, conducted using an ROV and seabed rock corers, was perfectly sufficient to identify apparently suitable sites on the surface of the Atlantis Bank platform; however, it could not accurately predict the fact that a moderate-sized fault zone existed at depth. Site AtBk6 was in fact carefully chosen to avoid faults resolved by the bathymetric data available to us. In theory, a modern high-resolution near-bottom bathymetry survey could map lineaments at the surface and predict their subsurface continuations; however, the degree of erosion of the platform summit and extent of carbonate deposition when Atlantis Bank was at or near sea level have modified and partially obscured the kinds of medium-scale tectonic features we encountered at depth.

Although the average recovery for the entire hole was high (63% of the cored interval) compared to most hard rock holes, it was disappointing compared to Holes 735B and U1309D, where it was 80%–90% throughout. This is a direct result of drilling into a fault system that extended down to 469 mbsf. In the course of drilling through this faulted and fractured zone we broke two bits and had to fish for cones several times in order to continue coring. After drilling (without coring) an interval to 510 mbsf to ensure we were past the problematic interval, we finally encountered excellent drilling conditions. From there to the bottom of the hole we had steady low torque, penetration rates of ~2 m/h, and an average recovery of 96% from 577.5 mbsf onward. This included the arguably longest single piece of igneous core ever recovered (2.85 m), consistent with long intervals of unfractured rocks.

The original location proposed in the SloMo Project for ultradeep penetration was Site 735, where we had proven the conditions at depth to be excellent on the basis of the results in Hole 735B. IODP engineers recommended a short offset from Hole 735B, to drill to 1500 m with a casing plan designed on the basis of the known conditions in Hole 735B, and then to core ahead to the crust/mantle boundary. Earlier versions of our SloMo proposal, over a period of almost 10 y, were based on this operational plan. However, the compromise of moving the site to another location on Atlantis Bank, and hence also collecting information on lateral heterogeneity of the lower crust and drilling a magnetic anomaly transition, was compelling to many, including the review panels. It was not of course known that the excellent drilling conditions encountered at both Sites 735 and 1105 were not to be replicated everywhere on Atlantis Bank.

Recommendations for future SloMo legs

Preamble

In 1994 ODP convened the Offset Drilling Workshop at Texas A&M University to discuss how to optimize strategies for drilling in hostile hard rock oceanic basement environments. Their principal recommendations were: (1) we need to learn how to drill in difficult places and (2) we need to learn how to find easy places to drill. In essence, the latter simply meant "invest the time to find a good place to drill first, then go for it." This echoes the ODP Drilling Superintendent's recommendation at the end of Leg 176 to come back to Site 735, offset a short distance from Hole 735B, drill to 1500 m without coring, log, install casing where appropriate (after logging), and drill ahead. This is how deep holes are done in industry: first a test hole, then engineer for a deep hole on that basis.

Our first recommendation is that we should not be diverted from the overall long-term plan for SloMo, which has been thoroughly and formally endorsed by the scientific community: that we continue to focus on the objective of drilling a ≥3 km deep hole to the crust/mantle boundary during Phase 1 of the program. Whether in Hole U1473A or a new hole at Site 735, nothing we encountered during Expedition 360 (SloMo Leg 1) suggests this is not feasible.

Taking advantage of a prepaid underused drilling platform

We propose to continue the SloMo Project in the short to medium term with an operational approach that takes full advantage of the three existing pilot holes on the Atlantis Bank (Holes 735B, 1105A, and U1473A). Our suggested approach for the next step is to take advantage of "tie-up" periods when the *JOIDES Resolution* is otherwise idle to conduct hole engineering, during which time few or no scientists need to be on board. The cost to the program for pursuing a long-term drilling project with the large-scale scope of SloMo, which most of all requires sustained periods of time on hole, would be minimal.

In the short term, in mid-2016, we propose that use be made of the 4 month period in which the *JOIDES Resolution* is tied up in South Africa to remediate Hole U1473A, ensure it is ready to be reoccupied for further scientific operations, and core ahead if possible (any core thus obtained can be described on shore). Once this is done we will be in a position to make the strategic decision as to whether Hole U1473A or Site 735 is the best location for drilling the 3 km hole to the crust/mantle boundary and completing SloMo Phase I.

In the slightly longer term we suggest that, instead of tying up the *JOIDES Resolution*, consideration be given to diverting the ship to conduct further engineering/coring operations at Atlantis Bank instead. These we propose could potentially include casing a hole that would be deepened (without coring) to the 1500 mbsf depth of the base of Hole 735B, from which point scientific coring expeditions could resume.

Specific proposals for next operational phase

The program should consider (at least) the following options below.

Scheduling a short-term ancillary program in Hole U1473A

The program should schedule an ancillary program in Hole U1473A during the upcoming long transit back to Colombo and/or the next best opportunity depending on weather and time available and carry out the following operations:

- Fish the junk in the hole.
- Enter the hole with a tricone bit and cement each of the three problem intervals sequentially, let the cement cure, and drill out the cement.
- Resume coring as time allows, potentially bringing along a couple of scientists to direct splitting of the core and to conduct a preliminary description of the material recovered. The cores would be split, labeled, run through the multisensor loggers, and then sealed in D-tubes and stored for the scientists to describe during a subsequent expedition to the site or at a core repository. This would make up for the lost drilling time because of the medical emergency and long transit and would potentially bring drilling in Hole U1473A back on schedule.

The upper 469 m of Hole U1473A is slightly problematical, in that material from the fractured intervals could continue to fall onto the drill collars and jam the pipe in hole, as happened on one occasion during Expedition 360. Enlargement of the hole in these fractured regions will continue as cuttings are pumped past them. The remedial cementing work proposed above is simple, routine, and should solve this problem.

Consider engineering a new deep hole at Site 735

Scientific ocean drilling has never previously drilled to a depth of 3 km, and doing so would be a turning point for the program in terms of both scientific accomplishment and a demonstration of its potential. The latter is critical for public support of ocean drilling. Drilling to the crust/mantle boundary, exploring for a new planetary biosphere, and drilling to the Moho are all things that excite the public interest as demonstrated by the enormous national and international publicity generated during Expedition 360 (and similarly during the Expedition 335 "Project Mohole" drilling operations in the Pacific Ocean), as documented elsewhere in this report. IODP should drill for success. It needs to demonstrate its capability to tackle large projects and carry them forward to success. This, more than anything else, is critical to the future of scientific ocean drilling.

Given the importance and challenge of such an endeavor, the program, together with scientific stakeholders of the SloMo Project, should thoroughly evaluate all alternatives for the location of the ≥3 km deep hole and eventual ultradeep Mohole, based on analysis of pilot Holes 735B and U1473A. If this were to conclude that Site 735 is the best option, an engineering leg would be required to drill a new hole to 1500 m as close to Hole 735B as possible before then coring ahead. A casing plan would need to be made in advance based on the drilling conditions encountered in Hole 735B to ensure the cleanest possible hole in the best condition for attempting ≥3 km deep drilling. Such an engineering leg would be a relatively low cost affair, as it would not require sailing a scientific party and could take advantage of the fact that most of the costs beyond the reentry cone, casing and bits, and fuel are already carried by the program. It would also have the advantage that nearby Hole U1473A would provide an ideal backup site with the as yet to be accomplished major scientific objective of drilling through a magnetic reversal. Thus, it would minimize the risks involved in scheduling the forthcoming SloMo scientific legs back to back, with consequent savings in transit time and fuel costs in using Mauritius as a port.

References

Adams, F.D., and Coker, E.G., 1906. An investigation into the elastic constants of rocks, more especially with reference to cubic compressibility. *American Journal of Science* (Series 4), 22(128):95–123. **http://dx.doi.org/10.2475/ajs.s4-22.128.95**

Adams, L.H., and Williamson, E.D., 1923. On the compressibility of minerals and rocks at high pressure. *Journal of the Franklin Institute,* 195(4):475–529. **http://dx.doi.org/10.1016/S0016-0032(23)90314-5**

Allerton, S., and Tivey, M.A., 2001. Magnetic polarity structure of the lower oceanic crust. *Geophysical Research Letters,* 28(3):423–426. **http://dx.doi.org/10.1029/2000GL008493**

Arai, S., Dick, H.J.B., and Scientific Party, 2000. *Cruise Report, Mode 2000* (*Kairei/Kaiko* KR00-06): Yokosuka, Japan (Japanese Agency for Marine-Earth Science and Technology).

Baines, A.G., Cheadle, M.J., Dick, H.J.B., Hosford Scheirer, A., John, B.E., Kusznir, N.J., and Matsumoto, T., 2003. Mechanism for generating the anomalous uplift of oceanic core complexes: Atlantis Bank, Southwest Indian Ridge. *Geology,* 31(12):1105–1108. **http://dx.doi.org/10.1130/G19829.1**

Baines, A.G., Cheadle, M.J., Dick, H.J.B., Hosford Scheirer, A., John, B.E., Kusznir, N.J., and Matsumoto, T., 2007. The evolution of the Southwest Indian Ridge from 55°45′E–62°E: changes in plate-boundary geometry since 26 Ma. *Geochemistry, Geophysics, Geosystems,* 8(6):Q06022. **http://dx.doi.org/10.1029/2006GC001559**

Baines, A.G., Cheadle, M.J., John, B.E., and Schwartz, J.J., 2008. The rate of oceanic detachment faulting at Atlantis Bank, SW Indian Ridge. *Earth and Planetary Science Letters,* 273(1–2):105–114. **http://dx.doi.org/10.1016/j.epsl.2008.06.013**

Biddle, J.F., Fitz-Gibbon, S., Schuster, S.C., Brenchley, J.E., and House, C.H., 2008. Metagenomic signatures of the Peru margin subseafloor biosphere show a genetically distinct environment. *Proceedings of the National Academy of Sciences of the United States of America,* 105(30):10583–10588. **http://dx.doi.org/10.1073/pnas.0709942105**

Blackman, D.K., Ildefonse, B., John, B.E., Ohara, Y., Miller, D.J., Abe, N., Abratis, M., Andal, E.S., Andreani, M., Awaji, S., Beard, J.S., Brunelli, D., Charney, A.B., Christie, D.M., Collins, J., Delacour, A.G., Delius, H., Drouin, M., Einaudi, F., Escartín, J. Frost, B.R., Früh-Green, G., Fryer, P.B., Gee, J.S., Godard, M., Grimes, C.B., Halfpenny, A., Hansen, H.-E., Harris, A.C., Tamura, A., Hayman, N.W., Hellebranc, E., Hirose, T., Hirth, J.G., Ishimaru, S., Johnson, K.T.M., Karner, G.D., Linek, M., MacLeod, C.J., Maeda, J., Mason, O.U., McCaig, A.M., Michibayashi, K., Morris, A., Nakagawa, T., Nozaka, T., Rosner, M., Searle, R.C., Suhr, G., Tominaga, M., von der Handt, A., Yamasaki, T., and Zhao, X., 2011. Drilling constraints on lithospheric accretion and evolution at Atlantis Massif, Mid-Atlantic Ridge, 30°N. *Journal of Geophysical Research: Solid Earth,* 116(B7):B07103. **http://dx.doi.org/10.1029/2010JB007931**

Blackman, D.K., Ildefonse, B., John, B.E., Ohara, Y., Miller, D.J., MacLeod, C.J., and the Expedition 304/305 Scientists, 2006. *Proceedings of the Integrated Ocean Drilling Program,* 304/305: College Station, TX (Integrated Ocean Drilling Program Management International, Inc.). **http://dx.doi.org/10.2204/iodp.proc.304305.2006**

Blumenfeld, P., and Bouchez, J.-L., 1988. Shear criteria in granite and migmatite deformed in the magmatic and solid states. *Journal of Structural Geology,* 10(4):361–372. **http://dx.doi.org/10.1016/0191-8141(88)90014-4**

Cann, J.R., Blackman, D.K., Smith, D.K., McAllister, E., Janssen, B., Mello, S., Avgerinos, E., Pascoe, A.R., and Escartin, J., 1997. Corrugated slip surfaces formed at ridge–transform intersections on the Mid-Atlantic Ridge. *Nature,* 385(6614):329–332. **http://dx.doi.org/10.1038/385329a0**

Cannat, M., Mével, C., and Stakes, D., 1991. Normal ductile shear zones at an oceanic spreading ridge: tectonic evolution of Site 735 gabbros (southwest Indian Ocean). *In* Von Herzen, R.P., Robinson, P.T., et al., *Proceedings of the Ocean Drilling Program, Scientific Results,* 118: College Station, TX (Ocean Drilling Program), 415–429. **http://dx.doi.org/10.2973/odp.proc.sr.118.157.1991**

Cannat, M., Sauter, D., Mendel, V., Ruellan, E., Okino, K., Escartin, J., Combier, V., and Baala, M., 2006. Modes of seafloor generation at a melt-poor ultraslow-spreading ridge. *Geology,* 34(7):605–608. **http://dx.doi.org/10.1130/G22486.1**

Casey, J.F., Banerji, D., and Zarian, P., 2007. Leg 179 synthesis: geochemistry, stratigraphy, and structure of gabbroic rocks drilled in ODP Hole 1105A, Southwest Indian Ridge. *In* Casey, J.F., and Miller, D.J. (Eds.), *Proceedings of the Ocean Drilling Program, Scientific Results,* 179: College Station, TX (Ocean Drilling Program), 1–125. **http://dx.doi.org/10.2973/odp.proc.sr.179.001.2007**

Cowen, J.P., Giovannoni, S.J., Kenig, F., Johnson, H.P., Butterfield, D., Rappé, M.S., Hutnak, M., and Lam, P., 2003. Fluids from aging ocean crust that support microbial life. *Science,* 299(5603):120–123. **http://dx.doi.org/10.1126/science.1075653**

Delacour, A., Früh-Green, G.L., Bernasconi, S.M., Schaeffer, P., and Kelley, D.S., 2008. Carbon geochemistry of serpentinites in the Lost City hydrothermal system (30°N, MAR). *Geochimica et Cosmochimica Acta,* 72(15):3681–3702. **http://dx.doi.org/10.1016/j.gca.2008.04.039**

Dick, H.J.B., Arai, S., Hirth, G., John, B.J., KROO-06 Scientific Party, 2001. A subhorizontal cross-section through the crust mantle boundary at the SW Indian Ridge. *Geophysical Research Abstracts,* 3:794.

Dick, H.J.B., MacLeod, C.J., Robinson, P.T., Allerton, S., and Tivey, M.A., 1999. Bathymetry of Atlantis Bank—Atlantis II Fracture Zone: Southwest Indian Ridge. *In* Dick, H.J.B., Natland, J.H., Miller, D.J., et al., *Proceedings of the Ocean Drilling Program, Initial Reports,* 176: College Station, TX (Ocean Drilling Program), 1–13. **http://dx.doi.org/10.2973/odp.proc.ir.176.104.1999**

Dick, H.J.B., Meyer, P.S., Bloomer, S., Kirby, S., Stakes, D., and Mawer, C., 1991a. Lithostratigraphic evolution of an in-situ section of oceanic Layer 3. *In* Von Herzen, R.P., Robinson, P.T., et al., *Proceedings of the Ocean Drilling Program, Scientific Results,* 118: College Station, TX (Ocean Drilling Program), 439–538. **http://dx.doi.org/10.2973/odp.proc.sr.118.128.1991**

Dick, H.J.B., Natland, J.H., Alt, J.C., Bach, W., Bideau, D., Gee, J.S., Haggas, S., Hertogen, J.G.H., Hirth, G., Holm, P.M., Ildefonse, B., Iturrino, G.J., John, B.E., Kelley, D.S., Kikawa, E., Kingdon, A., LeRoux, P.J., Maeda, J., Meyer, P.S., Miller, D.J., Naslund, H.R., Niu, Y.-L., Robinson, P.T., Snow, J., Stephen, R.A., Trimby, P.W., Worm, H.-U., and Yoshinobu, A., 2000. A long in situ section of the lower ocean crust: results of ODP Leg 176 drilling at the Southwest Indian Ridge. *Earth and Planetary Science Letters,* 179(1):31–51. **http://dx.doi.org/10.1016/S0012-821X(00)00102-3**

Dick, H.J.B., Natland, J.H., and Ildefonse, B., 2006. Past and future impact of deep drilling in the oceanic crust and mantle. *Oceanography,* 19(4):72–80. **http://dx.doi.org/10.5670/oceanog.2006.06**

Dick, H.J.B., Natland, J.H., Miller, D.J., et al., 1999. *Proceedings of the Ocean Drilling Program, Initial Reports,* 176: College Station, TX (Ocean Drilling Program). **http://dx.doi.org/10.2973/odp.proc.ir.176.1999**

Dick, H.J.B., Ozawa, K., Meyer, P.S., Niu, Y., Robinson, P.T., Constantin, M., Hebert, R., Maeda, J., Natland, J.H., Hirth, J.G., and Mackie, S.M., 2002. Primary silicate mineral chemistry of a 1.5-km section of very slow spreading lower ocean crust: ODP Hole 735B, Southwest Indian Ridge. *In* Natland, J.H., Dick, H.J.B, Miller, D.J., and Von Herzen, R.P. (Eds.), *Proceedings of the Ocean Drilling Program, Scientific Results,* 176: College Station, TX (Ocean Drilling Program), 1–60. **http://dx.doi.org/10.2973/odp.proc.sr.176.001.2002**

Dick, H.J.B., Schouten, H., Meyer, P.S., Gallo, D.G., Bergh, H., Tyce, R., Patriat, P., Johnson, K.T.M., Snow, J., and Fisher, A., 1991b. Tectonic evolution of the Atlantis II fracture zone. *In* Von Herzen, R.P., Robinson, P.T., et al., *Proceedings of the Ocean Drilling Program, Scientific Results,* 118: College Station, TX (Ocean Drilling Program), 359–398. **http://dx.doi.org/10.2973/odp.proc.sr.118.156.1991**

Dick, H.J.B., Tivey, M.A., and Tucholke, B.E., 2008. Plutonic foundation of a slow-spreading ridge segment: oceanic core complex at Kane Megamullion, 23°30′N, 45°20′W. *Geochemistry, Geophysics, Geosystems,* 9(5):Q05014. **http://dx.doi.org/10.1029/2007GC001645**

Drouin, M., Godard, M., Ildefonse, B., Bruguier, O., and Garrido, C.J., 2009. Geochemical and petrographic evidence for magmatic impregnation in the oceanic lithosphere at Atlantis Massif, Mid-Atlantic Ridge (IODP Hole U1309D, 30°N). *Chemical Geology,* 264(1–4):71–88. **http://dx.doi.org/10.1016/j.chemgeo.2009.02.013**

Edgcomb, V.P., Beaudoin, D., Gast, R., Biddle, J.F., and Teske, A., 2011. Marine subsurface eukaryotes: the fungal majority. *Environmental Microbiology,* 13(1):172–183. **http://dx.doi.org/10.1111/j.1462-2920.2010.02318.x**

Escartín, J., Mével, C., MacLeod, C.J., and McCaig, A.M., 2003. Constraints on deformation conditions and the origin of oceanic detachments: the Mid-Atlantic Ridge core complex at 15°45′N. *Geochemistry, Geophysics, Geosystems,* 4(8):1067. **http://dx.doi.org/10.1029/2002GC000472**

Expedition 304/305 Scientists, 2006. Expedition 304/305 summary. *In* Blackman, D.K., Ildefonse, B., John, B.E., Ohara, Y., Miller, D.J., MacLeod, C.J., and the Expedition 304/305 Scientists, *Proceedings of the Integrated Ocean Drilling Program,* 304/305: College Station, TX (Integrated Ocean Drilling Program Management International, Inc.). **http://dx.doi.org/10.2204/iodp.proc.304305.101.2006**

Fisher, R.L., and Sclater, J.G., 1983. Tectonic evolution of the southwest Indian Ocean since the mid-Cretaceous: plate motions and stability of the pole of Antarctica/Africa for at least 80 Myr. *Geophysical Journal International,* 73(2):553–576. **http://dx.doi.org/10.1111/j.1365-246X.1983.tb03330.x**

Fisk, M.R., Giovannoni, S.J., and Thorseth, I.H., 1998. Alteration of oceanic volcanic glass: textural evidence of microbial activity. *Science,* 281(5379):978–980. **http://dx.doi.org/10.1126/science.281.5379.978**

Gillis, K.M., Snow, J.E., Klaus, A., Abe, N., Adrião, Á.B., Akizawa, N., Ceuleneer, G., Cheadle, M.J., Faak, K., Falloon, T.J., Friedman, S.A., Godard, M., Guerin, G., Harigane, Y., Horst, A.J., Hoshide, T., Ildefonse, B., Jean, M.M., John, B.E., Koepke, J., Machi, S., Maeda, J., Marks, N.E., McCaig, A.M., Meyer, R., Morris, A., Nozaka, T., Python, M., Saha, A., and Wintsch, R.P., 2014. Primitive layered gabbros from fast-spreading lower oceanic crust. *Nature,* 505(7482):204–207. **http://dx.doi.org/10.1038/nature12778**

Godard, M., Awaji, S., Hansen, H., Hellebrand, E., Brunelli, D., Johnson, K., Yamasaki, T., Maeda, J., Abratis, M., Christie, D., Kato, Y., Mariet, C., and Rosner, M., 2009. Geochemistry of a long in-situ section of intrusive slow-spread oceanic lithosphere: results from IODP Site U1309 (Atlantis Massif, 30°N Mid-Atlantic-Ridge). *Earth and Planetary Science Letters,* 279(1–2):110–122. **http://dx.doi.org/10.1016/j.epsl.2008.12.034**

Gradstein, F.M., Ogg, J.G., Schmitz, M.D., and Ogg, G.M. (Eds.), 2012. *The Geological Time Scale 2012:* Amsterdam (Elsevier).

Handy, M., Hirth, G., Burgmann, R., 2007. Continental fault structure and rheology from the frictional-to-viscous transition downward. *In* Handy, M., Hirth, G., and Hovius, N. (Eds.), *Tectonic Faults: Agents of Change on a Dynamic Earth (Dahlem Workshop Reports):* Cambridge, Massachusetts (The MIT Press), 139–181.

Hess, H.H., 1960. The evolution of ocean basins. *In* Hill, M.N., Goldberg, E., Munk, W., and Iselin, O.D. (Eds.), *The Sea, Ideas and Observations:* New York (Interscience Publishers), 1–38.

Hess, H.H., 1962. History of ocean basins. *In* Engel, A.E.J. et al. (Eds.), *Petrological Studies: A Volume in Honor of A.F. Buddington:* Boulder, CO (Geological Society of America), 599–620. **http://dx.doi.org/10.1130/Petrologic.1962.599**

Hosford, A., Tivey, M., Matsumoto, T., Dick, H., Schouten, H., and Kinoshita, H., 2003. Crustal magnetization and accretion at the Southwest Indian Ridge near the Atlantis II Fracture Zone, 0–25 Ma. *Journal of Geophysical Research: Solid Earth,* 108(B3):2169. **http://dx.doi.org/10.1029/2001JB000604**

Inagaki, F., Hinrichs, K.-U., Kubo, Y., Bowles, M.W., Heuer, V.B., Long, W.-L., Hoshino, T., Ijiri, A., Imachi, H., Ito, M., Kaneko, M., Lever, M.A., Lin, Y.-S., Methé, B.A., Morita, S., Morono, Y., Tanikawa, W., Bihan, M., Bowden, S.A., Elvert, M., Glombitza, C., Gross, D., Harrington, G.J., Hori, T., Li, K., Limmer, D., Liu, C.-H., Murayama, M., Ohkouchi, N., Ono, S., Park, Y.-S.,

Phillips, S.C., Prieto-Mollar, X., Purkey, M., Riedinger, N., Sanada, Y., Sauvage, J., Snyder, G., Susilawati, R., Takano, Y., Tasumi, E., Terada, T., Tomaru, H., Trembath-Reichert, E., Wang, D.T., and Yamada, Y., 2015. Exploring deep microbial life in coal-bearing sediment down to ~2.5 km below the ocean floor. *Science,* 349(6246):420–424. **http://dx.doi.org/10.1126/science.aaa6882**

Inagaki, F., Nunoura, T., Nakagawa, S., Teske, A., Lever, M., Lauer, A., Suzuki, M., Takai, K., Delwiche, M., Colwell, F.S., Nealson, K.H., Horikoshi, K., D'Hondt, S., and Jørgensen, B.B., 2006. Biogeographical distribution and diversity of microbes in methane hydrate-bearing deep marine sediments on the Pacific Ocean margin. *Proceedings of the National Academy of Science of the United States of America,* 103(8):2815–2820. **http://dx.doi.org/10.1073/pnas.0511033103**

Jungbluth, S.P., Grote, J., Lin, H.-T., Cowen, J.P., and Rappé, M.S., 2013. Microbial diversity within basement fluids of the sediment-buried Juan de Fuca Ridge flank. *The ISME Journal,* 7:161–172. **http://dx.doi.org/10.1038/ismej.2012.73**

Kikawa, E., and Pariso, J.E., 1991. Magnetic properties of gabbros from Hole 735B, Southwest Indian Ridge. *In* Von Herzen, R.P., Robinson, P.T., et al., *Proceedings of the Ocean Drilling Program, Scientific Results,* 118: College Station, TX (Ocean Drilling Program), 285–307. **http://dx.doi.org/10.2973/odp.proc.sr.118.148.1991**

Kinoshita, H., Dick, H.J.B., and Shipboard Scientific Party, 2001. *Atlantis II Fracture Zone: MODE'98 Preliminary Report:* Yokosuka, Japan (JAMSTEC Deep Sea Research).

Kinoshita, J., Dick, H., and Shipboard Party JAMSTEC/WHOI, 1999. Deep sea diving expedition in SW Indian Ridge (paper presented in honor of Don Heinrichs for his dedication in Marine Geosciences of NSF), *Eos, Transactions of the American Geophysical Union,* 80(46):F526.

Koepke, J., Feig, S.T., Snow, J., and Freise, M., 2004. Petrogenesis of oceanic plagiogranites by partial melting of gabbros: an experimental study. *Contributions to Mineralogy and Petrology,* 146(4):414–432. **http://dx.doi.org/10.1007/s00410-003-0511-9**

Lavier, L., Buck, W.R., and Poliakov, A.N.B., 1999. Self-consistent rolling-hinge model for the evolution of large-offset low-angle normal faults. *Geology,* 27(12):1127–1130. **http://dx.doi.org/10.1130/0091-7613(1999)027<1127:SCRHMF>2.3.CO;2**

Lever, M.A., Rouxel, O., Alt, J.C., Shimizu, N., Ono, S., Coggon, R.M., Shanks, W.C., III, Laphan, L., Elvert, M., Prieto-Mollar, X., Hinrichs, K.-U., Inagaki, F., and Teske, A., 2013. Evidence for microbial carbon and sulfur cycling in deeply buried ridge flank basalt. *Science,* 339(6125):1305–1308. **http://dx.doi.org/10.1126/science.1229240**

Lissenberg, C.J., MacLeod, C.J., Howard, K.A., and Godard, M., 2013. Pervasive reactive melt migration through fast-spreading lower oceanic crust (Hess Deep, equatorial Pacific Ocean). *Earth and Planetary Science Letters,* 361:436–447. **http://dx.doi.org/10.1016/j.epsl.2012.11.012**

MacLeod, C.J., Dick, H.J.B., Allerton, S., Robinson, P.T., Coogan, L.A., Edwards, S.J., Galley, A., Gillis, K.M., Hirth, G., Hunter, A.G., Hutchinson, D., Kvassnes, A.J., Natland, J.H., Salisbury, M., Schandl, E.S., Stakes, D.S., Thompson, G.M., and Tivey, M.A., 1998. Geological mapping of slow-spread lower ocean crust: a deep-towed video and wireline rock drilling survey of Atlantis Bank (ODP Site 735, SW Indian Ridge). *InterRidge News,* 7(2):39–43.

MacLeod, C.J., Escartin, J., Banerji, D., Banks, G.J., Gleeson, M., Irving, D.H.B., Lilly, R.M., McCaig, A.M., Niu, Y., Allerton, S., and Smith, D.K., 2002. Direct geological evidence for oceanic detachment faulting: the Mid-Atlantic Ridge, 15°45′N. *Geology,* 30(10):879–882. **http://dx.doi.org/10.1130/0091-7613(2002)030<0879:DGEFOD>2.0.CO;2**

MacLeod, C.J., Searle, R.C., Murton, B.J., Casey, J.F., Mallows, C., Unsworth, S.C., Achenbach, K.L., and Harris, M., 2009. Life cycle of oceanic core complexes. *Earth and Planetary Science Letters,* 287(3–4):333–344. **http://dx.doi.org/10.1016/j.epsl.2009.08.016**

MacLeod, C.J., Wright, W.P., Perry, C.T., and Dick, H.J.B., 2000. Tectonic evolution and uplift/subsidence history of Atlantis Bank, a Transverse Ridge near the Atlantis II Fracture Zone, SW Indian Ridge. *Eos, Transactions of the American Geophysical Union,* 81:1129.

Mason, O.U., Nakagawa, T., Rosner, M., Van Nostrand, J.D., Zhou, J., Maruyama, A., Fisk, M.R., and Giovannoni, S.J., 2010. First investigation of the microbiology of the deepest layer of ocean crust. *PLoS One,* 5(11):e15399. **http://dx.doi.org/10.1371/journal.pone.0015399**

Matsumoto, T., Dick, H.J.B., and Scientific Party, 2002. Investigation of Atlantis Bank and the SW Indian Ridge from 568E to 588E: Preliminary Report: Tokyo (Japanese Agency for Marine-Earth Science and Technology).

Mendel, V., Sauter, D., Parson, L., and Vanney, J.-R., 1997. Segmentation and morphotectonic variations along a super slow-spreading center: the Southwest Indian Ridge (57° E–70° E). *Marine Geophysical Research,* 19(6):505–533. **http://dx.doi.org/10.1023/A:1004232506333**

Mendel, V., Sauter, D., Rommevaux-Jestin, C., Patriat, P., Lefebvre, F., and Parson, L.M., 2003. Magmato-tectonic cyclicity at the ultra-slow spreading Southwest Indian Ridge: evidence from variations of axial volcanic ridge morphology and abyssal hills pattern. *Geochemistry, Geophysics, Geosystems,* 4(5):9102. **http://dx.doi.org/10.1029/2002GC000417**

Ménez, B., Pasini V., and Brunelli, D., 2012. Life in the hydrated suboceanic mantle. *Nature Geoscience,* 5(2):133–137. **http://dx.doi.org/10.1038/ngeo1359**

Miller, D.J., and Christensen, N.I., 1997. Seismic velocities of lower crustal and upper mantle rocks from the slow-spreading Mid-Atlantic Ridge, south of the Kane Transform Zone (MARK). *In* Karson, J.A., Cannat, M., Miller, D.J., and Elthon, D. (Eds.), *Proceedings of the Ocean Drilling Program, Scientific Results,* 153: College Station, TX (Ocean Drilling Program), 437–454. **http://dx.doi.org/10.2973/odp.proc.sr.153.043.1997**

Minshull, T.A., Muller, M.R., Robinson, C.J., White, R.S., and Bickle, M.J., 1998. Is the oceanic Moho a serpentinization front? *In* Mills, R.A., and Harrison, K. (Eds.), *Modern Ocean Floor Processes and the Geological Record.* Geological Society Special Publications, 148(1):71–80. **http://dx.doi.org/10.1144/GSL.SP.1998.148.01.05**

Miranda, E.A., and John, B.E., 2010. Strain localization along the Atlantis Bank oceanic detachment fault system, Southwest Indian Ridge. *Geochemistry, Geophysics, Geosystems,* 11(4):Q04002. **http://dx.doi.org/10.1029/2009GC002646**

Muller, M.R., Minshull, T.A., and White, R.S., 2000. Crustal structure of the Southwest Indian Ridge at the Atlantis II Fracture Zone. *Journal of Geophysical Research: Solid Earth,* 105(B11):25809–25828. **http://dx.doi.org/10.1029/2000JB900262**

Muller, M.R., Robinson, C.J., Minshull, T.A., White, R.S., and Bickle, M.J., 1997. Thin crust beneath Ocean Drilling Program Borehole 735B at the Southwest Indian Ridge? *Earth and Planetary Science Letters,* 148(1–2):93–107. **http://dx.doi.org/10.1016/S0012-821X(97)00030-7**

Mutter, J.C., and Karson, J.A., 1992. Structural processes at slow-spreading ridges. *Science,* 257(5070):627–634. **http://dx.doi.org/10.1126/science.257.5070.627**

Natland, J.H., Meyer, P.S., Dick, H.J.B., and Bloomer, S.H., 1991. Magmatic oxides and sulfides in gabbroic rocks from Hole 735B and the later development of the liquid line of descent. *In* Von Herzen, R.P., Robinson, P.T., et al., *Proceedings of the Ocean Drilling Program, Scientific Results,* 118: College Station, TX (Ocean Drilling Program), 75–111. **http://dx.doi.org/10.2973/odp.proc.sr.118.163.1991**

Natland, J.H., and Dick, H.J.B., 2001. Formation of the lower ocean crust and the crystallization of gabbroic cumulates at a very slowly spreading ridge. *Journal of Volcanology and Geothermal Research,* 110(3–4):191–233. **http://dx.doi.org/10.1016/S0377-0273(01)00211-6**

Natland, J.H., and Dick, H.J.B., 2002. Stratigraphy and composition of gabbros drilled in Ocean Drilling Program Hole 735B, Southwest Indian Ridge: a synthesis of geochemical data. *In* Natland, J.H., Dick, H.J.B., Miller, D.J., and Von Herzen, R.P. (Eds.), *Proceedings of the Ocean Drilling Program, Scientific Results,* 176: College Station, TX (Ocean Drilling Program), 1–69. **http://dx.doi.org/10.2973/odp.proc.sr.176.002.2002**

Orcutt, B.N., Wheat, C.G., Rouxel, O., Hulme, S., Edwards, K.J., and Bach, W., 2013. Oxygen consumption rates in subseafloor basaltic crust derived from a reaction transport model. *Nature Communications,* 4:2539. **http://dx.doi.org/10.1038/ncomms3539**

Orsi, W., Biddle, J.F., and Edgcomb, V., 2013a. Deep sequencing of subseafloor eukaryotic rRNA reveals active fungi across marine subsurface provinces.

PLoS ONE, 8(2):e56335. **http://dx.doi.org/10.1371/journal.pone.0056335**

Orsi, W.D., Edgcomb, V.P., Christman, G.D., and Biddle, J.F., 2013b. Gene expression in the deep biosphere. *Nature,* 499(7457):205–208. **http://dx.doi.org/10.1038/nature12230**

Palmiotto, C., Corda, L., Ligi, M., Cipriani, A., Dick, H.J.B., Douville, E., Gasperini, L., Montagna, P., Thil, F., Borsetti, A.M., Balestra, B., and Bonatti, E., 2013. Nonvolcanic tectonic islands in ancient and modern oceans. *Geochemistry, Geophysics, Geosystems,* 14(10):4698–4717. **http://dx.doi.org/10.1002/ggge.20279**

Parkes, R.J., Cragg, B.A., Bale, S.J., Getliff, J.M., Goodman, K., Rochelle, P.A., Fry, J.C., Weightman, A.J., and Harvey, S.M., 1994. Deep bacterial biosphere in Pacific Ocean sediments. *Nature,* 371(6496):410–413. **http://dx.doi.org/10.1038/371410a0**

Pettigrew, T.L., Casey, J.F., Miller, D.J., et al., 1999. *Proceedings of the Ocean Drilling Program, Initial Reports,* 179: College Station, TX (Ocean Drilling Program). **http://dx.doi.org/10.2973/odp.proc.ir.179.1999**

Proskurowski, G., Lilley, M.D., Seewald, J.S., Früh-Green, G.L., Olson, E.J., Lupton, J.E., Sylva, S.P., and Kelley, D.S., 2008. Abiogenic hydrocarbon production at Lost City hydrothermal field. *Science*, 319(5863):604–607. **http://dx.doi.org/10.1126/science.1151194**

Robinson, P.T., Von Herzen, R., et al., 1989. *Proceedings of the Ocean Drilling Program, Initial Reports,* 118: College Station, TX (Ocean Drilling Program). **http://dx.doi.org/10.2973/odp.proc.ir.118.1989**

Sauter, D., Cannat, M., Rouméjon, S., Andreani, M., Birot, D., Bronner, A., Brunelli, D., Carlut, J., Delacour, A., Guyader, V., MacLeod, C.J., Manatschal, G., Mendel, V., Ménez, B., Pasini, V., Ruellan, E., and Searle, R., 2013. Continuous exhumation of mantle-derived rocks at the Southwest Indian Ridge for 11 million years. *Nature Geoscience,* 6(4):314–320. **http://dx.doi.org/10.1038/ngeo1771**

Sauter, D., Carton, H., Mendel, V., Munschy, M., Rommevaux-Jestin, C., Schott, J.-J., and Whitechurch, H., 2004. Ridge segmentation and the magnetic structure of the Southwest Indian Ridge (at 50°30′E, 55°30′E, and 66°20′E): implications for magmatic processes at ultraslow-spreading centers. *Geochemistry, Geophysics, Geosystems,* 5(5):Q05K08. **http://dx.doi.org/10.1029/2003GC000581**

Schroeder, T., and John, B.E., 2004. Strain localization on an oceanic detachment fault system, Atlantis Massif, 30°N, Mid-Atlantic Ridge. *Geochemistry, Geophysics, Geosystems,* 5:Q11007. **http://dx.doi.org/10.1029/2004GC000728**

Shock, E.L., 2009. Minerals as energy sources for microorganisms. *Economic Geology,* 104(8):1235–1248. **http://dx.doi.org/10.2113/gsecongeo.104.8.1235**

Sinton, J.M., and Detrick, R.S., 1992. Mid-ocean ridge magma chambers. *Journal of Geophysical Research: Solid Earth,* 97(B1):197–216. **http://dx.doi.org/10.1029/91JB02508**

Smith, D.K., Cann, J.R., and Escartin, J., 2006. Widespread active detachment faulting and core complex formation near 13°N on the Mid-Atlantic Ridge. *Nature,* 442(7101):440–443. **http://dx.doi.org/10.1038/nature04950**

Sylvan, J.B., Hoffman, C.L., Momper, L.M., Toner, B.M., Amend, J.P., and Edwards, K.J., 2015. *Bacillus rigiliprofundi* sp. nov., an endospore-forming, Mn-oxidizing, moderately halophilic bacterium isolated from deep subseafloor basaltic crust. *International Journal of Systematic and Evolutionary Microbiology,* 65:1992–1998. **http://dx.doi.org/10.1099/ijs.0.000211**

Till, J.L., and Moskowitz, B., 2013. Magnetite deformation mechanism maps for better prediction of strain partitioning. *Geophysical Research Letters,* 40(4):697–702. **http://dx.doi.org/10.1002/grl.50170**

Tucholke, B.E., Lin, J., and Kleinrock, M.C., 1998. Megamullions and mullion structure defining oceanic metamorphic core complexes on the Mid-Atlantic Ridge. *Journal of Geophysical Research: Solid Earth,* 103(B5):9857–9866. **http://dx.doi.org/10.1029/98JB00167**

Wrinch, D., and Jeffreys, H., 1923. On the seismic waves from the Oppau explosion of 1921 Sept. 21. *Geophysical Journal International,* 1(Supplement s2):15–22 **http://dx.doi.org/10.1111/j.1365-246X.1923.tb06565.x**

Table T1. Coring summary, Hole U1473A. For more information on bottom-hole assembly (BHA) runs, see Table **T2**. DSF = drilling depth below seafloor, CSF-A = core depth below seafloor, method A. Core type: G = ghost, M = miscellaneous, R = rotary core barrel, numeric core type = drilled interval. MBR = mechanical bit release. (Continued on next page.)

Core, type	Top depth drilled DSF (m)	Bottom depth drilled DSF (m)	Advanced (m)	Recovered length (m)	Curated length (m)	Top depth cored CSF-A (m)	Bottom depth recovered CSF-A (m)	Recovery (%)	Date on deck	Time on deck UTC (h)	Sections (*N*)	BHA run number	Operational episode description
360-U1473A-													
11			****Drilled interval from 0.00 to 9.5 m DSF*****						18 Dec 2015	1445	0	2	Install reentry system
2R	9.5	12.8	3.3	2.25	2.45	9.5	11.95	68	19 Dec 2015	2345	2	3	Coring Episode 1
3R	12.8	22.4	9.6	4.24	5.10	12.8	17.90	44	20 Dec 2015	0535	4		
4R	22.4	32.0	9.6	6.27	8.41	22.4	30.81	65	20 Dec 2015	1230	6		
5R	32.0	41.6	9.6	2.07	2.05	32.0	34.05	22	20 Dec 2015	1615	2		
6R	41.6	51.3	9.7	3.08	4.08	41.6	45.68	32	20 Dec 2015	1950	3		
7R	51.3	61.0	9.7	1.92	2.27	51.3	53.57	20	21 Dec 2015	0005	2		
8R	61.0	70.7	9.7	4.92	5.82	61.0	66.82	51	21 Dec 2015	0610	4		
9R	70.7	80.4	9.7	5.92	7.14	70.7	77.84	61	21 Dec 2015	1045	5		
10R	80.4	90.1	9.7	3.07	3.43	80.4	83.83	32	22 Dec 2015	0355	3	4	
11R	90.1	99.8	9.7	6.19	7.01	90.1	97.11	64	22 Dec 2015	0820	5		
12R	99.8	109.5	9.7	6.30	6.68	99.8	106.48	65	22 Dec 2015	1135	5		
13R	109.5	119.2	9.7	5.42	5.85	109.5	115.35	56	22 Dec 2015	1625	5		
14R	119.2	128.9	9.7	6.09	7.16	119.2	126.36	63	22 Dec 2015	2225	5		
15R	128.9	138.6	9.7	7.21	8.70	128.9	137.60	74	23 Dec 2015	0340	7		
16R	138.6	148.3	9.7	7.84	8.83	138.6	147.43	81	23 Dec 2015	1010	6		
17R	148.3	158.0	9.7	5.94	7.06	148.3	155.36	61	23 Dec 2015	1550	5		
18R	158.0	167.7	9.7	4.64	5.48	158.0	163.48	48	23 Dec 2015	2350	4		
19R	167.7	177.4	9.7	2.30	3.01	167.7	170.71	24	24 Dec 2015	1305	2	5	
20R	177.4	180.1	2.7	2.15	2.44	177.4	179.84	80	24 Dec 2015	1530	2		
21R	180.1	187.1	7.0	4.00	4.60	180.1	184.70	57	25 Dec 2015	1225	4		
22R	187.1	196.8	9.7	1.56	1.95	187.1	189.05	16	25 Dec 2015	1510	2		
23R	196.8	206.5	9.7	4.12	5.69	196.8	202.49	42	25 Dec 2015	1815	4		
24R	206.5	216.2	9.7	3.67	4.83	206.5	211.33	38	25 Dec 2015	2135	4		
25R	216.2	225.9	9.7	2.65	3.33	216.2	219.53	27	26 Dec 2015	0130	3		
26R	225.9	235.6	9.7	3.28	4.24	225.9	230.14	34	26 Dec 2015	0615	3		
27R	235.6	245.3	9.7	7.48	8.23	235.6	243.83	77	26 Dec 2015	1000	6		
28R	245.3	255.0	9.7	7.22	7.35	245.3	252.65	74	26 Dec 2015	1400	5		
29R	255.0	264.7	9.7	6.82	7.34	255.0	262.34	70	26 Dec 2015	1820	5		
30R	264.7	274.4	9.7	5.79	6.64	264.7	271.34	60	26 Dec 2015	2135	5		
31R	274.4	284.1	9.7	2.70	3.65	274.4	278.05	28	27 Dec 2015	0010	3		
32R	284.1	293.8	9.7	7.43	8.72	284.1	292.82	77	27 Dec 2015	0400	6		
33R	293.8	303.5	9.7	6.03	6.65	293.8	300.45	62	27 Dec 2015	0810	5		
34R	303.5	313.2	9.7	6.77	7.53	303.5	311.03	70	27 Dec 2015	1210	6		
35R	313.2	322.9	9.7	2.40	2.89	313.2	316.09	25	28 Dec 2015	0220	2	6	
36R	322.9	332.6	9.7	3.02	3.92	322.9	326.82	31	28 Dec 2015	0530	3		
37R	332.6	342.3	9.7	4.57	5.90	332.6	338.50	47	28 Dec 2015	0855	4		
38R	342.3	352.0	9.7	4.36	5.06	342.3	347.36	45	28 Dec 2015	1415	4		
39R	352.0	361.7	9.7	7.06	8.37	352.0	360.37	73	28 Dec 2015	1850	6		
40R	361.7	371.4	9.7	2.17	2.41	361.7	364.11	22	29 Dec 2015	0040	2		
41R	371.4	381.1	9.7	7.09	7.99	371.4	379.39	73	29 Dec 2015	0520	6		
42R	381.1	390.8	9.7	4.06	4.92	381.1	386.02	42	29 Dec 2015	0935	4		
43R	390.8	400.5	9.7	9.25	10.02	390.8	400.82	95	29 Dec 2015	1440	8		
44R	400.5	410.2	9.7	5.44	6.42	400.5	406.92	56	29 Dec 2015	2140	5		
45M	410.2	410.8	0.6	0.50	1.25	410.2	411.45	83	7 Jan 2016	1130	1	10	Fishing for roller cones
46R	410.8	420.5	9.7	2.59	3.94	410.8	414.74	27	8 Jan 2016	0425	3	11	Coring Episode 2 and two roller cones lost and found
47R	420.5	430.2	9.7	4.04	5.29	420.5	425.79	42	8 Jan 2016	0815	4		
48R	430.2	439.9	9.7	2.69	3.83	430.2	434.03	28	8 Jan 2016	1035	3		
49R	439.9	449.6	9.7	0.98	1.31	439.9	441.21	10	8 Jan 2016	1830	1		
50R	449.6	459.3	9.7	3.52	4.50	449.6	454.10	36	9 Jan 2016	0015	3		
51R	459.3	469.0	9.7	5.72	6.40	459.3	465.70	59	9 Jan 2016	0505	5		
52R	469.0	469.6	0.6	0.42	0.49	469.0	469.49	70	9 Jan 2016	0725	1		
53R	469.6	470.6	1.0	0.00	0.00	469.6	469.60	0	11 Jan 2016	0045	0	14	Advance limited; recovery prevented by roller cone stuck in bit
54R	470.6	480.3	9.7	0.00	0.00	470.6	470.60	0	11 Jan 2016	0635	0		
55R	480.3	481.7	1.4	0.00	0.00	480.3	480.30	0	11 Jan 2016	1100	0		
561			*****Drilled interval from 481.7 to 519.2 m DSF*****						13 Jan 2016	1130	0	16	Drilling without coring
57R	519.2	519.6	0.4	0.40	0.40	519.2	519.60	100	14 Jan 2016	0400	1	17	Coring Episode 3
58R	519.6	529.2	9.6	9.48	10.35	519.6	529.95	99	14 Jan 2016	0750	8		
59R	529.2	538.8	9.6	6.50	6.84	529.2	536.04	68	14 Jan 2016	1315	5		
60R	538.8	548.4	9.6	5.16	6.19	538.8	544.99	54	14 Jan 2016	1845	5		

Table T1 (continued).

Core, type	Top depth drilled DSF (m)	Bottom depth drilled DSF (m)	Advanced (m)	Recovered length (m)	Curated length (m)	Top depth cored CSF-A (m)	Bottom depth recovered CSF-A (m)	Recovery (%)	Date on deck	Time on deck UTC (h)	Sections (*N*)	BHA run number	Operational episode description
61R	548.4	558.1	9.7	6.72	7.61	548.4	556.01	69	15 Jan 2016	0040	6		
62R	558.1	567.8	9.7	7.01	7.63	558.1	565.73	72	15 Jan 2016	0420	6		
63R	567.8	577.5	9.7	2.22	2.72	567.8	570.52	23	15 Jan 2016	0830	2		
64R	577.5	587.2	9.7	9.37	9.76	577.5	587.26	97	15 Jan 2016	1350	9		
65R	587.2	596.9	9.7	9.32	9.77	587.2	596.97	96	15 Jan 2016	2045	7		
66R	596.9	606.6	9.7	8.74	9.06	596.9	605.96	90	16 Jan 2016	0235	7		
67R	606.6	616.3	9.7	9.73	10.32	606.6	616.92	100	16 Jan 2016	2125	8	18	
68R	616.3	626.0	9.7	9.23	9.67	616.3	625.97	95	17 Jan 2016	0235	7		
69R	626.0	635.7	9.7	9.80	10.26	626.0	636.26	101	17 Jan 2016	0850	8		
70R	635.7	645.4	9.7	8.87	9.09	635.7	644.79	91	17 Jan 2016	1415	8		
71R	645.4	648.4	3.0	3.62	3.76	645.4	649.16	121	17 Jan 2016	1805	3		
72R	648.4	651.9	3.5	3.60	3.71	648.4	652.11	103	18 Jan 2016	1145	3	19	
73R	651.9	654.6	2.7	1.85	2.03	651.9	653.93	69	19 Jan 2016	0050	2	20	
74R	654.6	664.3	9.7	10.09	10.35	654.6	664.95	104	19 Jan 2016	0605	9		
75R	664.3	674.0	9.7	9.88	10.28	664.3	674.58	102	19 Jan 2016	1120	8		
76R	674.0	680.7	6.7	5.16	5.31	674.0	679.31	77	19 Jan 2016	1710	5		
77R	680.7	683.7	3.0	2.29	2.42	680.7	683.12	76	19 Jan 2016	2115	2		
78R	683.7	693.4	9.7	9.94	10.56	683.7	694.26	102	20 Jan 2016	0330	8		
79R	693.4	703.1	9.7	8.94	9.54	693.4	702.94	92	20 Jan 2016	0805	8		
80R	703.1	712.8	9.7	9.86	10.26	703.1	713.36	102	20 Jan 2016	1440	9		
81R	712.8	721.3	8.5	7.62	8.55	712.8	721.35	90	20 Jan 2016	2155	6		
82R	721.3	731.0	9.7	9.80	10.01	721.3	731.31	101	21 Jan 2016	1745	8	21	
83R	731.0	740.7	9.7	9.64	10.00	731.0	741.00	99	22 Jan 2016	0205	9		
84R	740.7	750.4	9.7	9.52	9.75	740.7	750.45	98	22 Jan 2016	0705	7		
85R	750.4	756.1	5.7	5.04	5.27	750.4	755.67	88	22 Jan 2016	1325	4		
86R	756.1	760.1	4.0	3.27	3.38	756.1	759.48	82	22 Jan 2016	1720	3		
87R	760.1	769.8	9.7	9.64	9.88	760.1	769.98	99	22 Jan 2016	2340	9		
88R	769.8	779.5	9.7	9.39	9.72	769.8	779.52	97	23 Jan 2016	0445	8		
89R	779.5	789.2	9.7	9.73	10.06	779.5	789.56	100	23 Jan 2016	1000	8		
90G	9.5	789.2	779.7	0.25	0.25	9.5	9.75		25 Jan 2016	1500	1	22	Successful logging (MBR problem)
91M	789.2	789.7	0.5	0.50	0.50	789.2	789.70	100	27 Jan 2016	0230	1	24	
		Total:	1569.4	469.4									

Table T2. Operational summary information by bottom-hole assembly (BHA) run number. For coring summary, see Table **T1**. XCB = extended core barrel, RCB = rotary core barrel, TC = tricone, FM = fishing magnet, RCJB = reverse circulation junk basket. DIC = drill-in casing. WOW = waiting on weather. MBR = mechanical bit release. NA = not applicable.

BHA run	Bit type/ instance	Reentry date	Reentry time UTC + 4 (h)	Reentry number	Run advance (m)	Run recovery (m)	Run recovery (%)	Comment	Major operational episode	Episode advance (m)	Episode recovery (m)	Episode recovery (%)
1	XCB							Seafloor survey to select drill site	Install reentry system	9.5	NA	NA
2	TC 1	18 Dec 2015	0530		9.5			Bare-rock spud-in with mud motor and DIC				
3	RCB 1	19 Dec 2015	1535	1	70.9	30.7	43	Coring Run 1	Coring Episode 1	400.7	207.0	52
4	RCB 2	21 Dec 2015	2335	2	87.3	52.7	60	Coring Run 2				
5	RCB 3	24 Dec 2015	1137	3	145.5	74.2	51	Coring Run 3				
		25 Dec 2015	1122	4				Reentry after WOW (13.25 h)				
6	RCB 4	28 Dec 2015	0008	5	97.0	49.4	51	Coring Run 4; lost three roller cones				
7	FM 1	30 Dec 2015	1244	6	0.0			FM did not retrieve roller cones	Fishing for roller cones (and medivac)	0.6	0.5	83
8	FM 2	5 Jan 2016	2146	7	0.0			Recovered little metal, no cone				
9	RCJB 1	6 Jan 2016	1330	8	0.0			Recovered gravel but no cone				
10	RCJB 2	7 Jan 2016	0555	9	0.6	0.5	83	RCJB took a core (but none of three cones)!				
11	RCB 5	7 Jan 2016	2320	10	58.8	20.0	34	Lost a roller cone	Coring Episode 2 and two roller cones lost and found	70.9	20.0	28
12	RCJB 3	9 Jan 2016	2007	11	0.0			Recovered gravel but no cone				
13	RCJB 4	10 Jan 2016	0846	12	0.0			RCJB recovered cobble and a roller cone!				
14	RCB 6	10 Jan 2016	2037	13	12.1	0.0	0	Slow advance, no recovery; depluggers; lost cone				
15	FM 3	12 Jan 2016	0321	14	0.0			Recovered roller cone!				
16	TC 2	12 Jan 2016	1545	15	37.5			Drilled interval	Drilling without coring	37.5	NA	NA
17	RCB 7	14 Jan 2016	0210	16	87.4	64.9	74		Coring Episode 3	270.0	241.4	89
18	RCB 8	16 Jan 2016	1424	17	41.8	41.3	99	Ended in WOW				
19	RCB 9	18 Jan 2016	0653	18	3.5	3.6	103	Got stuck at 1215 h				
20	RCB 9	18 Jan 2016	2315	19	69.4	65.6	95	Reused previous bit, worn out at the end				
21	RCB 10	21 Jan 2016	1038	20	67.9	66.0	97	Dropped bit on seafloor using MBR				
	Log	23 Jan 2016	2145	21				Three successful logging runs	Successful logging (and MBR problem)	0.5	0.5	100
22	FM 4	25 Jan 2016	1012	22				MBR sleeve retainer ring not recovered				
23	RCB 11	25 Jan 2016	2230	23	0.0	0.0	0	No advance achieved				
24	RCJB 5	26 Jan 2016	1420	24	0.5	0.5	100	Recovered cobbles with clear tool marks				
									Totals including drilled intervals:	789.7	469.4	59
									Totals including only cored intervals:	742.7	469.4	63

Table T3. Webcasts conducted during Expedition 360.

Country	Number of webcasts	Number of participants
USA	47	2081
France	42	2566
UK	8	193
Canada	6	195
Japan	3	148
Italy	3	206
Portugal	2	96
Germany	2	120
China	1	60
Thailand	1	10
Switzerland	1	30
Philippines	1	25
Danemark	1	42
Berlin	1	70
Belgium	1	70
Romania	1	35
Total:	120	5947

Table T4. Readership (post views) and engagement (likes, shares, or replies to posts) of the *JOIDES Resolution* social media networks during Expedition 360. NA = not available.

Website	Posts	Reach	Engagements
Twitter	87	126,903	3,089
Facebook	92	200,265	12,326
Instagram	42	NA	544
Blog	53	22,897	NA
Totals	274	350,065	15,959

Table T5. Media highlights published or broadcast during Expedition 360. See Table **T6** for complete list of coverage. NA = not available.

Agency	Country	Language	Type of media	Date	Title	Estimated reach of publication	URL
BBC	UK	English	Website	1 Dec 2015	Bid to Drill Deep Inside Earth	800,000 (article specific readers)	http://www.bbc.com/news/science-environment-34967750
Nature	US	English	Magazine/ Website	1 Dec 2015	Quest to Drill into Earth's Mantle Restarts	3,000,000 (online); 54,000 (print)	http://www.nature.com/news/quest-to-drill-into-earth-s-mantle-restarts-1.18921
BBC World News	UK	English	Television	6 Dec 2015	Drilling Expedition: Scientists on their way to Indian Ocean	NA	NA
ABC The World	Australia	English	Television	18 Dec 2015	Scientists are Preparing to Drill Deeper into the Earth Than Ever Before	NA	NA
Boston Globe	US	English	Newspaper/ Website	22 Dec 2015	A Woods Hole Scientist Attempts to Drill Through Earth's Crust	250,000 (print)	http://www.bostonglobe.com/ideas/2015/12/22/brainiac-drilling/qqacEhZAgzylDfsW2H6rPN/story.html
La Repubblica	Italy	Italian	Newspaper	24 Dec 2015	Viaggio Sotto La Crosta Della Terra. Due Italiani Nel Team	300,000 (print)	NA
de Volkskant	Netherlands	Dutch	Newspaper/ Website	9 Jan 2016	Boren Waar Niemand Ooit Heeft Geboord	250,000 (print)	http://www.volkskrant.nl/wetenschap/boren-waar-niemand-ooit-heeft-geboord~a4221009/
CBBC	UK	English	Television	14 Jan 2016	Mission to Drill Deep into the Earth's Crust	NA	http://www.bbc.co.uk/newsround/35304334
Science Friday	US	English	Radio	22 Jan 2016	Digging Deep into the Crust of the Earth	1,500,000	http://www.sciencefriday.com/segments/digging-deep-into-the-crust-of-the-earth/
Smithsonian	US	English	Magazine/ Website	26 Jan 2016	A Decades-Long Quest to Drill Into Earth's Mantle may Soon Hit Pay Dirt	2,000,000 (print)	http://www.smithsonianmag.com/science-nature/decades-long-quest-drill-earths-mantle-may-soon-hit-pay-dirt-180957908/
Xinhua News Agency	China	Mandarin	Newspapers/ Websites	Entire expedition	30 news reports, 100 photographs	NA	Multiple

Table T6. All media coverage published or broadcast during Expedition 360. NA = not available. (Continued on next two pages.)

Agency	Country	Language	Type of media	Date	Title	Estimated reach of publication	URL
Huffington Post UK	UK	English	Website	1 Dec 2015	Scientists Plan World-Record Drilling Attempt To Go Deeper Into The Earth's Crust Than Ever Before	NA	http://www.huffingtonpost.co.uk/2015/12/01/scientists-plan-world-record-drilling-attempt-to-go-deeper-into-the-earths-crust-than-ever-before_n_8686536.html
The Reveille	Pakistan	English	Website	1 Dec 2015	Environmental Sciences: Bid to drill deep inside Earth	NA	http://www.thereveillenwu.com/2015/12/01/environmental-sciences-bid-to-drill-deep-inside-earth/
Next Big Future	US	English	Website	1 Dec 2015	Researchers hope to drill through crust to the Mantle at the crusts thinnest point	NA	http://nextbigfuture.com/2015/12/researchers-hope-to-drill-through-crust.html
Yahoo News	US	English	Website	1 Dec 2015	This week, geologists will attempt to drill through Earth's crust and into the mantle	NA	http://finance.yahoo.com/news/starting-week-scientists-attempt-drill-212156427.html
BBC	UK	English	Website	1 Dec 2015	Bid to Drill Deep Inside Earth	800,000 (article specific readers)	http://www.bbc.com/news/science-environment-34967750
Nature	US	English	Magazine/ Website	1 Dec 2015	Quest to Drill into Earth's Mantle Restarts	3,000,000 (online); 54,000 (print)	http://www.nature.com/news/quest-to-drill-into-earth-s-mantle-restarts-1.18921
Daily Express	UK	English	Website	2 Dec 2015	WARNING: Scientists could spark MEGAQUAKE as they drill below Earth's crust for first time	488,000	http://www.express.co.uk/news/science/623518/Fears-scientists-fracking-volcanic-sea-bed-trigger-mega-earthquake
IFLScience	UK	English	Website	2 Dec 2015	Scientists Plan To Drill Beneath The Earth's Crust For The First Time	NA	http://www.iflscience.com/journey-centre-earth-begins
International Business Times	US	English	Website	2 Dec 2015	Scientists to enter Earth's mantle for the first time	NA	http://www.ibtimes.com.au/scientists-enter-earths-mantle-first-time-1488723

Table T6 (continued). (Continued on next page).

Agency	Country	Language	Type of media	Date	Title	Estimated reach of publication	URL
Daily Mail	UK	English	Newspaper/ Website	2 Dec 2015	Mission to drill into our planet's crust will search for samples in the super-hot rock	1,700,000	http://www.dailymail.co.uk/sciencetech/article-3342572/Is-life-hidden-Earth-s-mantle-Mission-drill-planet-s-crust-search-samples-super-hot-rock.html
Global Research	Canada	English	Website	3 Dec 2015	A Mission to Drill Right through the Earth's Crust	NA	http://www.globalresearch.ca/a-mission-to-drill-right-through-the-earths-crust/5499100
Science Alert	Australia	English	Website	3 Dec 2015	A mission to drill right through Earth's crust begins this week	NA	http://www.sciencealert.com/a-mission-to-drill-right-through-earth-s-crust-begins-this-week
The Age	Australia	English	Website	4 Dec 2015	Planned journey to the mantle of the Earth will break records	131,000	http://www.theage.com.au/technology/sci-tech/planned-journey-to-the-mantle-of-the-earth-will-break-records-20151203-glel8i.html
Jimmy Fallon	US	English	Television	4 Dec 2015	Molologue joke: "It'll all be worth it if they find a candy center"	3,900,000	NA
Gizmodo	US	English	Website	5 Dec 2015	Humans Are Once Again Attempting to Reach Earth's Mantle	NA (alexa rank: 421)	http://gizmodo.com/humans-are-once-again-attempting-to-reach-earths-mantle-1746388432
BBC World News	UK	English	Television	6 Dec 2015	Drilling Expedition: Scientists on their way to Indian Ocean	NA	NA
BBC Radio	UK	English	Radio	6 Dec 2015	NA	NA	http://www.bbc.co.uk/programmes/p039jtt7
Le Monde	France	French	Website	9 Dec 2015	Pourquoi des chercheurs vont percer la croûte terrestre	NA	http://passeurdesciences.blog.lemonde.fr/2015/12/09/pourquoi-des-chercheurs-vont-percer-la-croute-terrestre/
Care2	US	English	Website	13 Dec 2015	Scientists Are Getting Ready to Drill Into Earth's Mantle	NA	http://www.care2.com/causes/scientists-are-getting-ready-to-drill-into-earths-mantle.html
ABC The World	Australia	English	Television	18 Dec 2015	Scientists are Preparing to Drill Deeper into the Earth Than Ever Before	NA	NA
Boston Globe	US	English	Newspaper/ Website	22 Dec 2015	A Woods Hole Scientist Attempts to Drill Through Earth's Crust	250,000 (print)	https://www.bostonglobe.com/ideas/2015/12/22/brainiac-drilling/qqacEhZAgzylDfsW2H6rPN/story.html
La Repubblica	Italy	Italian	Newspaper	24 Dec 2015	Viaggio Sotto La Crosta Della Terra. Due Italiani Nel Team	300,000 (print)	NA
The Globe and Mail	Canada	English	Website	30 Dec 2015	Fire up your neurons with The Globe's 2015 science quiz	NA	http://www.theglobeandmail.com/technology/science/2015-science-quiz/article27957224/
How Stuff Works	US	English	Website	30 Dec 2015	This Ship Hopes to Be the First to Drill Beneath the Earth's Crust	NA	http://now.howstuffworks.com/2015/12/29/ship-drill-earth-crust
Beijing News	China	Mandarin	Newspaper/ Website	1 Jan 2016	Drilling in the thinnest crust	NA	http://www.bjnews.com.cn/world/2016/01/01/390188.html
Spudouest Dimanche	France	French	Newspaper	3 Jan 2016	Elle dispense ses cours depuis l'Océan indien	NA	NA
WBUR: Radio Boston	US	English	Radio	5 Jan 2016	NA	NA	NA
de Volkskant	Netherlands	Dutch	Newspaper/ Website	9 Jan 2016	Boren Waar Niemand Ooit Heeft Geboord	250,000 (print)	http://www.volkskrant.nl/wetenschap/boren-waar-niemand-ooit-heeft-geboord~a4221009/
MeteoWeb	Italy	Italian	Website	11 Jan 2016	JOIDES Resolution, nuovo tentativo di perforare la crosta terrestre fino al mantello	NA	NA
CBBC	UK	English	Television	14 Jan 2016	Mission to Drill Deep into the Earth's Crust	NA	http://www.bbc.co.uk/newsround/35304334
ISTOÉ Independente	Portugal	Portugese	Magazine/ Website	15 Jan 2016	Viagem ao centro da Terra	362,000	http://www.istoe.com.br/reportagens/444711_VIAGEM+AO+CENTRO+DA+TERRA
Livingston County News	US	English	Newspaper/ Website	20 Jan 2016	Avon students make virtual visit to scientific drilling ship	NA	http://www.thedailynewsonline.com/lcn05/avon-students-make-virtual-visit-to-scientific-drilling-ship-20160120&
UW News	US	English	Website	21 Jan 2016	UW Researcher Part of Indian Ocean Expedition to Drill to the Earth's Core	NA	http://www.uwyo.edu/uw/news/2016/01/uw-researcher-part-of-indian-ocean-expedition-to-drill-to-the-earths-core.html
Science Friday	US	English	Radio	22 Jan 2016	Digging Deep into the Crust of the Earth	1,500,000	http://www.sciencefriday.com/segments/digging-deep-into-the-crust-of-the-earth/
Halesowen News	UK	English	Newspaper/ Website	22 Jan 2016	Halesowen students celebrate live link up with boffins aboard Indian Ocean ship	NA	http://www.halesowennews.co.uk/news/14223572.Halesowen_students_celebrate_live_link_up_with_boffins_aboard_Indian_Ocean_ship/
La Provincia Pavese	Italy	Italian	Newspaper	23 Jan 2016	Al centro della terra La sfida nell'Oceano	15,700	NA
WAZ	Germany	German	Newspaper/ Website	24 Jan 2016	Mendener Forscher: "Eine Mischung aus Technologie und Magie"	580,000	http://www.derwesten.de/panorama/mendener-forscher-eine-mischung-aus-technologie-und-magie-id11487079.html
Popular Mechanics	US	English	Magazine/ Website	25 Jan 2016	Scientists Are Working to Drill a Mile-and-a-Half Hole Into the Earth	1,200,000	http://www.popularmechanics.com/science/environment/a19120/scientists-drill-into-earths-mantle/

Table T6 (continued).

Agency	Country	Language	Type of media	Date	Title	Estimated reach of publication	URL
Smithsonian	US	English	Magazine/ Website	26 Jan 2016	A Decades-Long Quest to Drill Into Earth's Mantle may Soon Hit Pay Dirt	2,000,000 (print)	**http://www.smithsonianmag.com/science-nature/decades-long-quest-drill-earths-mantle-may-soon-hit-pay-dirt-180957908/**
Inverse	US	English	Website	26 Jan 2016	Researchers Drill for the Earth's Mantle	NA	**https://www.inverse.com/article/10608-researchers-drill-for-the-earth-s-mantle**
Il Giorno	Italy	Italian	Newspaper	26 Jan 2016	Da Pavia nelle viscere della terra Il songo di due geologi si realizza	69,000	NA
KCBS San Francisco	US	English	Radio	27 Jan 2016	NA	NA	NA
Xinhua News Agency	China	Mandarin	Newspapers/ Websites	Entire expedition	30 news reports, 100 photographs	NA	Multiple

Figure F1. 3-D perspective view of the Atlantis II Transform, looking north-northeast. Data compiled from multibeam data collected during *Conrad* Cruise C2709, *James Clark Ross* Cruise JR31, *Yokosuka* and *Kairei* site survey cruises, and several French multibeam expeditions, combined with satellite gravity seafloor data and the Global Multi-Resolution Topography database (**http://www.marine-geo.org/portals/gmrt/**) (see also Mendel et al., 1997, 2003; Dick et al., 1999; Kinoshita et al., 2001; Matsumoto et al., 2002; Sauter et al., 2004; Baines et al., 2007).

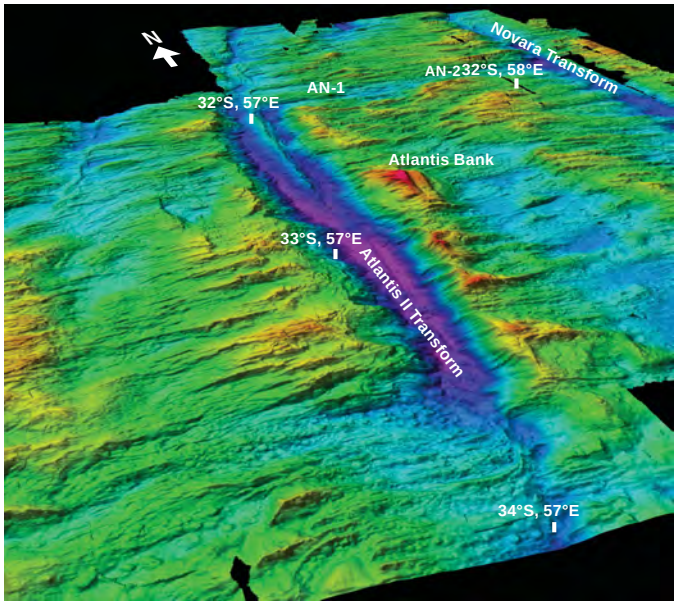

Figure F2. Alternative models for the lower crust and mantle (modified from Dick et al., 2006).

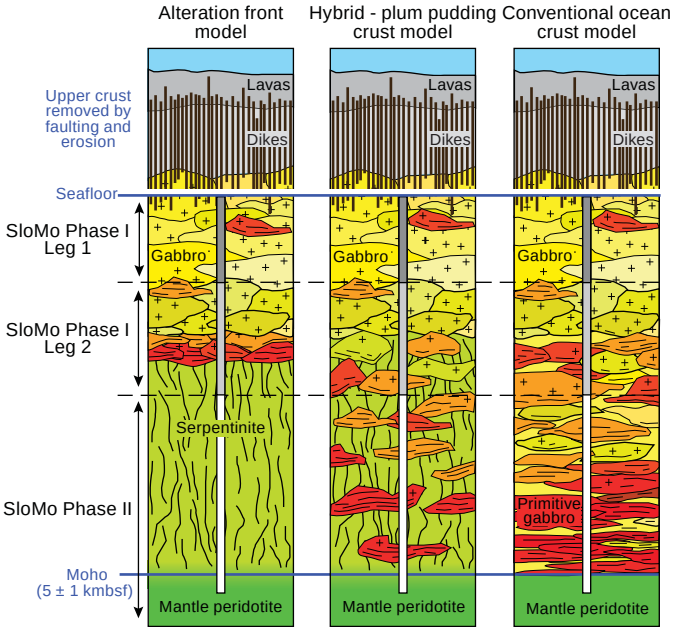

Figure F3. A. Bathymetry of Atlantis Bank area, with ODP/IODP drill sites marked. B. Summary of mapping of the same area, with geological interpretation by H.J.B. Dick based on site survey results (MacLeod et al., 1998; Kinoshita et al., 2001; Matsumoto et al., 2002).

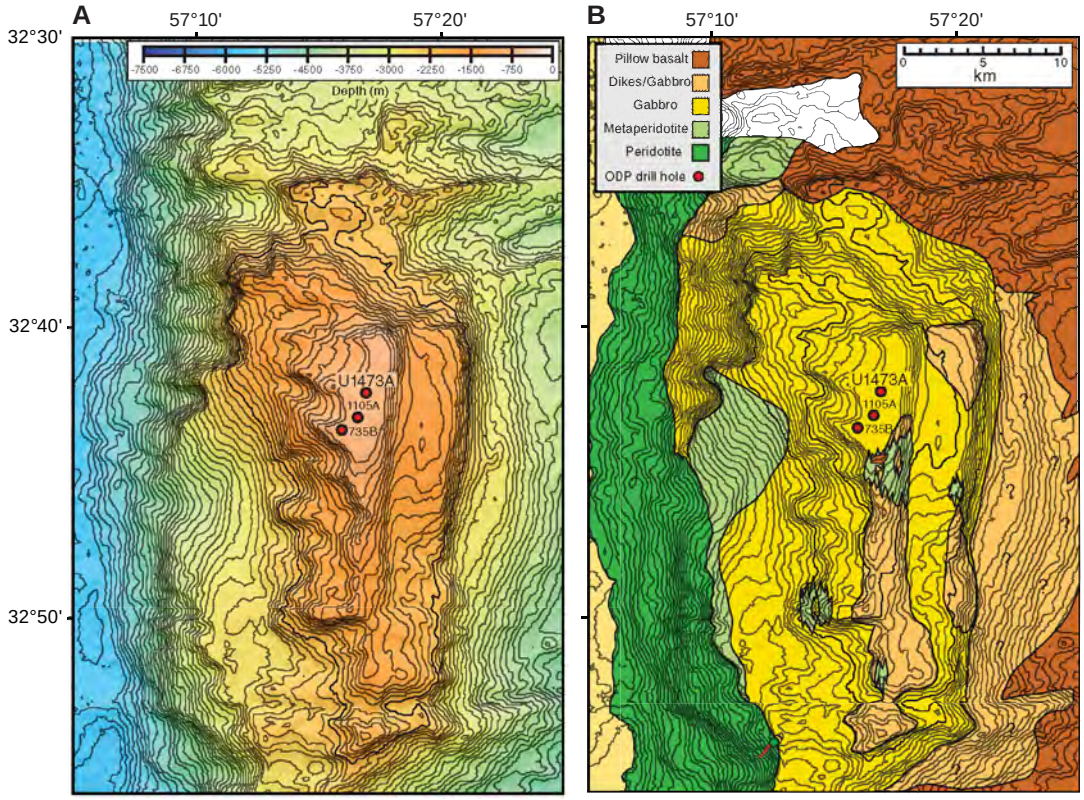

Figure F4. Velocity models for north–south seismic Line CAM101 over Atlantis Bank, together with principal drill sites (modified after Muller et al., 2000). Green line = depth of Hole U1473A drilled during Expedition 360, orange line = projected penetration during the remainder of SloMo Phase I, red line = projected penetration during SloMo Phase II (riser drilling). Velocity contours are 0.4 km/s. Upper panel shows an undifferentiated Layer 3; lower panel shows a lower serpentinized mantle Layer 3 and an upper gabbroic Layer 3. The models fit the data equally well. Triangles mark ocean-bottom hydrophones. Hole U1473A lies on the line, and Hole 735B is projected from a kilometer to the west. Moho gaps are due to ocean-bottom seismometer placement and are not real (R.S. White, pers. comm., 2000).

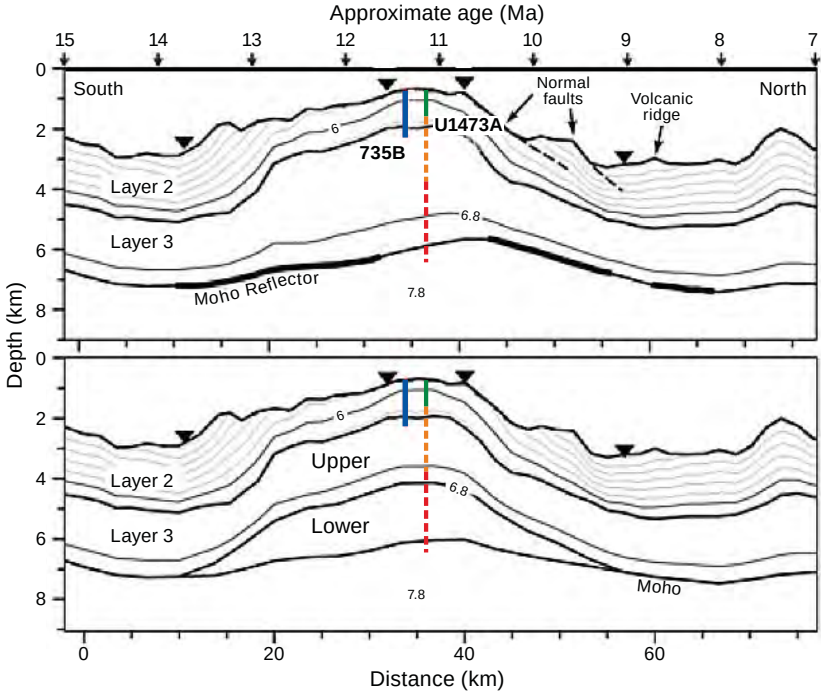

Figure F5. High-resolution contoured narrow-beam bathymetry map of Atlantis Bank wave-cut platform (Dick et al., 1999), showing ROV and submersible dive tracks plus locations of shallow and deep drill holes (MacLeod et al., 1998).

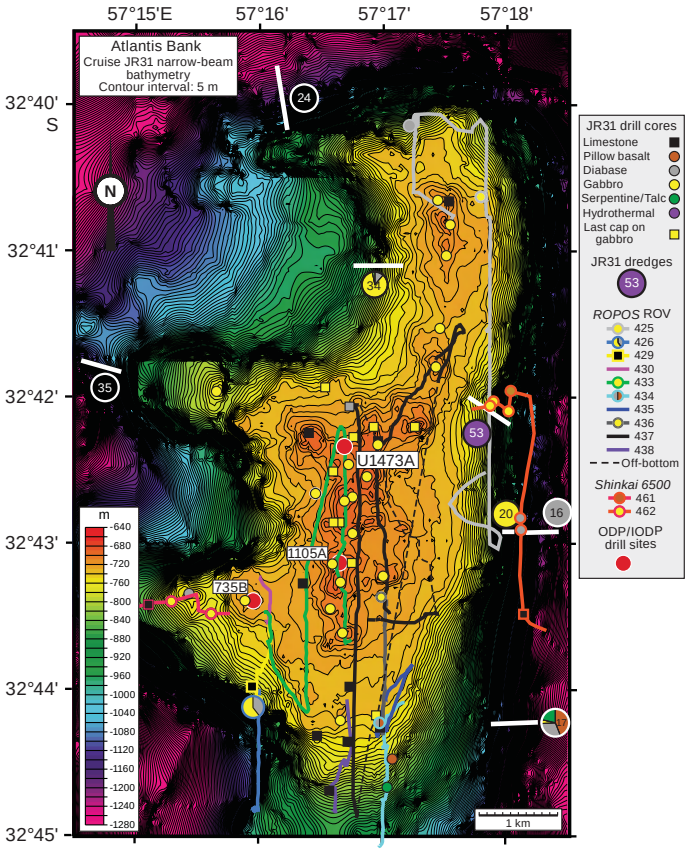

Figure F6. Running average (20 m) of lithologies, crystal-plastic deformation intensity, and whole-rock Mg# ([Mg × 100]/[Mg + Fe]) for Holes 735B and U1309D (Mid-Atlantic Ridge at 30°N), modified from Dick et al. (2000), Blackman et al. (2011), and Expedition 304/305 Scientists (2006). Different symbols for points in whole-rock Mg# diagram represent different lithologies based on modal mineralogy; definitions can be found in the Leg 118 and 176 *Initial Reports* volumes (Robinson, Von Herzen, et al., 1989; Dick, Natland, Miller, et al., 1999) and the Expedition 304/305 *Proceedings* volume (Blackman, Ildefonse, John, Ohara, Miller, MacLeod, and the Expedition 304/305 Scientists, 2006). These sections represent descriptions from two different scientific parties, and although both followed American Geophysical Institute conventions on nomenclature, exact definitions for each lithology described may vary. Lithologic plots differ from those previously presented, as the lithologies from both holes were grouped in the same manner to facilitate comparison. Gray dotted lines at Mg# = 80 emphasize overall chemical differences between the sections. Primary melts emerging from the mantle would be in equilibrium with gabbroic cumulates and dunites with an Mg# ≥ 90, largely missing from both sections.

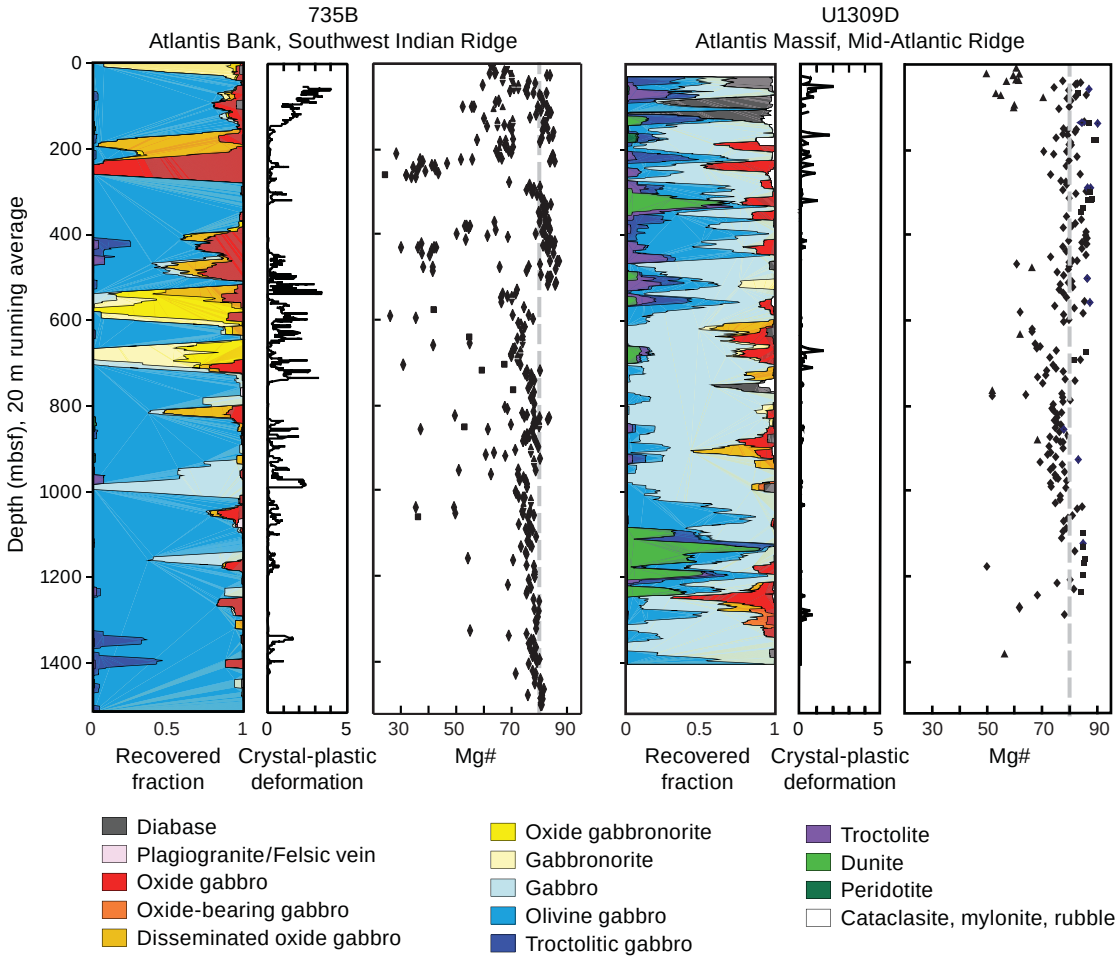

Figure F7. A. Location and magnetization of Atlantis Bank platform drill cores. B. Contoured deep-towed magnetization. C. Magnetic anomaly models with positions of Holes 735B and U1473A.

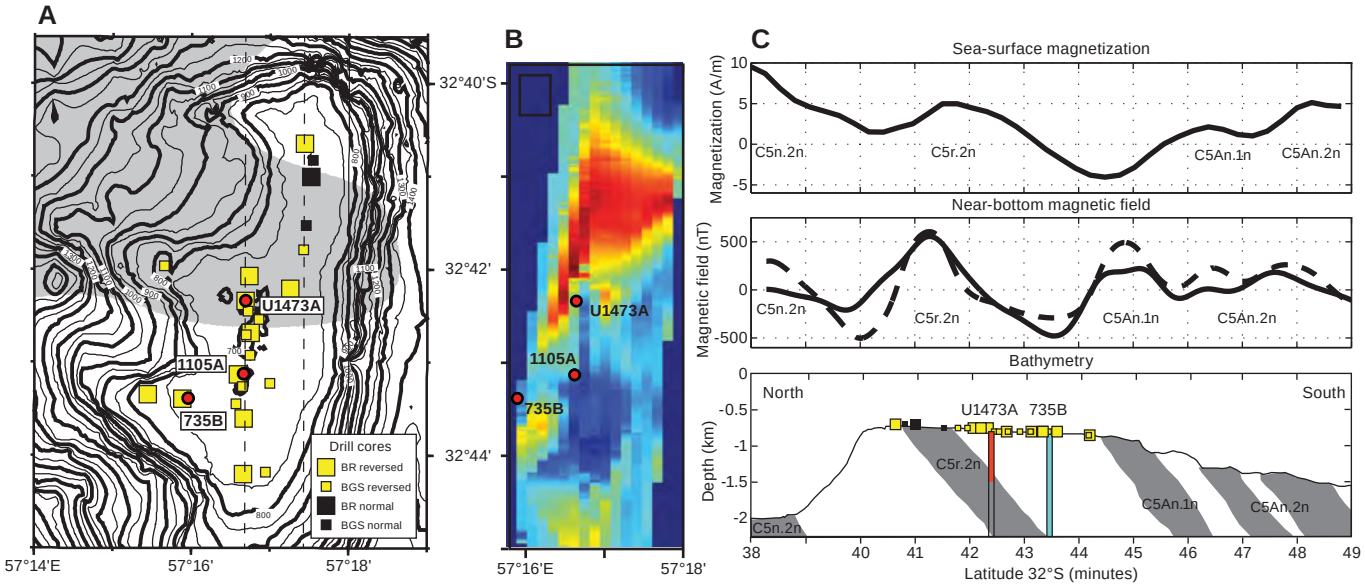

Figure F8. Bottom photo of target area selected for deep drill site (proposed Site AtBk6), showing flat bare-rock pavement (with echinoid) and thin carbonate in distance. The leg of the BRIDGE seabed rock drill is in the foreground; drilling here (Site JR31-BR8) yielded 1.1 m of oxide-bearing olivine gabbronorite cut by a thin mylonitic shear zone. Field of view = ~4–5 m.

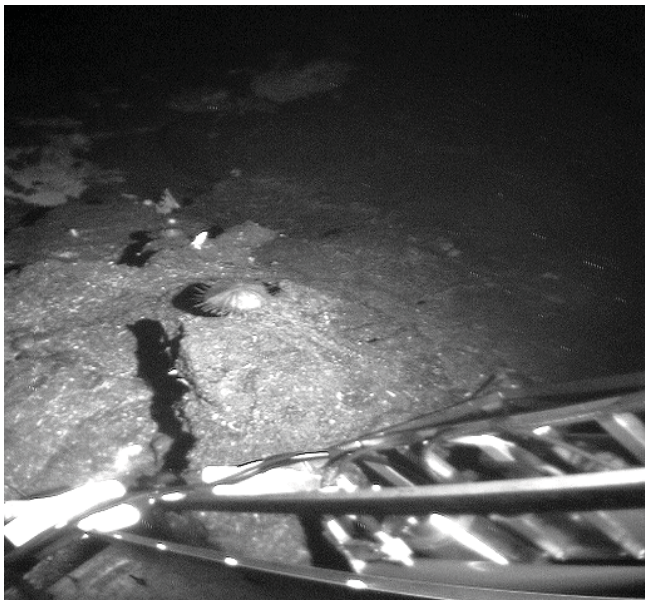

Figure F9. Track map of the subsea camera system during Site AtBk6/U1473 survey. The initial 50 m × 50 m box was extended south and west when it was clear that the seafloor at and around the original Site AtBk6 location (Waypoint 1) was dominated by sediment and scattered blocks of gabbro. Local bathymetry was derived from pipe length measurements combined with estimate of distance of pipe off the bottom for each minute of the survey.

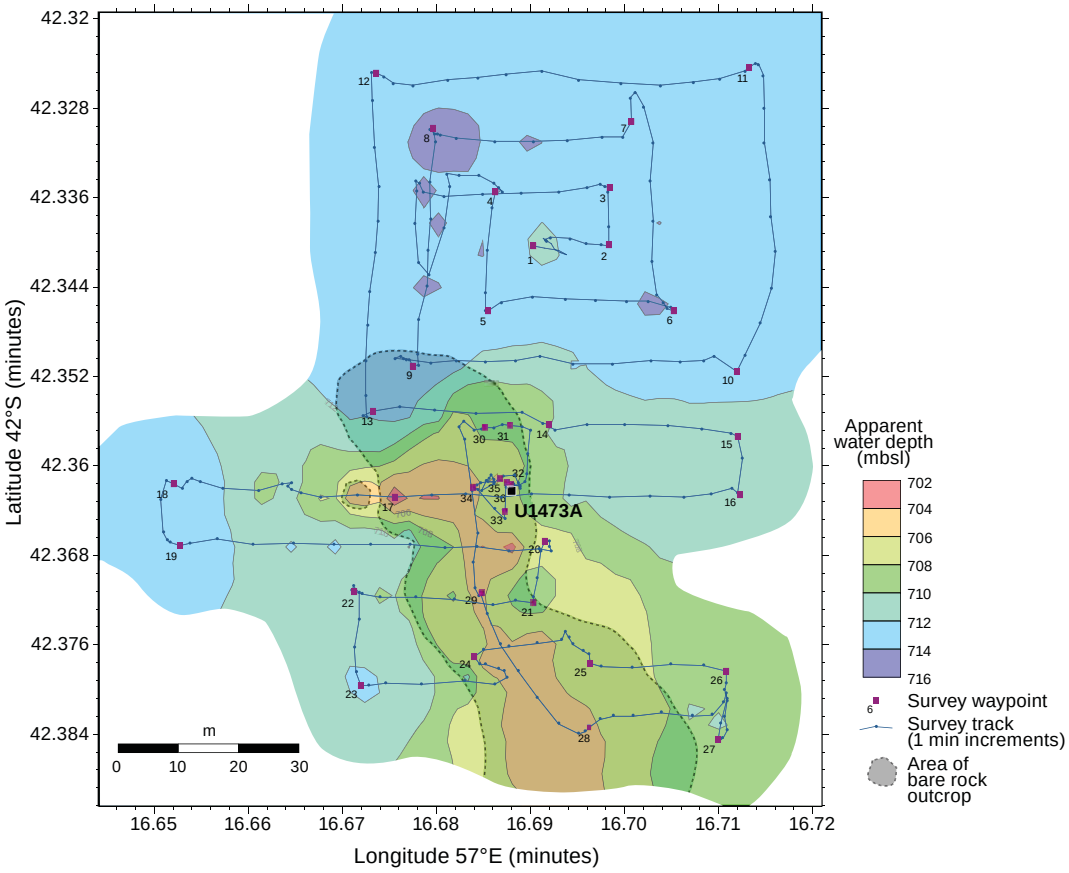

Figure F10. A–E. Photographs from various stages of the site survey (locations shown in Figure **F9**). Dark lineaments in D are believed to be east-west–trending amphibole veins. F. Hole U1473A hard rock reentry system in place on seafloor. Drill pipe is 9⅞ inches in diameter (~25 cm).

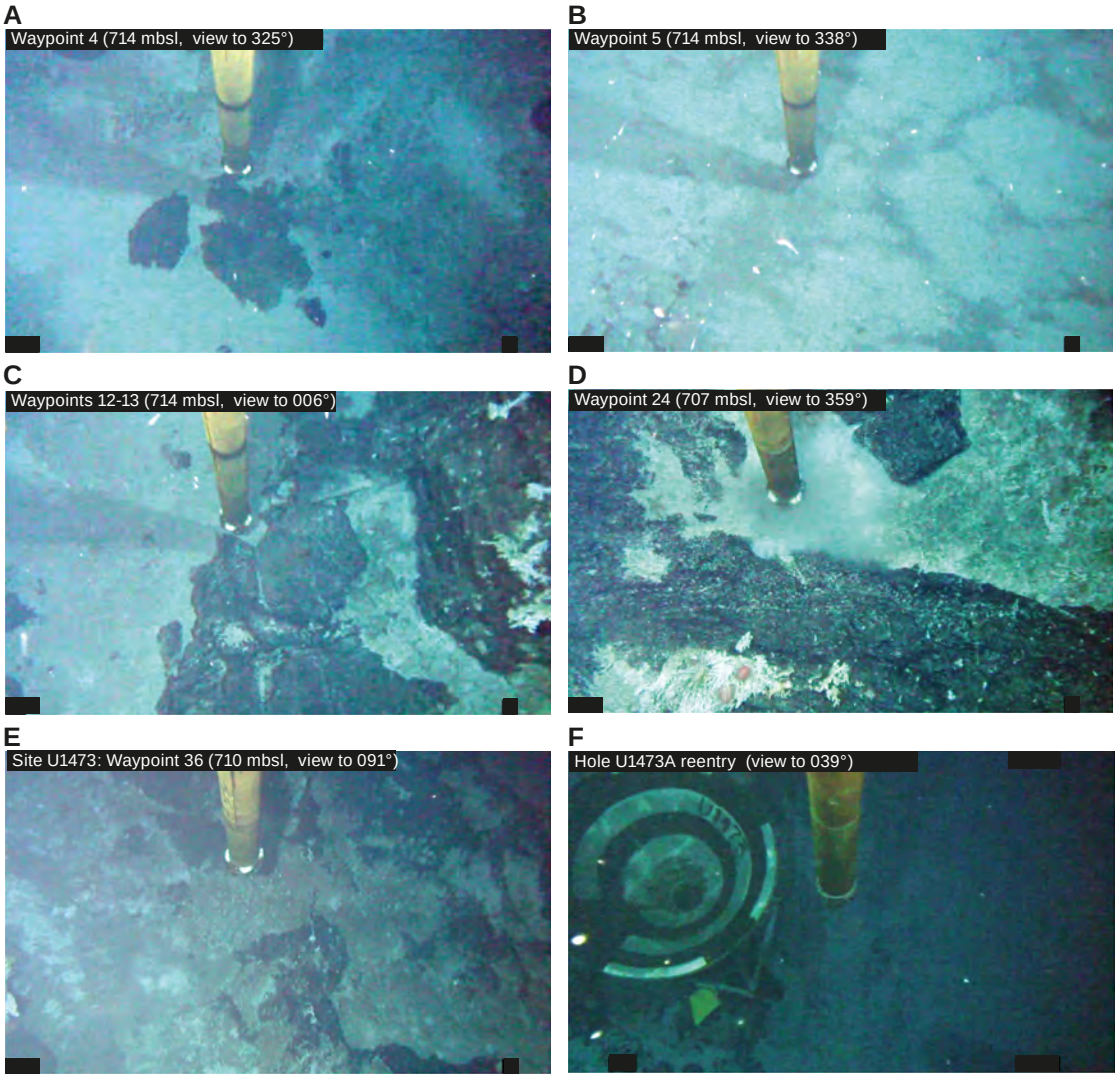

Figure F11. Lithostratigraphic variations, Hole U1473A. Relative abundances of lithologies are averaged over 20 m. Dashed lines = unit boundaries. Histograms document proportion of felsic veins per section and number of igneous layers identified every 5 m. CCSF = core composite depth below seafloor.

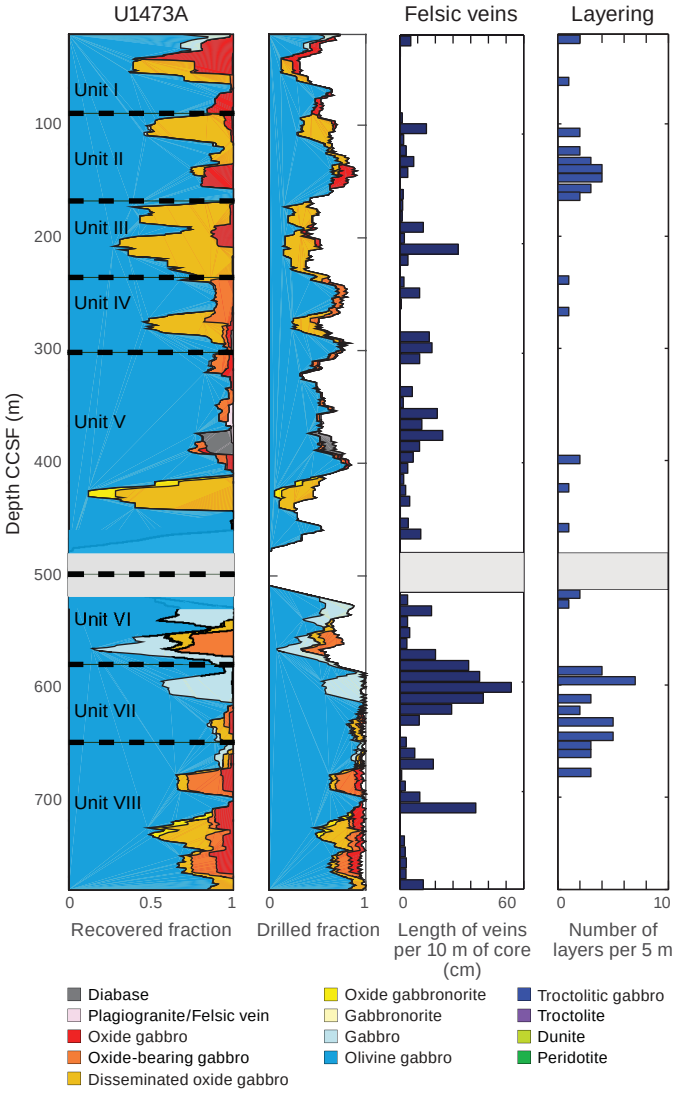

Figure F12. A. Lithostratigraphic variations in Hole U1473A compared with lithostratigraphic columns of other holes drilled at Atlantis Bank (Holes 735B and 1105A) and Atlantis Massif (Hole U1309D). Relative abundances of rocks are averaged over 20 m. In Holes 735B and U1309D, oxide gabbro includes both oxide gabbro and oxide-bearing gabbro.

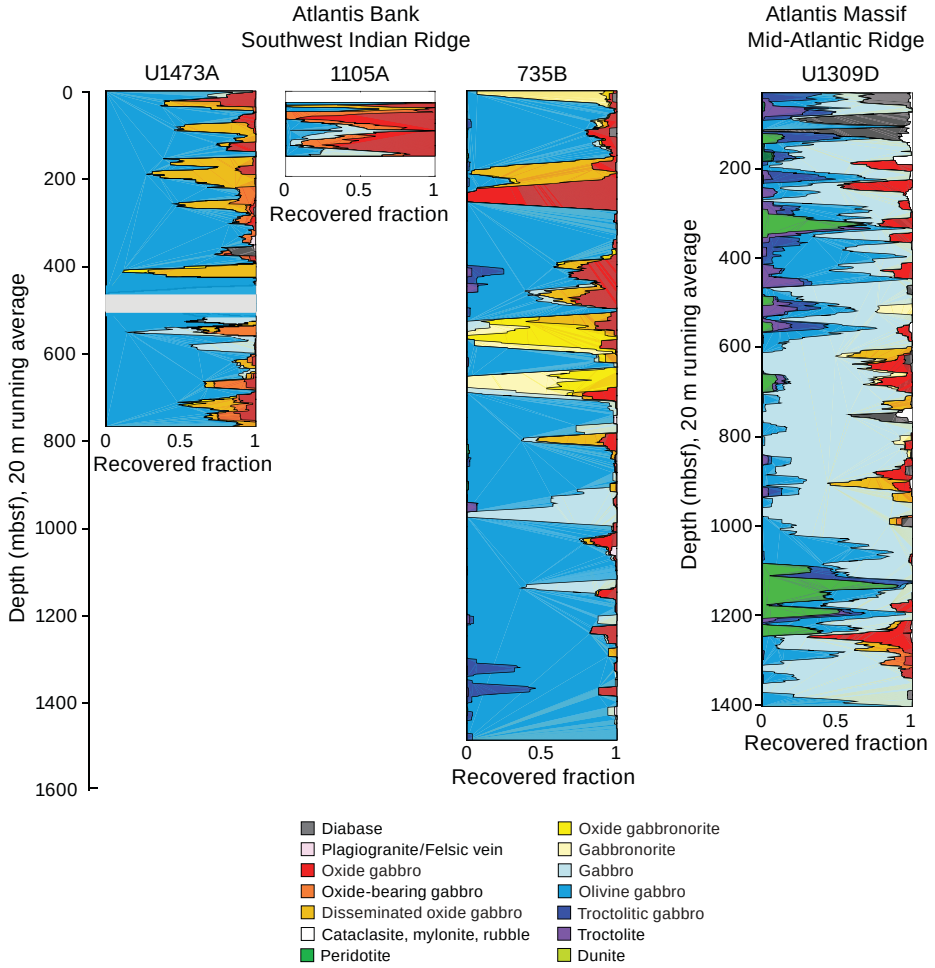

Figure F13. Chemical variations as a function of depth, Hole U1473A. Mg# decreases over most of the hole with discontinuities at ~60, ~300, and 700 mbsf (dotted lines). Ni and Cr data define geochemical boundaries with abrupt changes in concentration at ~60, 300, and 700 mbsf. Olivine gabbros collected to investigate alteration are distinguished.

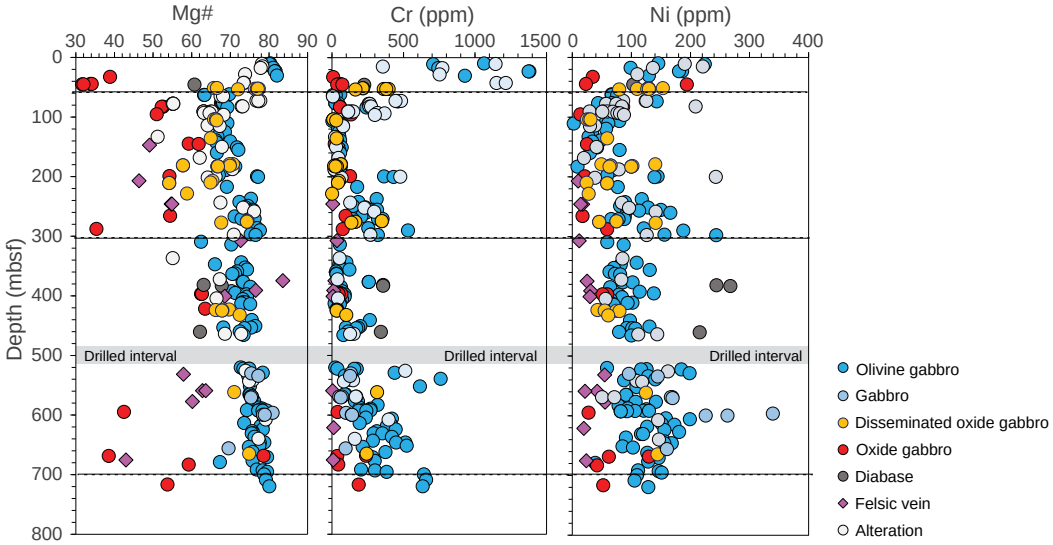

Figure F14. Downhole variation of primary igneous phase mineral alteration intensity, reddish clay mineral occurrences after olivine, magmatic vein occurrence, and vein filling minerals, Hole U1473A. Alteration intensity: 0 = <3%, 1 = 3%–9%, 2 = 10%–29%, 3 = 30%–59%, 4 = 60%–90%, 5 = >90%. Vein filling proportion: 0 = <10%, 1 = 10%–29%, 2 = 30%–59%, 3 = 60%–90%, 4 = >90%.

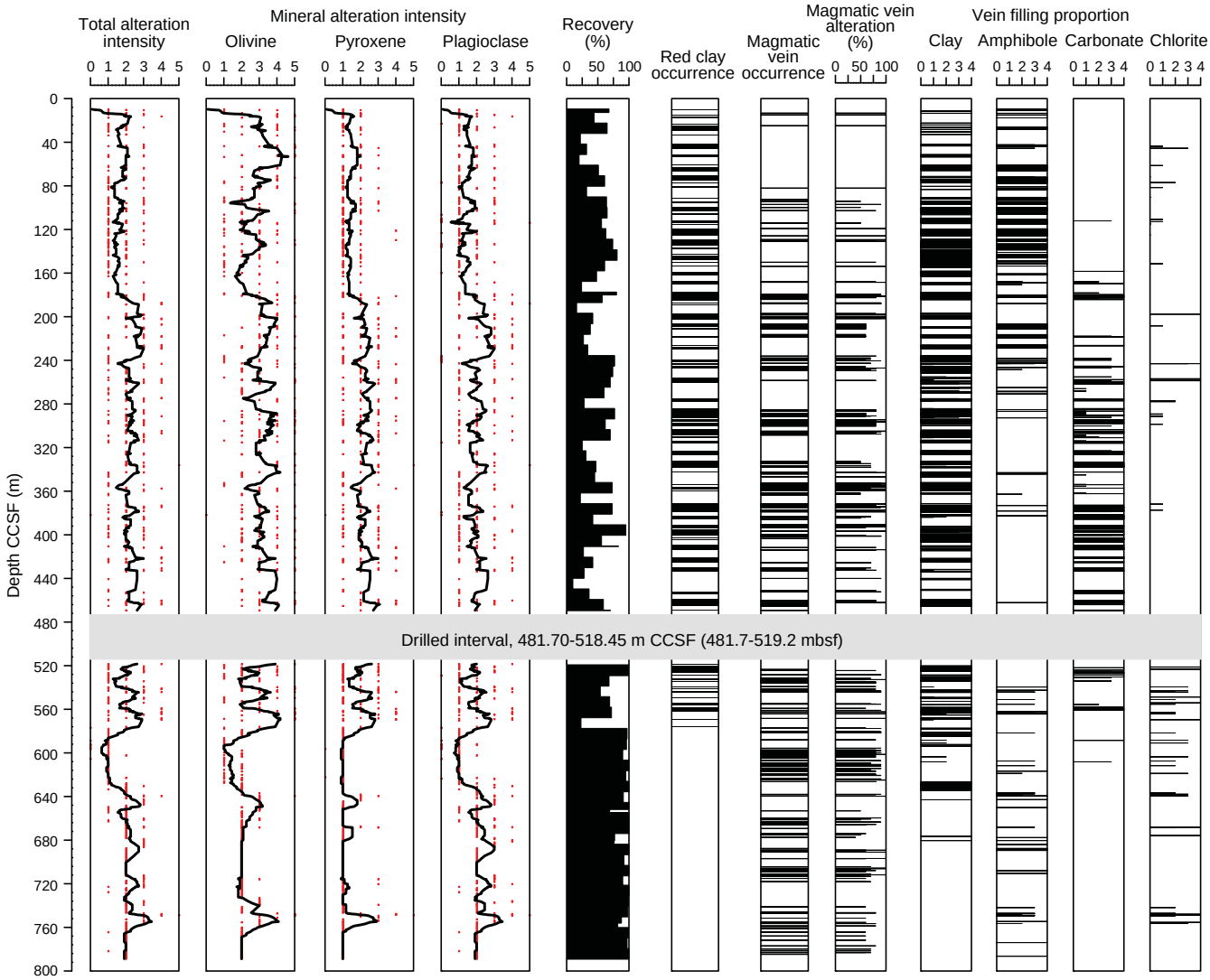

Figure F15. Distribution of crystal-plastic fabric intensity, dip variation, and shear sense with depth, Hole U1473A. Red lines = raw data, black curves = 5 cell thickness corrected running averages of intensity.

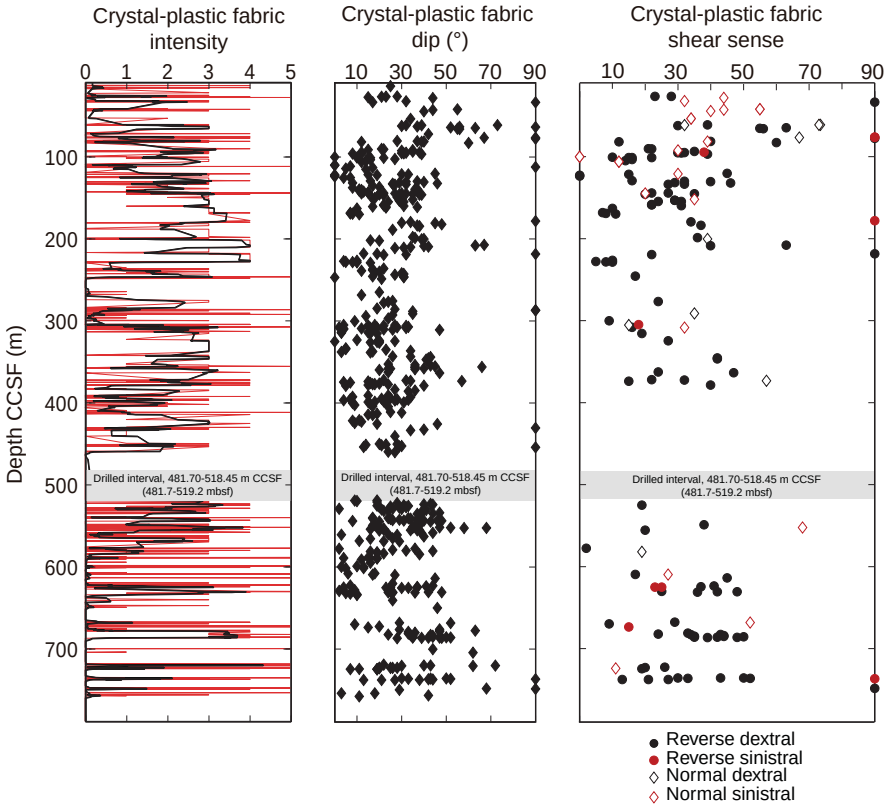

Figure F16. Metamorphic vein density and amphibole, clay, and carbonate vein frequency with depth, Hole U1473A. Vein density: 0 = no veins, 1 = <1/10 cm, 2 = 1–5/10 cm, 3 = 5–10/10 cm, 4 = 10–20/10 cm, 5 = >20/10 cm. Black curve = 11 point running average, horizontal dash-dotted lines = fault zone locations, dark gray bar = major fault location.

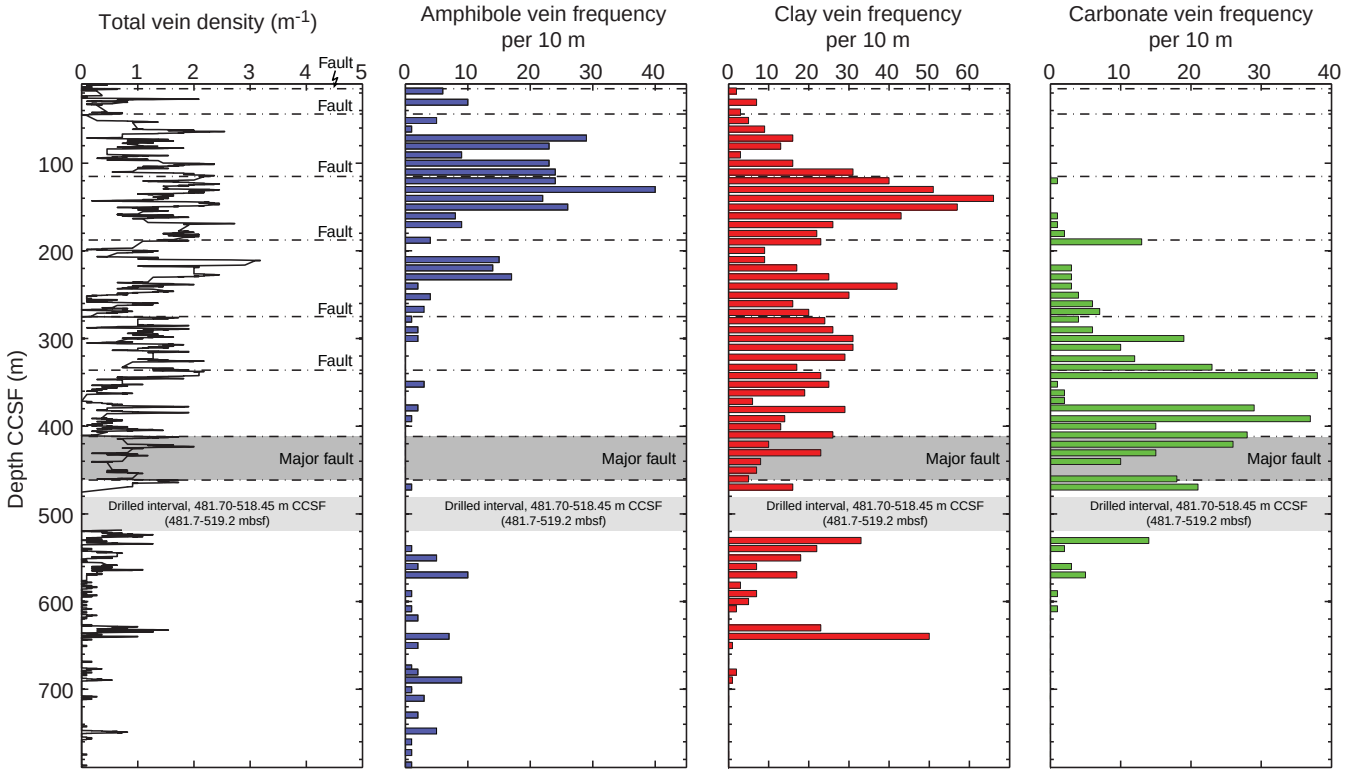

Figure F17. Fault rock intensity (1 = minor fracturing, 2 = moderate fracturing, 3 = incipient breccia, 4 = fault breccia, 5 = cataclasite) and fracture density (1 = 1 fracture/10 cm, 2 = 1–5 fractures/10 cm, 3 = >5 fractures/10 cm) with depth in Hole U1473A, raw data plotted. Fault rock intensity and fracture density are plotted as 11 cell (10 cm interval per cell) running averages (black curves). Red lines = raw fault rock intensity data, gray bars = seven major fault systems.

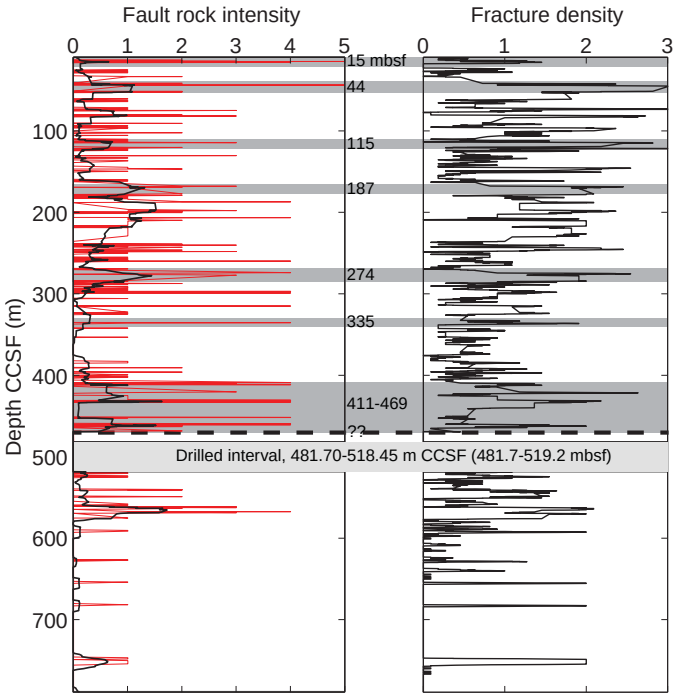

Figure F18. Summary of inclination data from Hole U1473A based on quality-filtered principal components determined from the 25–50 mT alternating field demagnetization data before (green) and after (orange) piece averaging. The data define five distinct inclination zones.

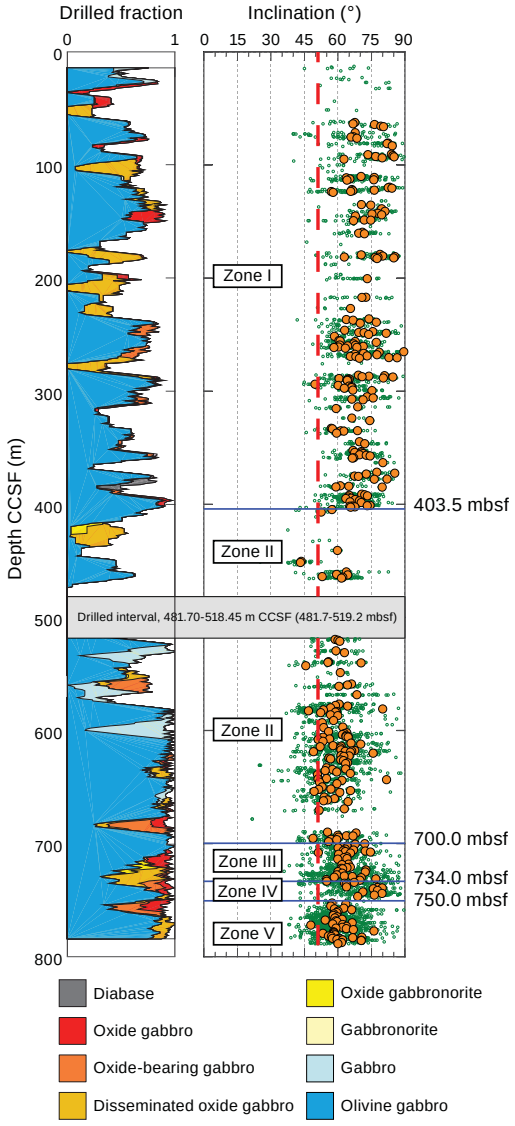

Figure F19. Expedition 360 operational time distribution. Left: Proportional time by major operational categories (desired activities [greens and purple], operational problems [reds], and logistics problems [blue and gray]). Right: Timeline of operational categories, each vertical bar represents 1 day.